Application of High-Throughput Sequencing Methods to Spider Phylogenomics and Speciation with a Focus on the Mygalomorph Genus *Aptostichus*

by

Nicole L. Garrison

A dissertation submitted to the Graduate Faculty of
Auburn University
in partial fulfillment of the
requirements for the Degree of
Doctor of Philosophy

Auburn, Alabama
May 5, 2018

Keywords: phylogenomics, molecular systematics, mygalomorph spiders, transcriptome, species delimitation

Approved by

Dr. Jason E. Bond, Chair, Professor and Department Chair of Biological Sciences
Dr. Rita Graze, Professor of Biological Sciences
Dr. Scott Santos, Professor of Biological Sciences
Dr. Michael Wooten, Professor of Biological Sciences

Abstract

Spiders are massively abundant generalist arthropod predators that are found in nearly every ecosystem on the planet and have persisted for over 380 million years. Spiders have long served as evolutionary models for studying complex mating and web spinning behaviors, key innovation and adaptive radiation hypotheses, and have been inspiration for important theories like sexual selection by female choice. Unfortunately, past major attempts to reconstruct spider phylogeny typically employing the "usual suspect" genes have been unable to produce a well-supported phylogenetic framework for the entire order. To further resolve higher level spider evolutionary relationships, I assembled a transcriptome-based data set comprising 70 ingroup spider taxa and executed phylogenomic analyses of a core ortholog supermatrix (Chapter I). To address questions at the species/population level, I employed a combination of two genomic sequencing approaches – targeted enrichment (anchored hybrid enrichment) and restriction enzyme based (genotyping-by-sequencing) – to evaluate relationships within the *Aptostichus atomarius* species complex (Chapter II). Finally, to understand the genomic basis of species diversity at the level of transcription, I compared transcriptomes of eight closely related species including ingroup *A. atomarius* complex members and outgroup taxa. Within the transcribed genes I detected gene families under selection and recovered sequences potentially associated with dune endemic lineages (Chapter III). All three chapters are designed with a single overarching goal: to move spider evolutionary biology and systematics forward by generating and utilizing next-generation sequence data and resources.

Table of Contents

Abstract ii

List of Tables vi

List of Figures vii

Chapter I Spider Phylogenomics: Untangling the Spider Tree of Life 1

Introduction 1

Materials and Methods 5

Sampling, Extraction, Assembly 5

Core Ortholog Approach and Data Processing 6

Phylogenetics 10

Results 13

Summary of Genomic Data 13

Phylogenetic Analyses 14

Discussion 16

Data Characteristics and Development of Spider Core Orthologs 17

A Modified View of Spider Evolution and Key Innovations 18

Spider Systematics 21

Conclusions 27

Data Accessibility 28

References 29

Chapter II Species Delimitation in a Californian Trapdoor Spider Species Complex 49
Introduction 49
Materials and Methods 52
GBS Sequencing and Filtering 53
Species/Population Discovery 54
AHE Loci Capture and Processing 55
Phylogenomic Analyses 56
Species Validation 57
Species Boundary Refinement 58
Results 59
GBS Data Clustering Analyses 60
Phylogenomic Relationships 61
Species Delimitation and Refinement 62
Discussion 63
Cryptic Speciation 64
Sympatry and Species Diagnoses 65
Sister Species of Metapopulations? 66
Conclusions 68
References 71
Chapter III Transcriptome Characterization and Signatures of Selection in the *Aptostichus atomarius* Species Complex 85

Background 85
Materials and Methods 87
Assembly and Assessment of Completeness 88
Functional Annotation 90
Detection of Gene Families Under Selection 91
Results and Discussion 92
Conclusions 98
References 100
Appendix I 116

List of Tables

Chapter I

Table 1: Major Spider Lineages 39

Table 2: Summary of Phylogenomic Analyses 40

Table 3: BEAST statistics 41

Chapter II

Table 1: Sampling Locality Data 75

Chapter III

Table 1: Sequence Metadata and Annotation Summary 106

Table 2: OrthoFinder Summary 106

Table 3: COATS Top 20 107

List of Figures

Chapter I

Figure 1: Summary, Preferred Tree of Spider Relationships 43

Figure 2: Summary Tree of Phylogenomic Analyses 44

Figure 3: ASTRAL Gene Tree 45

Figure 4: Chronogram 46

Figure 5: Time Calibrated Phylogeny and BAMM Analysis 47

Figure 6: ML Ancestral State Reconstruction 48

Chapter II

Figure 1: Sampling Locality Map 78

Figure 2: STRUCTURE and LEA for D1 79

Figure 3: STRUCTURE and LEA for D2 79

Figure 4: STRUCTURE and LEA for D3 79

Figure 5: ML Reconstruction 644 Loci 80

Figure 6: ML Reconstruction 141 Loci 80

Figure 7: ASTRAL Species Tree 644 Loci 81

Figure 8: ASTRAL Species Tree 141 Loci 82

Figure 9: BPP Result Summary 83

Figure 10: PHRAPL Asymmetric Analyses Summary 83

Figure 11: PHRAPL Symmetric Analyses Summary 84

Figure 12: Map of Adjusted Distributions 84

Chapter III

Figure 1: Distribution Map and Sampling Localities 108

Figure 2: COATS Pipeline 109

Figure 3: Isoform Counts 110

Figure 4 BUSCO Results 110

Figure 5: MCSC Taxonomic Distribution 111

Figure 6: Heatmap of Pairwise Sequence Values 112

Figure 7: OrthoVenn Output 113

Figure 8: MSA Aptostichus ICK Peptides 114

Figure 9: TMhmm Alignment of ICK 115

Figure 10: MSA Kunitz-type peptides 115

CHAPTER I
Spider Phylogenomics: Untangling the Spider Tree of Life

Introduction:

Spiders (Order Araneae; Fig. 1) are a prototypical, hyperdiverse arthropod group comprising >45,000 described species (World Spider Catalog, 2016) distributed among 3,958 genera and 114 families; by some estimates the group may include more than 120,000 species (Agnarsson, Coddington & Kuntner, 2013). Spiders are abundant, generalist predators that play dominant roles in almost every terrestrial ecosystem. The order represents an ancient group that has continued to diversify taxonomically and ecologically since the Devonian (>380 mya). They are relatively easy to collect and identify, and are one of few large arthropod orders to have a complete online taxonomic catalog with synonymies and associated literature (World Spider Catalog, 2016).

In addition to their remarkable ecology, diversity, and abundance, spiders are known for producing extraordinary biomolecules like venoms and silks as well as their utility as models for behavioral and evolutionary studies (reviewed in Agnarsson, Coddington & Kuntner, 2013). Stable and complex venoms have evolved over millions of years to target predators and prey alike. Stable and complex venoms have evolved over millions of years to target predators and prey alike. Although few are dangerous to humans, spider venoms hold enormous promise as economically important insecticides and therapeutics (Saez et al., 2010; King & Hardy, 2013). Moreover, no other animal lineage can claim a more varied and elegant use of silk. A single species may have as many as eight different silk glands, producing a variety of super-strong silks deployed in almost every aspect of a spider's life (Garb, 2013): safety lines, dispersal,

reproduction (sperm webs, eggsacs, pheromone trails), and prey capture (Blackledge, Kuntner & Agnarsson, 2011). Silken prey capture webs, particularly the orb, have long been considered a key characteristic contributing to the ecological and evolutionary success of this group (reviewed in Bond & Opell, 1998). Moreover, spider silks are promising biomaterials, already benefiting humans in myriad ways - understanding the phylogenetic basis of such super-materials will facilitate efforts to reproduce their properties in biomimetic materials like artificial nerve constructs, implant coatings, and drug delivery systems (Blackledge, Kuntner & Agnarsson, 2011; Schacht & Scheibel, 2014).

The consensus on major spider clades has changed relatively little in the last two decades since the summary of Coddington & Levi (1991) and Coddington (2005). Under the classical view, Araneae comprises two clades (see Table 1 and Fig. 1 for major taxa discussed throughout; node numbers (Fig. 1) referenced parenthetically hereafter), Mesothelae (Node 2) and Opisthothelae (Node 3). Mesotheles are sister to all other spiders, possessing a plesiomorphic segmented abdomen and mid-ventral (as opposed to terminal) spinnerets. Opisthothelae contains two clades: Mygalomorphae (Node 4) and Araneomorphae (Node 8). Mygalomorphae is less diverse (~6 % of described Araneae diversity) and retains several plesiomorphic features (e.g. two pairs of book lungs, few and biomechanically 'weak' silks (Dicko et al., 2008; Starrett et al., 2012). Within Araneomorphae, Hypochilidae (Paleocribellatae; Node 9) is sister to Neocribellatae, within which Austrochiloidea are sister to the major clades Haplogynae (Node 10) and Entelegynae (Node 11), each weakly to moderately supported by few morphological features. Haplogynes have simple genitalia under muscular control whereas entelegynes have hydraulically activated, complex genitalia, with externally sclerotized female epigyna. Entelegynes comprise multiple, major, hyperdiverse groups, including the "RTA clade" (RTA =

retrolateral tibial apophysis, Node 13), its subclade Dionycha (e.g. jumping spiders; Ramirez, 2014, Node 14), and the Orbiculariae – the cribellate and ecribellate orb weavers and relatives (see Hormiga & Griswold, 2014).

Beginning with early higher-level molecular phylogenetic studies, it gradually became clear that major "stalwart" and presumably well-supported spider groups like the Neocribellatae, Haplogynae, Palpimanoidea, Orbiculariae, Lycosoidea, and others (generally only known to arachnologists) were questionable. Subsequent studies focusing on mygalomorph (Hedin & Bond, 2006; Bond et al., 2012) and araneomorph (Blackledge et al., 2009; Dimitrov et al., 2012) relationships continued to challenge the consensus view based largely on morphological data, finding polyphyletic families and ambivalent support for major clades, which were sometimes "rescued" by adding non-molecular data; molecular signal persistently contradicted past verities. In Agnarsson, Coddington & Kuntner (2013), a meta-analysis of available molecular data failed to recover several major groups such as Araneomorphae, Haplogynae, Orbiculariae, Lycosoidea, and others (Table 1). Although these authors criticized the available molecular data as insufficient, their results actually presaged current spider phylogenomic inferences Bond et al., 2014. Incongruence between the traditional spider classification scheme and (non-phylogenomic) molecular systematics likely has one primary cause: too few data. Non-molecular datasets to date have been restricted to a relatively small set of morphological and/or behavioral characters whereas molecular analyses addressing deep spider relationships have largely employed relatively few, rapidly evolving loci (e.g., 28S and 18S rRNA genes, Histone 3, and a number of mitochondrial DNA markers).

The first analyses of spider relationships using genome-scale data, scored for 40 taxa by Bond et al. (2014) and for 14 taxa by Fernández, Hormiga & Giribet (2014), considerably refined

understanding of spider phylogeny, the former explicitly calling into question long held notions regarding the tempo and mode of spider evolution. Using transcriptome-derived data, Bond et al. (2014) recovered the monophyly of some major groups (araneomorphs and mygalomorphs) but reshuffled several araneomorph lineages (haplogynes, paleocribellates, orbicularians, araneoids (Node 12) and the RTA clade). Notably, Bond et al. (2014) and Fernández, Hormiga & Giribet (2014) rejected Orbiculariae, which included both cribellate (Deinopoidea) and ecribellate orb weavers (Araneoidea). Instead they suggested either that the orb web arose multiple times, or, more parsimoniously, that it arose once and predated the major diversification of spiders. Despite significant advances in understanding of spider phylogeny, only a small percentage of spider families were sampled and monophyly of individual families could not be tested in previous phylogenomic studies. Denser taxon sampling is needed to warrant changes in higher classification and to more definitively address major questions about spider evolution.

Herein, we apply a spider-specific core ortholog approach with significantly increased taxon and gene sampling to produce a more complete and taxon specific set of alignments for phylogenetic reconstruction and assessment of spider evolutionary pattern and process. Existing genome-derived protein predictions and transcriptome sequences from a representative group of spiders and arachnid outgroups were used to create a custom core ortholog set specific to spiders. Taxon sampling was performed to broadly sample Araneae with an emphasis on lineages whose phylogenetic placement is uncertain and included previously sequenced transcriptomes, gene models from completely sequenced genomes, and novel transcriptome sequences generated by our research team. This resulted in a data set comprising 70 spider taxa plus five additional arachnid taxa as outgroups. We test long-held notions that the orb web, in conjunction with ecribellate adhesive threads, facilitated diversification among araneoids and present the most

completely sampled phylogenomic data set for spiders to date using an extensive dataset of nearly 3,400 putative genes (~700K amino acids). Further, we test the hypothesis of a non-monophyletic Orbiculariae, assess diversification rate shifts across the spider phylogeny, and provide phylogenomic hypotheses for historically difficult to place spider families. Our results clearly demonstrate that our understanding of spider phylogeny and evolution requires major reconsideration and that several long-held and contemporary morphologically-derived hypotheses are likely destined for falsification.

Materials and Methods:

Sampling, Extraction, Assembly

Spider sequence data representing all major lineages were collected from previously published transcriptomic and genomic resources (N=53) and supplemented with newly sequenced transcriptomes (N=22) to form the target taxon set for the current study. Existing sequence data were acquired via the NCBI SRA database (http://www.ncbi.nlm.nih.gov/sra). Raw transcriptome sequences were downloaded, converted to fastq file format, and assembled using Trinity (Grabherr et al., 2011). Genomic data sets in the form of predicted proteins were downloaded directly from the literature (Sanggaard et al., 2014) for downstream use in our pipeline. Newly sequenced spiders were collected from a variety of sources, extracted using the TRIzol total RNA extraction method, purified with the RNeasy mini kit (Qiagen) and sequenced in-house at the Auburn University Core Genetics and Sequencing Laboratory using an Illumina Hi-Seq 2500. This produced 100bp paired end reads for each newly sequenced spider transcriptome, which were then assembled using Trinity. Proteins were predicted from each transcriptome using the program TransDecoder (Haas et al., 2013).

Core Ortholog Approach and Data Processing

We employed a core ortholog approach for putative ortholog selection and implicitly compared the effect of using a common arthropod core ortholog set and one compiled for spiders; the arthropod core ortholog set was deployed as described in Bond et al. (2014). To generate the spider core ortholog set, we used an all-versus-all BLASTP method (Altschul et al., 1990) to compare the transcripts of the amblypygid *Damon variegatus*, and the spiders *Acanthoscurria geniculata*, *Dolomedes triton*, *Ero leonina*, *Hypochilus pococki*, *Leucauge venusta*, *Liphistius malayanus*, *Megahexura fulva*, *Neoscona arabesca*, *Stegodyphus mimosarum*, and *Uloborus sp*. *Acanthoscurria geniculata*) and *Stegodyphus mimosarum* were represented by predicted transcripts from completely sequenced genomes while the other taxa were represented by our new Illumina transcriptomes. An e-value cut-off of 10-5 was used. Next, based on the BLASTP results, Markov clustering was conducted using OrthoMCL 2.0 (Li, Stoeckert & Roos, 2003) with an inflation parameter of 2.1.

The resulting putatively orthologous groups (OGs) were processed with a modified version of the bioinformatics pipeline employed by Kocot et al. (2011). First, sequences shorter than 100 amino acids in length were discarded. Next, each candidate OG was aligned with MAFFT (Katoh, 2005) using the automatic alignment strategy with a maxiterate value of 1,000. To screen OGs for evidence of paralogy, an "approximately maximum likelihood tree" was inferred for each remaining alignment using FastTree 2 (Price, Dehal & Arkin, 2010). Briefly, this program constructs an initial neighbor-joining tree and improves it using minimum evolution with nearest neighbor interchange (NNI) subtree rearrangement. FastTree subsequently uses minimum evolution with subtree pruning regrafting (SPR) and maximum likelihood using NNI to further improve the tree. We used the "slow" and "gamma" options; "slow" specifies a more

exhaustive NNI search, while "gamma" reports the likelihood under a discrete gamma approximation with 20 categories, after the final round of optimizing branch lengths.

PhyloTreePruner (Kocot, Citarella & Halanych, 2013) was then employed as a tree-based approach to screen each candidate OG for evidence of paralogy. First, nodes with support values below 0.95 were collapsed into polytomies. Next, the maximally inclusive subtree was selected where all taxa were represented by no more than one sequence or, in cases where more than one sequence was present for any taxon, all sequences from that taxon formed a monophyletic group or were part of the same polytomy. Putative paralogs (sequences falling outside of this maximally inclusive subtree) were then deleted from the input alignment. In cases where multiple sequences from the same taxon formed a clade or were part of the same polytomy, all sequences but the longest were deleted. Lastly, in order to eliminate orthology groups with poor taxon sampling, all groups sampled for fewer than 7 of the 11 taxa and all groups not sampled for *Megahexura fulva* (taxon with greatest number of identified OGs) were discarded. The remaining alignments were used to build profile hidden Markov models (pHMMs) for HaMStR with hmmbuild and hmmcalibrate from the HMMER package (Eddy, 2011).

For orthology inference, we employed HaMStR v13.2.3 (Ebersberger, Strauss & Von Haeseler, 2009), which infers orthology based on predefined sets of orthologs. Translated transcripts for all taxa were searched against the new set of 4,934 spider-specific pHMMs (available for download from the Dryad Data Repository) and an arthropod core ortholog set previously employed in Bond et al. (2014). In the spider core ortholog analysis, the genome-derived *Acanthoscurria geniculata* OGs were used as the reference protein set for reciprocal best hit scoring. *Daphnia pulex* was used as the reference species for putative ortholog detection in the arthropod core ortholog analysis. Orthologs sharing a core identification number were pooled

together for all taxa and processed using a modified version of the pipeline used to generate the custom spider ortholog set. In both analyses, sequences shorter than 75 amino acids were deleted first. OGs sampled for fewer than 10 taxa were then discarded. Redundant identical sequences were removed with the perl script uniqhaplo.pl (available at http://raven.iab.alaska.edu/~ntakebay/) leaving only unique sequences for each taxon. Next, in cases where one of the first or last 20 characters of an amino acid sequence was an X (corresponding to a codon with an ambiguity, gap, or missing data), all characters between the X and that end of the sequence were deleted and treated as missing data. Each OG was then aligned with MAFFT (mafft --auto --localpair --maxiterate 1000; Katoh, 2005). Alignments were then trimmed with ALISCORE (Misof & Misof, 2009) and ALICUT (Kück, 2009) to remove ambiguously aligned regions. Next, a consensus sequence was inferred for each alignment using the EMBOSS program infoalign (Rice, Longden & Bleasby, 2000). For each sequence in each single-gene amino acid alignment, the percentage of positions of that sequence that differed from the consensus of the alignment were calculated using infoalign's "change" calculation. Any sequence with a "change" value greater than 75 was deleted. Subsequently, a custom script was used to delete any mistranslated sequence regions of 20 or fewer amino acids in length surrounded by ten or more gaps on either side. This step was important, as sequence ends were occasionally mistranslated or misaligned. Alignment columns with fewer than four non-gap characters were subsequently deleted. At this point, alignments shorter than 75 amino acids in length were discarded. Lastly, we deleted sequences that did not overlap with all other sequences in the alignment by at least 20 amino acids, starting with the shortest sequence not meeting this criterion. This step was necessary for downstream single-gene phylogenetic tree reconstruction. As a final filtering step, OGs sampled for fewer than 10 taxa were discarded.

In some cases, a taxon was represented in an OG by two or more sequences (splice variants, lineage-specific gene duplications [=inparalogs], overlooked paralogs, or exogenous contamination). In order to select the best sequence for each taxon and exclude any overlooked paralogs or exogenous contamination, we built trees in FastTree 2 (Price, Dehal & Arkin, 2010) and used PhyloTreePruner to select the best sequence for each taxon as described above. Remaining OGs were then concatenated using FASconCAT (Kück & Meusemann, 2010). The OGs selected by our bioinformatic pipeline were further screened in seven different ways (subsets listed in Table 2). OGs were first sorted based on amount of missing data; the half with the lowest levels was pulled out as matrix 2 (1699 genes). From matrix 2, a smaller subset of OGs optimized for gene occupancy was extracted, resulting in matrix 3 (850 genes). The full supermatrix (matrix 1) was also optimized using the programs MARE (Meyer, Meusemann & Misof, 2011) and BaCoCa (Base Composition Calculator; Kück & Struck, 2014). MARE assesses the supermatrix by partition, providing a measure of tree-likeness for each gene and optimizes the supermatrix for information content. The full supermatrix was optimized with an alpha value of 5, to produce matrix 7 (1488 genes, 58 taxa). From the MARE-reduced matrix, genes having no missing partitions for any of the remaining taxa (n=50) were extracted to form a starting matrix for the BEAST analyses (details below). Matrix assessment was also conducted using BaCoCa, which provides a number of descriptive supermatrix statistics for evaluating bias in amino acid composition and patterns in missing data. This program was used to assess for patterns of non-random clusters of sequences in the data, which could potentially mislead phylogenetic analyses. Matrix 4 represents a 50 % reduction of the full supermatrix using BaCoCa derived values for phylogenetically informative sites as a guide; essentially reducing missing data from absent partitions and gaps. This matrix is similar, but not identical to matrix

2. Matrix 5 resulted from application of arthropod core OGs from Bond et al. (2014) to the extended taxon set. Matrix 6 represents the full spider core OG matrix (matrix 1) with *Stegodyphus* pruned from the tree. OGs for each matrix were concatenated using FASconCAT (Kück & Meusemann, 2010).

Phylogenetics

Table 2 summarizes run parameters of the seven individual maximum likelihood analyses conducted for each of the supermatrices. We selected the optimal tree for each supermatrix using the computer program ExaML ver. 3.0.1 (Kozlov, Aberer & Stamatakis, 2015). Models of amino acid substitution were selected using the AUTOF command in ExaML. Bootstrap data sets and starting parsimony trees for each matrix were generated using RAxML (Stamatakis, 2014) and each individually analyzed in ExaML. We generated 225-300 replicates for each matrix which were then used to construct a majority-rule bootstrap consensus tree; a custom python script was used to automate the process and write a bash script to execute the analyses on a high-performance computing (HPC) cluster. The arthropod core OG bootstrap analysis was conducted using RAxML. All analyses were conducted on the Auburn University CASIC HPC and Atrax (Bond Lab, Auburn University).

A coalescent-based method as implemented in ASTRAL (Accurate Species TRee ALgorithm; Mirarab et al., 2014) was used to infer a species tree from a series of unrooted gene trees. The ASTRAL approach is thought to be more robust to incomplete lineage sorting, or deep coalescence, than maximum likelihood analysis of concatenated matrices and works quickly on genome-scale datasets (Mirarab et al., 2014). We first constructed individual gene trees for all partitions contained within matrix 1. Gene trees were generated using ML based on 100 RAxML random addition sequence replicates followed by 100 bootstrap replicates (Table 2). Subsequent

species tree estimation was inferred using ASTRAL v4.7.6, from all individual unrooted gene trees (and bootstrap replicates), under the multi-species coalescent model.

A chronogram was inferred in a Bayesian framework under an uncorrelated lognormal relaxed clock model (Drummond et al., 2006, Drummond, 2007) using Beast v1.8.1 (Drummond et al., 2012). For this analysis we used 43 partitions of a matrix which included complete partitions for all taxa derived from the MARE-optimized matrix 7. The model of protein evolution for each partition was determined using the perl script ProteinModelSelection.pl in RAxML. BEAST analyses were run separately for each partition using eight calibration points based on fossil data. The most recent common ancestor (MRCA) of Mesothelae + all remaining spiders was given a lognormal prior of (mean in real space) 349 Ma (SD=0.1) based on the Mesothelae fossil *Palaeothele montceauensis* (Selden, 1996). The MRCA of extant araneomorphs was given a lognormal prior of (mean in real space) 267 Ma (SD=0.2) based on the fossil *Triassaraneus andersonorum* (Selden et al., 1999). The MRCA of extant mygalomorphs was given a lognormal prior of (mean in real space) 278 Ma (SD=0.1) based on the fossil *Rosamygale grauvogeli* (Selden & Gall, 1992). The MRCA of Haplogynae + Hypochilidae was given a lognormal prior of (mean in real space) 278 Ma (SD=0.1) based on the fossil *Eoplectreurys gertschi* (Selden & Penney, 2010). The MRCA of Deinopoidea (cribellate orb-weavers) was given a lognormal prior of (mean in real space) 195 Ma (SD=0.3) based on the fossil *Mongolarachne jurassica* (Selden, Shih & Ren, 2013). The MRCA of ecribellate orb-weavers was given a lognormal prior of (mean in real space) 168 Ma (SD=0.4) based on the fossil *Mesozygiella dunlopi* (Penney & Ortu, 2006). The MRCA of Nemesiidae, excluding *Damarchus*, was given a lognormal prior of (mean in real space) 168 Ma (SD=0.4) based on the nemesiid fossil *Cretamygale chasei* (Selden, 2002). Finally, the MRCA of Antrodiaetidae was

given a lognormal prior of (mean in real space) 168 Ma (SD=0.4) based on the fossil *Cretacattyma raveni* (Eskov & Zonstein, 1990). Two or more independent Markov Chain Monte Carlo (MCMC) searches were performed until a parameter effective sample size (ESS) >200 was achieved. ESS values were examined in Tracer v1.5. Independent runs for each partition were assembled with LogCombiner v1.7.5 and 10 % percent of generations were discarded as burn-in. Tree files for each partition where then uniformly sampled to obtain 10,000 trees. A total of 430,000 trees (10,000 trees from each partition) were assembled with LogCombiner v1.7.5 and a consensus tree was produced using TreeAnnotator v1.8.1. A chronogram containing all taxa was generated using a penalized likelihood method in r8s v1.8 (Sanderson, 2002). The 95 % highest posterior density dates obtained for the BEAST analysis were incorporated as constraints for node ages of the eight fossil calibrated nodes. The analysis was performed using the TN algorithm, cross validation of branch-length variation and rate variation modeled as a gamma distribution with an alpha shape parameter.

To detect diversification rate shifts, we performed a Bayesian analysis of diversification in BAMM (Bayesian Analysis of Macroevolutionary Mixtures; Rabosky et al., 2014). For this analysis we used the chronogram obtained by the r8s analysis in order to maximize taxon sampling. To account for non-random missing speciation events, we quantified the percentage of taxa sampled per family (World Spider Catalog, 2015) and incorporated these into the analysis. We also accounted for missing families sampled at various taxonomic levels. The MCMC chain was run for 100,000,000 generations, with sampling every 10,000 generations. Convergence diagnostics were examined using coda (Plummer et al., 2006) in R. Ten percent of the runs were discarded as burn-in. The 95 % credible set of shift configurations was plotted in the R package BAMMtools (Rabosky et al., 2014).

Character state reconstructions of web type following Blackledge et al. (2009) were performed using a maximum likelihood approach. The ML approach was implemented using the rayDISC command in the package corHMM (Beaulieu, O'Meara & Donoghue, 2013) in R (Ihaka & Gentleman, 1996). This method allows for multistate characters, unresolved nodes, and ambiguities (polymorphic taxa or missing data). Three models of character evolution were evaluated under the ML method: equal rates (ER), symmetrical (SYM) and all rates different (ARD). A likelihood-ratio test was performed to select among these varying models of character evolution.

Results:

Summary of Genomic Data

Twenty-one novel spider transcriptomes were sequenced, with an average of 72,487 assembled contigs (contiguous sequences) ranging from 6,816 (*Diguetia sp*.) to 191,839 (*Segestria sp.*); specimen data and transcriptome statistics for each sample are summarized in Supplemental Tables S1 and S2 respectively. Median contig length for the novel transcriptomes was 612 bp. The complete taxon set, including spider and outgroup transcriptomes from the SRA database, had an average contig number of 53,740 and a range of 5,158 (*Paratropis sp*.) to 202,311 (*Amaurobius ferox*) with a median contig length of 655. The newly constructed spider-specific core ortholog group (OG) set contained 4,934 OGs, more than three times the number of arthropod core orthologs used in a prior spider analysis Bond et al. (2014) and represents a significant step forward in generating a pool of reasonably well-vetted orthologs for spider phylogenomic analyses. The arthropod and spider core orthology sets had 749 groups in common; 4,185 OGs in the spider core were novel. Of the spider-core groups, 4,249 (86 %) were

present in the sequenced genome of our HaMStR reference taxon of choice *Acanthoscurria geniculata* (Sanggaard et al., 2014) and were retained for use in downstream ortholog detection. The number of TransDecoder predicted proteins and ortholog detection success for each taxon is summarized in Table S2. Annotations for the arthropod set can be found in Bond et al. (2014); Supplemental Table S3 summarizes gene annotations for the spider core ortholog set generated for this study. Our new HaMStR spider core ortholog set and *Acanthoscurria geniculata* BLAST database file can be downloaded from the Dryad Data Repository at doi:10.5061/dryad.6p072.

Phylogenetic Analyses

Seven super matrices were generated for downstream non time-calibrated analyses (Fig. 2), one drawn from the arthropod core set and six using the spider core set. Data set sizes, summarized in Table 2, ranged from a maximum of 3,398 OGs with a higher percentage of missing cells (38.5%), 850 OGs with 19.6% missing, to 549 OGs (arthropod core set) with 33% missing data. Two matrices were generated using automated filtering approaches implemented by BaCoCa (Kuck & Struck, 2014) and MARE (Meyer, Meusemann & Misof, 2011). In BaCoCa we sorted partitions using number of informative sites, capturing the top half (~1700 OGs) of the matrix containing the most informative sites. RCFV values generated by BaCoCa were <0.05 for all taxa in all partitions for each of the matrices, indicating homogeneity in base composition. Additionally, there was no perceptible taxonomic bias observed in shared missing data (Figs. S1-S6). The MARE optimized matrix comprised 58 taxa and 1,488 genes with 19.6% missing data. For graphical representations of gene occupancy for each matrix, see Figures S7-S12. Blast2GO (Conesa et al., 2005) gene ontology distributions of molecular function for OGs recovered from both the spider and arthropod ortholog sets (Figs. S13 and S14) can be found in the supplemental materials.

Our phylogenetic analyses (see Table 2 and Discussion), the results of which are summarized in Figure 2, consistently recover many well-supported monophyletic groups: Araneae, Mygalomorphae, Araneomorphae, Synspermiata (i.e., Haplogynae excluding Filistatidae and Leptonetidae), Entelegynae, the RTA clade, Dionycha, and Lycosoidea. Within Mygalomorphae, Atypoidina and Avicularioidea are monophyletic; Nemesiidae is polyphyletic. Filistatidae (*Kukulcania*) emerges as the sister group to *Hypochilus*. Interestingly, Leptonetidae emerges as the sister group to Entelegynae. Eresidae is sister to Araneoidea, similar to findings of Miller et al. (2010). Deinopoidea is polyphyletic. Oecobiidae is sister to Uloboridae, which are together sister to Deinopidae plus the RTA clade. Homalonychidae and by implication the entire Zodarioidea (Miller et al., 2010), is sister to Dionycha plus Lycosoidea. Hahniidae, represented by the cryphoecine *Calymmaria*, is sister to Dictynidae. Thomisidae belongs in Lycosoidea as proposed by Homann (1971) and Polotow, Carmichael & Griswold (2015) (see also Ramirez, 2014). Coalescent-based species-tree analysis in ASTRAL employed unrooted gene trees based on the 3,398 gene matrix as input and inferred a well-supported tree (most nodes >95 % bs; Fig. 3). With few exceptions the topology recovered using this approach was congruent with the likelihood-based supermatrix analysis. Conflicting nodes, some corresponding to key araneomorph lineages, which were moderately to weakly supported in concatenated analyses, are summarized in Figure 2.

A chronogram based on 43 partitions with no missing data (matrix 7, see Table 2) is shown in Figure 4. MRCA divergence time estimates are summarized in Table 3: Mesothelae - Opisthothelae at 340 Ma (95 % CI[287-398]); Mygalomorphae - Araneomorphae at 308 Ma (95 % CI[258-365]); Synspermiata + Hypochilidae - Entelegynae at 276 Ma (95 % CI[223-330]); RTA + Deinopoidea - *Stegodyphus* + Araneoidea at 214 Ma (95 % CI[154-280]); RTA -

Dionycha at 138.8 Ma (Fig. 4). Diversification rate shift analysis estimated three instances of significant diversification shifts within spiders (95 % credibility). The highest rate shift is within the RTA + Dionycha + Lycosoidea (Fig. 5) followed by Avicularioidea and within Araneoidea (f = 0.23; 0.21; Fig. 5).

Maximum likelihood ancestral state reconstruction of web type (Fig. 6) shows that the spider common ancestor likely foraged from a subterranean burrow, sometimes sealed by a trapdoor. The ancestral condition for araneomorphs may have been a stereotypical aerial sheet. Entelegynae ancestors probably spun orbs, which were subsequently lost at least three times. RTA taxa largely abandoned webs to become hunting spiders. Precise location of these character state shifts depends upon sufficient sampling; denser sampling reduces the number of unobserved evolutionary events. While this analysis contains only 47 of 114 spider families, the sequence and overall mapping to the spider backbone phylogeny is strongly supported.

Discussion:

Our phylogenomic analyses represent the largest assessment of spider phylogeny to date using genomic data, both in terms of taxa and number of orthologs sampled. Our results are largely congruent with earlier work (Bond et al., 2014): we recover all of the major backbone lineages (Mygalomorphae, Araneomorphae, RTA, etc.), but reiterate that our understanding of spider evolutionary pattern and process needs thorough reconsideration. This expanded study reinforces the ancient origin of the orb web hypothesis (Bond et al., 2014) and shows that rates of spider species diversification appear to be associated with web change or loss – or with modification of the male palp rather than the origin of the orb web. It shows that the Haplogynae are polyphyletic with Filistatidae as sister to Hypochilidae and Leptonetidae as sister to

Entelegynae. It also suggests a position for two enigmatic families – Hahniidae and Homalonychidae – and provides an alternate view of RTA relationships and the contents of Dionycha clade.

Data Characteristics and Development of Spider Core Orthologs

Transcriptome analyses are unquestionably data rich. Thousands of assembled sequences emerge from even modest RNA-seq experiments, providing, among other things, a basis for identifying phylogenetically informative orthologs. This bounty comes with a few caveats. Isoforms, paralogous sequences, and assembly artifacts (chimeric contigs) can mislead inference of single-copy orthologous genes. The data represent one snapshot – a specific organism, point in time, and combination of tissues – that can lead to gaps in downstream supermatrices due to stochastic sampling issues. Large amounts of missing data, due to missing loci and indels introduced during alignment, can arise post-assembly in the ortholog detection and filtering stages of phylogenomic analyses (Bond et al., 2014; Fernandez, Hormiga & Giribet, 2014). Lemmon et al. (2009) and a number of other authors (Roure, Baurain & Philippe, 2013; Dell'Ampio et al., 2014; Xia, 2014) have discussed the potential negative effects of such missing data in large phylogenomic (transcriptome-based) datasets. Recent studies argue that the phylogenetic signal from transcriptomes can conflict with alternative reduced representation approaches like targeted sequence capture (Jarvis et al., 2014; Brandley et al., 2015; Prum et al., 2015). From vast amounts of bird genome protein-coding data, Jarvis et al. (2014) concluded that these loci were not only insufficient (low support values), but also misleading due to convergence and high levels of incomplete lineage sorting during rapid radiations.

Simulation studies now predict that 10's-100's of loci will resolve most phylogenies, albeit sensitive to factors such as population size or speciation tempos (Knowles & Kubatko,

2011; Leache & Rannala, 2011; Liu & Yu, 2011). To mitigate the impacts of paralogy, incomplete lineage sorting, and missing data, we developed *a priori* a set of spider core orthologs that comprise a database consisting of over 4,500 genes that are expected to be recovered from most whole spider RNA extractions and are likely orthologous. We summarize the annotations for each of the genes in the HaMStR pHMM file in Supplemental table S3.

Our approach enhances repeatability, downstream assessment, scalability (taxon addition), and data quality. Studies that employ pure clustering approaches like OMA stand-alone (Altenhoff et al., 2013) may produce more data (i.e., more "genes") on the front end; however, they present some problems in terms of ease of scalability. Although adding more genes is one strategy, it is increasingly clear that taxon sampling and data quality are also very important (Lemmon & Lemmon, 2013; Bond et al., 2014).

A Modified View of Spider Evolution and Key Innovations

Once considered the "crowning achievement of aerial spiders" (Gertsch, 1979), the orb web and consequent adaptive radiation of araneoid spiders (ecribellate orb weavers and their relatives) captured the imagination of spider researchers for over a century. The evolution of adhesive threads and the vertical orientation of the orb web, positioned to intercept and retain flying insects, has been long considered a "key innovation" that allowed spiders to inhabit a new adaptive zone (Bond & Opell, 1998). It is important to note that several prior authors speculated about orb web adaptive value, such as Levi (1980), Opell (1979), Opell (1982), and Coddington (1986) although Bond & Opell (1998) quantified the pattern in a formal phylogenetic framework. Over 25 % of all spider species are araneoids. Given orb weaver monophyly on quantitative phylogenies (Griswold et al., 1998; Blackledge et al., 2009), rigorous empirical studies tended to confirm the orb as a prime cause of spider diversification (Bond & Opell, 1998). Nevertheless, a

lack of correlation of the orb web and species richness has been apparent for some time. Griswold et al. (1998) noted that over 50 % of Araneoidea no longer build recognizable orb webs and suggested that "the orb web has been an evolutionary base camp rather than a summit."

Bond et al. (2014) tested two alternative evolutionary scenarios for orb web evolution, reflecting different analytical results; parsimony implied multiple independent origins, and maximum likelihood implied one origin and subsequent multiple losses. The current study (Fig. 6) favors the latter: the orb evolves at the base of the araneoid + deinopoid + RTA clade, but is lost at least three times independently. Large amounts of morphological and behavioral data (albeit often correlated with features essential to the orb) still support the single origin hypothesis (Coddington, 1986; Coddington, 1991; Scharff & Coddington, 1997; Griswold et al., 1998; Agnarsson, Coddington & Kuntner, 2013). Our results suggest both that the orb web originated earlier than previously supposed, and that heretofore-unsuspected clades of spiders descend from orb weavers. In a sense, this ancient origin hypothesis reconciles the implications of genomic data with the classical evidence for multiple, homologous, complex, co-adapted character systems.

Recent discoveries of large, cribellate orb web-weaving taxa from the late Triassic agree with our molecular dates. Diverse Mesozoic deinopoids (Selden, Ren & Shih, 2015) are consistent with the "orb web node" at 213 Ma (Fig. 4, Table 3). Under this view, modern uloborids and deinopids are distinct remnants of this diverse group. Selden, Ren & Shih (2015) previously noted that if other extant taxa "emerged from the deinopoid stem or crown group it would render the whole-group Deinopoidea paraphyletic"; we discuss this scenario in detail below.

Contrary to the contemporary paradigm that the evolution of the orb web and adhesive sticky threads elevated rates of diversification among the araneoid spiders, our BAMM analysis (Fig. 5) indicates that the highest rates of diversification likely occurred among the RTA spiders followed by mygalomorphs and then araneoids as a distant third, the latter driven--in part--by the secondarily non-orb weaving theridiids and linyphiids. These results imply that other foraging strategies (e.g. cursorial hunting and irregular sheets) were a more "successful" strategy than the orb. Indeed, the point estimate for the RTA node during the early Cretaceous (138.8 Ma; Fig. 4 and Table 3) precedes the subsequent diversification of the RTA clade at 125-100 Ma.

This date coincides with the Cretaceous Terrestrial Revolution (KTR). Angiosperms radiated extensively at 125-90 Ma (Crane & Friis, 1987; Wang, Zhang & Jarezembowski, 2013), as did various plant-dependent insect lineages, including beetles (McKenna et al., 2009; McKenna et al., 2015), lepidopterans (Wahlberg, Wheat & Pena, 2013), ants (Moreau et al., 2006), and holometabolous insects in general (Misof et al., 2014), although some insect lineages do not show a pulse (e.g., darkling beetles; Kergoat et al., 2014). Spiders, as important insect predators, may also have diversified rapidly along with their prey (e.g., Penney, Wheater & Selden, 2003; Penalver, 2006; Selden & Penney, 2010). The fossil and phylogenomic data presented here show that most spider lineages predate the KTR (Selden & Penney, 2010; Bond et al., 2014). Among these, the RTA clade especially, but also mygalomorphs and araneoids, diversified in response to the KTR insect pulse. That aerial web spinners specialized on rapidly radiating clades of flying insects is hardly surprising. Similarly, if forest litter habitats became more complex and spurred insect diversification (Moreau et al., 2006), ground-dwelling spiders may also have diversified at unusual rates. Perhaps the most dramatic change in insect abundances occurred with the origin and early diversification of social insects that today

dominate animal biomass on the planet (Holldobler & Wilson, 1990) and beetles (McKenna et al., 2015). Both groups date back to 150-125 my and diversified during the KTR (LaPolla, Dlussky & Perrichot, 2013; Ward, 2014; Legendre et al., 2015). A major increase in these insect groups may have favoured spiders that feed on cursorial prey and thus could help explain the concurrent increase in diversification in the RTA clade, mygalomorphs, and non-orb weaving araneoids such as cobweb weavers (Dziki et al., 2015).

Taken together, this new evidence on character evolution, divergence estimates, and rates of diversification indicates that previous conclusions regarding the timing and rate of spider evolution were imprecise. Our data support an ancient orb web hypothesis that is further bolstered by a wealth of fossil data showing that a cribellate deinopoid stem group likely diversified during the early Mesozoic. Molecular divergence clock estimates are consistent with the placement of the orb web further down the tree as well as suggesting that some of the greatest rates of species diversification coincided with the KTR. The latter suggests that spiders took advantage of increased abundance of cursorial prey. These findings likely diminish the hypothesis proposed by Bond & Opell (1998) that the vertically oriented orb web represented a key innovation, particularly in light of the fact that over half of araneoid species do not build an orb web (e.g. Theridiidae and Linyphiidae; noted by Griswold et al., 1998; Fernandez, Hormiga & Giribet, 2014). We already knew that major orb web-weaving groups are very successful in spite of abandoning the orb (Blackledge et al., 2009).

Spider Systematics

Although our results show that many classical ideas in spider systematics require revision (e.g. mygalomorph families, Haplogynae, paleocribellates, higher araneoids, and RTA + dionychan lineages), they also robustly support many classical taxonomic concepts. Since Raven

(1985), Mygalomorphae (Table 1, Node 4) has continuously represented a challenge to spider systematics. As discussed by Hedin & Bond (2006) and Bond et al. (2012), nearly half the families are probably non-monophyletic. While our sampling here and previously (Bond et al., 2014) is far greater than any other published phylogenomic study (e.g., Fernandez, Hormiga & Giribet, 2014 included just one theraphosid), taxon sampling remains insufficient to address major issues aside from deeper level phylogenetic problems. However, the data (Fig. 2) support Euctenizidae as a monophyletic family, but not Nemesiidae. As indicated in Bond et al. (2014), the once controversial Atypoidina (Node 5) consistently has strong statistical support in all analyses. Alternatively, the placement of paratropidids, ctenizids, and idiopids remains questionable and warrants further sampling.

The traditional view of spider classification (Coddington, 2005) places Paleocribellatae and Austrochiloidea (Table 1) as sister groups to all the remaining Araneomorphae taxa – Haplogynae and Entelegynae; the latter terms are used primarily herein as clade names rather than specific reference to genitalic condition. Our current tree (Fig. 2) is congruent with Bond et al. (2014) in placing Paleocribellatae (Table 1, *Hypochilus*); Fig. 1, Node 9) as sister to Haplogynae. Filistatidae (*Kukulcania*), which is placed as sister to the ecribellate haplogynes (Synspermiata lineage as proposed in Michalik & Ramirez, 2014), pairs with *Hypochilus* as in Bond et al. (2014). This arrangement suggests that characters formerly considered "primitive" to araneomorphs, for example, mobile leg three cribellate silk carding, might instead be a synapomorphy for the new hypochilid-filistatid clade. Remaining haplogyne relationships are somewhat congruent with previously published analyses (Ramirez, 2000; Michalik & Ramirez, 2014). However, one of the more intriguing results is the placement of the morphologically intermediate "haplogyne" (Table 1) *Calileptoneta* (Leptonetidae) as sister to Entelegynae,

suggesting that leptonetids may represent intermediate genitalic forms between haplogyne and the relatively more complex entelegyne condition (Ledford & Griswold, 2010). As outlined by Ledford & Griswold (2010), a number of previous analyses (Platnick et al., 1991; Ramirez, 2000; Griswold et al., 2005) discussed the "rampant" homoplasy required to place leptonetids (sister to Telemidae) among haplogynes and suggest two possible scenarios – leptonetids are proto-entelegynes, or they are the sister group to the remaining Haplogynae. Our phylogenomic analyses support the former hypothesis favored by Ledford & Griswold (2010), and puts the discovery of the cribellate *Archoleptoneta* into better phylogenetic context. Additionally, these results provide further support for the concept of Synspermiata as proposed by Michalik & Ramirez (2014) and represent a robust phylogenetic framework for understanding the evolution of entelegyne genitalia.

Our reconstruction of araneoid relationships departs dramatically from the traditional classification scheme and a number of recently published molecular systematic studies (e.g., Blackledge et al., 2009; Dimitrov et al., 2012). Theridiidae (cobweb spiders) is sister to the remaining araneoids as opposed to occupying a more derived position within that clade. Comparisons to Dimitrov et al. (2012) should be viewed with caution: that analysis contained a large suite of taxa not included here, and many results of that analysis had only weak support. Nevertheless, our phylogenomic data agree in supporting the close relationship between Mysmenidae, Mimetidae, and Tetragnathidae. We also retain the more inclusive linyphioids as close relatives of Araneidae + Nephilidae as in Dimitrov et al. (2012). Unlike that study, we recover nesticids sister to linyphioids (Pimoidae plus Linyphiidae) rather than theridiids: Theridioid (Theridiidae and Nesticidae) diphyly is a surprising result, which has already been shown with standard markers by Agnarsson, Coddington & Kuntner (2013). Theridioids have

strikingly similar spinning organs and tarsus IV comb for throwing silk, but are otherwise genitalically distinct. Clearly relationships among the derived araneoids require more intensive sampling, especially of missing families (Theridiosomatidae, Malkaridae, Anapidae, etc.) to adequately resolve their phylogeny.

The addition of nearly 30 terminals to the Bond et al. (2014) dataset corroborates the non-monophyly of the classically defined Orbiculariae, although the orb and its behavioral, morphological, and structural constituents may be homologous. Deinopoidea, with these data, is polyphyletic (see also Dimitrov et al., 2012). Instead, a new clade, Uloboridae + Oecobiidae, is sister to Deinopidae + the RTA clade. Bootstrap support was consistently low for the node dividing these two groupings in all analyses except matrix 6 (Fig. 2), which omits the eresid exemplar *Stegodyphus* and matrix 8, the ASTRAL analysis. The placement of the two eresoid taxa (Table 1), *Stegodyphus* and *Oecobius* continues to present difficulties here as in previous published phylogenomic studies (Miller et al., 2010). Fernandez, Hormiga & Giribet (2014) found alternative placements for *Oecobius* whereas Bond et al. (2014) typically recovered *Stegodyphus* as the sister group to all entelegynes (recovered here as the sister group to araneoids) and *Oecobius* as a member of a clade comprising uloborid and deinopid exemplars, but with notably lower support. Disparities between the two analyses may be attributed to differences in taxon sampling. On the other hand, increased taxon sampling across the tree diminished node support in some places. However, it is worth noting that support was very strong in the ASTRAL species tree analysis, suggesting that while there may be some conflict among individual data partitions there is an overwhelming amount of signal in the data for a Deinopoidea + RTA relationship. This trend was noted by Bond et al. (2014) who found that only 2.4 % of all bootstrap replicates recovered a monophyletic Orbiculariae. Based on these

data and the putative rapid diversification that occurred once the orb web was abandoned, it is clear that resolving relationships at this point in spider evolutionary history remains a challenge. Finally, Bond et al. (2014) and Agnarsson, Coddington & Kuntner (2013) recovered an unexpected relationship between eresoid taxa and deinopoids that consistently rendered the Deinopoidea paraphyletic or polyphyletic if *Oecobius* was included in the analysis. Our results, here including an additional uloborid exemplar, still confirm Deinopoidea polyphyly. Perhaps careful examination of *Oecobius* web morphology and spinning behavior may provide independent corroboration of this molecular signal.

Although all of our analyses recover a monophyletic RTA clade, relationships among its members reflect some departure from the traditional view of RTA phylogeny but are largely consistent with a more recent morphology-based study. We recover a clade that comprises a mix of agelenoids (Agelenidae, Desidae, and Amphinectidae) as a sister group to Dictynidae + Hahniidae and Amaurobiidae. The taxonomic composition of Dictynidae, Hahniidae and Amaurobiidae, as well as their phylogenetic placement, remains problematic and in a state of flux (Coddington, 2005; Spagna, Crews & Gillespie, 2010; Miller et al., 2010). The typical hahniine hahniids have been difficult to place due to their long branches (Spagna & Gillespie, 2008, Miller et al., 2010). *Calymmaria*, has been moved into "Cybaeidae s.l." by Spagna Crews & Gillespie (2010), suggesting that the relationships among hahniids, cybaeids, and dictynids need further scrutiny.

Amaurobiids have also been hard to place, though this is in part because Amaurobiidae are a moving target. The term "Amaurobiids" needs to be clarified, as most of nine subfamilies discussed in Lehtinen (1967) are now placed elsewhere. We use *Callobius*, from the type subfamily of the family. Our amaurobiid placement, basal to an agelenoid and dictynoid

grouping corroborates previous findings (Miller et al., 2010; Spagna, Crews & Gillespie, 2010). Dictynids on the other hand were considered one of the unresolved sister groups to amaurobioids, zodarioids, and dionychans (Spagna, Crews & Gillespie, 2010). Here the placement of our dictynid exemplar *Cicurina* is more precise: sister group to the hahniid *Calymmaria* (as in Miller et al., 2010).

We also recover Homalonychidae (representing Zodarioidea) as the sister group to dionychans and lycosoids, once again, mirroring the results of Agnarsson, Coddington & Kuntner (2013). Previously Zodarioidea was placed closer to the base of the RTA clade (Miller et al., 2010). Dionychans here include salticids, anyphaenids, corinnids, and gnaphosids whereas crab spiders (Thomisidae) nest with the lycosoids containing a paraphyletic Pisauridae. Placement of Thomisidae within Lycosoidea goes back at least to Homann (1971) and was formally established by Bayer & Schonhofer (2013) and the total evidence analysis of Polotow, Carmichael & Griswold, 2015). Although Ramirez (2014) placed Thomisidae outside of Lycosoidea, in one of his slightly suboptimal results thomisids were included in Lycosoidea. The relationships we recover among dionychan and lycosoid taxa are largely congruent with those inferred by Ramirez (2014) in a massive morphological study of Dionycha and RTA exemplars. Given the general incongruence among previous morphological and molecular spider systematic studies, it will be interesting to see how Ramirez (2014) phylogeny and familial-level reevaluations compare as phylogenomic studies expand. Raven (1985) was a landmark study for mygalomorphs; perhaps Ramirez (2014) may serve in the same capacity for one of the most diverse branches on the spider tree of life.

Conclusions:

Following Coddington & Levi (1991), higher-level spider classification underwent a series of challenges from quantitative studies of morphology, producing provocative but weakly-supported hypotheses (Griswold et al., 1998; Griswold et al., 2005). Total evidence studies, for example, Wood, Griswold & Gillespie (2012a; Wood et al. (2012b) for Palpimanoidea, Polotow, Carmichael & Griswold (2015) for Lycosoidea, and Bond et al. (2012) for Mygalomorphae appear to have settled some local arrangements, but much of the backbone of the spider tree of life remains an open question only to be solved through increased taxon sampling. Phylogenomics has already brought data-rich, convincing solutions to long standing controversies, for example, phylogeny of the orb web (Bond et al., 2014; Fernandez, Hormiga & Giribet, 2014). Phylogenomics portends a new and exciting period for spider evolutionary biology. Recent advances in digital imaging, proteomics, silk biology and major fossil discoveries mean that our understanding of spider evolution will likely accelerate by leaps and bounds in the coming years. The tempo and mode of spider evolution is likely different than previously thought. At this point it seems reasonably clear that the orb web evolved earlier phylogenetically than previously thought, only to be subsequently lost at least three times independently during the Cretaceous. While the orb web has certainly been successful, a likely dramatic increase in the abundances of cursorial insects during the KTR, also impacted the success of other foraging strategies, including webless hunting. Our results and that of others like Ramirez (2014) show that spider systematics remains a work in progress with many questions yet to be answered.

Data Availability:

Illumina transcriptome sequence data are available from the NCBI short read archive (SRA) as BioProject PRJNA306047 (accession numbers SAMN04453329-SAMN04453350). Phylogenomics data matrices were deposited on 5 February 2016 in the Dryad Digital Repository at doi:10.5061/dryad.6p072. Supplemental Figures are available online with the publication: https://doi.org/10.7717/peerj.1719/supp-1 - https://doi.org/10.7717/peerj.1719/supp-19.

References:

Agnarsson I, Coddington JA, Kuntner M. 2013. Systematics—progress in the study of spider diversity and evolution. In: Penney D, ed. Spider research in the 21st century: trends and perspectives. Manchester: Siri Scientific Press, 58–111.

Altenhoff AM, Gil M, Gonnet GH, Dessimoz C. 2013. Inferring hierarchical orthologous groups from orthologous gene pairs. PLoS ONE 8(1):e53786 DOI 10.1371/journal.pone.0053786.

Altschul SF, Gish W, Miller W, Myers EW, Lipman DJ. 1990. Basic local alignment search tool. Journal of Molecular Biology 215:403–410 DOI 10.1016/S0022-2836(05)80360-2.

Bayer S, Schönhofer AL. 2013. Phylogenetic relationships of the spider family psechridae inferred from molecular data, with comments on the lycosoidea (arachnida: Araneae). Invertebrate Systematics 27(1):53–80 DOI 10.1071/IS12017.

Beaulieu JM, O'Meara BC, Donoghue MJ. 2013. Identifying hidden rate changes in the evolution of a binary morphological character: the evolution of plant habit in campanulid angiosperms. Systematic Biology 62(5):725–737 DOI 10.1093/sysbio/syt034.

Blackledge TA, Kuntner M, Agnarsson I. 2011. The form and function of spider orb webs: evolution from silk to ecosystems. In: Casas J, ed. Advances in insect physiology. Vol. 41. Burlington: Academic Press, 175–262.

Blackledge TA, Scharff N, Coddington JA, Szüts T, Wenzel JW, Hayashi CY, Agnarsson I. 2009. Reconstructing web evolution and spider diversification in the molecular era. Proceedings of the National Academy of Sciences of the United States of America 106(13):5229–5234 DOI 10.1073/pnas.0901377106.

Bond JE, Garrison NL, Hamilton CA, Godwin RL, Hedin M, Agnarsson I. 2014. Phylogenomics resolves a spider backbone phylogeny and rejects a prevailing paradigm for orb web evolution. Current Biology 24(15):1765–1771 DOI 10.1016/j.cub.2014.06.034.

Bond JE, Hendrixson BE, Hamilton CA, Hedin M. 2012. A reconsideration of the classification of the spider infraorder mygalomorphae (arachnida: Araneae) based on three nuclear genes and morphology. PLoS ONE 7(6):e38753 DOI 10.1371/journal.pone.0038753.

Bond JE, Opell BD. 1998. Testing adaptive radiation and key innovation hypotheses in spiders. Evolution 52(2):403–414 DOI 10.2307/2411077.

Brandley MC, Bragg JG, Singhal S, Chapple DG, Jennings CK, Lemmon AR, Lemmon EM, Thompson MB, Moritz C. 2015. Evaluating the performance of anchored hybrid enrichment at the tips of the tree of life: a phylogenetic analysis of Aus- tralian Eugongylus group scincid lizards. BMC Evolutionary Biology 15(62) DOI 10.1186/s12862-015-0318-0.

Coddington J. 1986. The monophyletic origin of the orb web. In: Shear W, ed. Spiders: webs, behavior, and evolution. Stanford, California: Stanford University Press, 319–363.

Coddington JA. 1991. Cladistics and spider classification: araneomorph phylogeny and the monophyly of orbweavers (Araneae: Araneomorphae; Orbiculariae). Acta Zoologica Fennica 190:75–87.

Coddington JA. 2005. Phylogeny and classification of spiders. In: Ubick P, Paquin P, Cushing P, Roth V, eds. Spiders of North America: an identification manual. American Arachnological Society, 18–24.

Coddington JA, Levi HW. 1991. Systematics and evolution of spiders (Araneae). Annual Review of Ecology and Systematics 22:565–592 DOI 10.1146/annurev.es.22.110191.003025.

Conesa A, Götz S, García-Gómez JM, Terol J, Talón M, Robles M. 2005. Blast2go: a universal tool for annotation, visualization and analysis in functional genomics research. Bioinformatics 21(18):3674–3676 DOI 10.1093/bioinformatics/bti610.

Crane P. 1987. The origin of angiosperms and their biological consequences. In: Friis E, Chaloner W, Crane P, eds. Vegetational consequences of the angiosperm diversification. Cambridge: Cambridge University Press, 105–144.

Dell'Ampio E, Meusemann K, Szucsich NU, Peters RS, Meyer B, Borner J, Petersen M, Aberer AJ, Stamatakis A, Walzl MG, Minh BQ, Von Haeseler A, Ebersberger I, Pass G, Misof B. 2014. Decisive data sets in phylogenomics: lessons from studies on the phylogenetic relationships of primarily wingless insects. Molecular Biology and Evolution 31(1):239–249 DOI 10.1093/molbev/mst196.

Dicko C, Porter D, Bond J, Kenney JM, Vollrath F. 2008. Structural disorder in silk proteins reveals the emergence of elastomericity. Biomacromolecules 9(1):216–221 DOI 10.1021/bm701069y.

Dimitrov D, Lopardo L, Giribet G, Arnedo MA, Alvarez-Padilla F, Hormiga G. 2012. Tangled in a sparse spider web: single origin of orb weavers and their spinning work unravelled by denser taxonomic sampling. Proceedings of the Royal Society B: Biological Sciences 279(1732):1341–1350 DOI 10.1098/rspb.2011.2011.

Drummond AJ, Ho S Y W, Phillips MJ, Rambaut A. 2006. Relaxed phylogenetics and dating with confidence. PLoS Biology 4(5):e88 DOI 10.1371/journal.pbio.0040088.

Drummond AJ, Rambaut A. 2007. BEAST: Bayesian evolutionary analysis by sampling trees. BMC Evolutionary Biology 7(1):214 DOI 10.1186/1471-2148-7-214.

Drummond AJ, Suchard MA, Xie D, Rambaut A. 2012. Bayesian phylogenetics with BEAUti and the BEAST 1.7. Molecular Biology and Evolution 29(8):1969–1973 DOI 10.1093/molbev/mss075.

Dziki A, Binford G, Coddington JA, Agnarsson I. 2015. Spintharus flavidus in the caribbean–a 30 million year biogeographical history and radiation of a 'widespread species'. PeerJ PrePrints 3:e1639 DOI 10.7287/peerj.preprints.1332v1.

Ebersberger I, Strauss S, Von Haeseler A. 2009. HaMStR: profile hidden markov model based search for orthologs in ESTs. BMC Evolutionary Biology 9(1):157 DOI 10.1186/1471-2148-9-157.

Eddy SR. 2011. Accelerated profile HMM searches. PLoS Computational Biology 7(10):e1002195 DOI 10.1371/journal.pcbi.1002195.

Eskov KY, Zonstein S. 1990. First Mesozoic mygalomorph spiders from the Lower Cretaceous of Siberia and Mongolia, with notes on the system and evolution of the infraorder Mygalomorphae (Chelicerata: Araneae). Neues Jahrbuch für Geologie und Paläontologie, Abhandlungen 178:325–368.

Fernández R, Hormiga G, Giribet G. 2014. Phylogenomic analysis of spiders reveals nonmonophyly of orb weavers. Current Biology 24(15):1772–1777 DOI 10.1016/j.cub.2014.06.035.

Garb J. 2013. Spider silk: an ancient biomaterial for the 21st century. In: Penney D, ed. Spider research in the 21st century: trends and perspectives. Manchester, UK: Siri Scientific Press, 252–281.

Gertsch WJ. 1979. American spiders. Second edition. New York: Van Nostrand Reinhold Co.

Grabherr MG, Haas BJ, Yassour M, Levin JZ, Thompson DA, Amit I, Adiconis X, Fan L, Raychowdhury R, Zeng Q, Chen Z, Mauceli E, Hacohen N, Gnirke A, Rhind N, Di Palma F, Birren BW, Nusbaum C, Lindblad-Toh K, Friedman N, Regev A. 2011. Full-length transcriptome assembly from RNA-Seq data without a reference genome. Nature Biotechnology 29(7):644–652 DOI 10.1038/nbt.1883.

Griswold CE, Coddington JA, Hormiga G, Scharff N. 1998. Phylogeny of the orb-web building spiders (Araneae, Orbiculariae: Deinopoidea, Araneoidea). Zoological Journal of the Linnean Society 123(1):1–99 DOI 10.1111/j.1096-3642.1998.tb01290.x.

Griswold CE, Ramírez M, Coddington J, Platnick N. 2005. Atlas of phylogenetic data for entelegyne spiders (Araneae: araneomorphae: Entelegynae), with comments on their phylogeny. Procceedings of the California Academy of Sciences 56:1–324.

Haas BJ, Papanicolaou A, Yassour M, Grabherr M, Blood PD, Bowden J, Couger MB, Eccles D, Li B, Lieber M, MacManes MD, Ott M, Orvis J, Pochet N, Strozzi F, Weeks N, Westerman R, William T, Dewey CN, Henschel R, LeDuc RD, Friedman N, Regev A. 2013. De novo transcript sequence reconstruction from RNA-seq using the Trinity platform for reference generation and analysis. Nature Protocols 8(8):1494–1512 DOI 10.1038/nprot.2013.084.

Hedin M, Bond JE. 2006. Molecular phylogenetics of the spider infraorder Mygalo- morphae using nuclear rRNA genes (18s and 28s): conflict and agreement with the current system of classification. Molecular Phylogenetics and Evolution 41(2):454–471 DOI 10.1016/j.ympev.2006.05.017.

Homann H. 1971. Die Augen der Araneae. Zeitschrift für Morphologie der Tiere 69(3):201–272 DOI 10.1007/BF00277623.

Hormiga G, Griswold CE. 2014. Systematics, phylogeny, and evolution of orb-weaving spiders. Annual Review of Entomology 59(1):487–512 DOI 10.1146/annurev-ento-011613-162046.

Hölldobler B, Wilson EO. 1990. The ants. Cambridge: Belknap Press.

Ihaka R, Gentleman R. 1996. R: a language for data analysis and graphics. Journal of Computational and Graphical Statistics 5(3):299–314.

Jarvis ED, Mirarab S, Aberer AJ, Li B, Houde P, Li C, Ho SY, Faircloth BC, Nabholz B, Howard JT, Suh A, Weber CC, Da Fonseca RR, Li J, Zhang F, Li H, Zhou L, Narula N, Liu L, Ganapathy G, Boussau B, Bayzid MS, Zavidovych V, Subramanian S, Gabaldon T, Capella-Gutierrez S, Huerta-Cepas J, Rekepalli B, Munch K, Schierup M, Lindow B, Warren WC, Ray D, Green RE, Bruford MW, Zhan X, Dixon A, Li S, Li N, Huang Y, Derryberry EP, Bertelsen MF, Sheldon FH, Brumfield RT, Mello CV, Lovell PV, Wirthlin M, Schneider MPC, Prosdocimi F, Samaniego JA, Velazquez AMV, Alfaro-Nunez A, Campos PF, Petersen B, Sicheritz-Ponten T, Pas A, Bailey T, Scofield P, Bunce M, Lambert DM, Zhou Q, Perelman P, Driskell AC, Shapiro B, Xiong Z, Zeng Y, Liu S, Li Z, Liu B, Wu K, Xiao J, Yinqi X, Zheng Q, Zhang Y, Yang H, Wang J, Smeds L, Rheindt FE, Braun M, Fjeldsa J, Orlando L, Barker FK, Jonsson KA, Johnson W, Koepfli K-P, O'Brien S, Haussler D, Ryder OA, Rahbek C, Willerslev E, Graves GR, Glenn TC, McCormack J, Burt D, Ellegren H, Alstrom P, Edwards SV, Stamatakis A, Mindell DP, Cracraft J, Braun EL, Warnow T, Jun W, Gilbert MTP, Zhang G. 2014. Whole-genome analyses resolve early branches in the tree of life of modern birds. Science 346(6215):1320–1331 DOI 10.1126/science.1253451.

Katoh K. 2005. MAFFT version 5: improvement in accuracy of multiple sequence alignment. Nucleic Acids Research 33(2):511–518 DOI 10.1093/nar/gki198.

Kergoat GJ, Soldati L, Anne-Laure C, Jourdan H, Jabbour-Zahab R, Genson G, Bouchard P, Condamine FL. 2014. Higher level molecular phylogeny of darkling beetles (Coleoptera: Tenebrionidae): Darkling beetle phylogeny. Systematic Entomol- ogy 39(3):486–499 DOI 10.1111/syen.12065.

King GF, Hardy MC. 2013. Spider-venom peptides: structure, pharmacology, and potential for control of insect pests. Annual Review of Entomology 58(1):475–496 DOI 10.1146/annurev-ento-120811-153650.

Knowles LL, Kubatko LS. 2011. Estimating species trees: practical and theoretical aspects. John Wiley and Sons.

Kocot KM, Cannon JT, Todt C, Citarella MR, Kohn AB, Meyer A, Santos SR, Schander C, Moroz LL, Lieb B, Halanych KM. 2011. Phylogenomics reveals deep molluscan relationships. Nature 477(7365):452–456 DOI 10.1038/nature10382.

Kocot ML, Citarella M, Halanych K. 2013. PhyloTreePruner: a phylogenetic tree-based approach for selection of orthologous sequences for phylogenomics. Evolutionary Bioinformatics 9:429–435 DOI 10.4137/EBO.S12813.

Kozlov AM, Aberer AJ, Stamatakis A. 2015. ExaML version 3: a tool for phy- logenomic analyses on supercomputers. Bioinformatics 31(15):2577–2579 DOI 10.1093/bioinformatics/btv184.

Kück P. 2009. ALICUT: a Perlscript which cuts ALISCORE identified RSS. version, 2. Bonn, Germany: Department of Bioinformatics, Zoologisches Forschungsmuseum A. Koenig (ZFMK).

Kück P, Meusemann K. 2010. FASconCAT: convenient handling of data matrices. Molec- ular Phylogenetics and Evolution 56(3):1115–1118 DOI 10.1016/j.ympev.2010.04.024.

Kück P, Struck TH. 2014. BaCoCa—a heuristic software tool for the parallel assessment of sequence biases in hundreds of gene and taxon partitions. Molecular Phylogenetics and Evolution 70:94–98 DOI 10.1016/j.ympev.2013.09.011.

LaPolla JS, Dlussky GM, Perrichot V. 2013. Ants and the fossil record. Annual Review of Entomology 58(1):609–630 DOI 10.1146/annurev-ento-120710-100600.

Leache AD, Rannala B. 2011. The accuracy of species tree estimation under simulation: a comparison of methods. Systematic Biology 60(2):126–137 DOI 10.1093/sysbio/syq073.

Ledford JM, Griswold CE. 2010. A study of the subfamily Archoleptonetinae (Araneae, Leptonetidae) with a review of the morphology and relationships for the Leptoneti- dae. Zootaxa 2391:1–32.

Legendre F, Nel A, Svenson GJ, Robillard T, Pellens R, Grandcolas P. 2015. Phylogeny of dictyoptera: dating the origin of cockroaches, praying mantises and termites with molecular data and controlled fossil evidence. PLoS ONE 10(7):e0130127 DOI 10.1371/journal.pone.0130127.

Lehtinen PT. 1967. Classification of the cribellate spiders and some allied families, with notes on the evolution of the suborder Araneomorpha. In: Annales zoologici fennici. Societas Zoologica Botanica Fennica Vanamo, 199–468.

Lemmon AR, Brown JM, Stanger-Hall K, Lemmon EM. 2009. The effect of ambiguous data on phylogenetic estimates obtained by maximum likelihood and Bayesian inference. Systematic Biology 58(1):130–145 DOI 10.1093/sysbio/syp017.

Lemmon EM, Lemmon AR. 2013. High-throughput genomic data in systematics and phylogenetics. Annual Review of Ecology, Evolution, and Systematics 44(1):99–121 DOI 10.1146/annurev-ecolsys-110512-135822.

Levi HW. 1980. Orb-webs: primitive or specialized. In: Gruber J,ed. Proceedings of the 8th international congress of arachnology, 367–370.

Li L, Stoeckert CJ, Roos DS. 2003. OrthoMCL: identification of ortholog groups for eukaryotic genomes. Genome Research 13(9):2178–2189 DOI 10.1101/gr.1224503.

Liu L, Yu L. 2011. Estimating species trees from unrooted gene trees. Systematic Biology 60(5):661–667 DOI 10.1093/sysbio/syr027.

McKenna DD, Sequeira AS, Marvaldi AE, Farrell BD. 2009. Temporal lags and overlap in the diversification of weevils and flowering plants. Proceedings of the National Academy of Sciences of the United States of America 106(17):7083–7088 DOI 10.1073/pnas.0810618106.

Mckenna DD, Wild AL, Kanda K, Bellamy CL, Beutel RG, Caterino MS, Farnum CW, Hawks DC, Ivie MA, Jameson ML, Leschen RAB, Marvaldi AE, Mchugh JV, Newton AF, Robertson JA, Thayer MK, Whiting MF, Lawrence JF, lipiski A, Maddison DR, Farrell BD. 2015. The beetle tree of life reveals that coleopteran survived end-permian mass extinction to diversify during the cretaceous terrestrial revolution. Systematic Entomology 40(4):835–880 DOI 10.1111/syen.12132.

Meyer B, Meusemann K, Misof B. 2011. MARE: MAtrix REduction—a tool to select optimized data subsets from supermatrices for phylogenetic inference. Bonn (Germany): Zentrum fuur molekulare Biodiversitätsforschung (zmb) am ZFMK . Version 01.2-rc. Available at http:// mare.zfmk.de.

Michalik P, Ramírez MJ. 2014. Evolutionary morphology of the male reproductive system, spermatozoa and seminal fluid of spiders (Araneae, Arachnida) – Current knowledge and future directions. Arthropod Structure & Development 43(4):291–322 DOI 10.1016/j.asd.2014.05.005.

Miller JA, Carmichael A, Ramírez MJ, Spagna JC, Haddad CR, Řezáč M, Johan- nesen J, Král J, Wang X-P, Griswold CE. 2010. Phylogeny of entelegyne spi- ders: Affinities of the family Penestomidae (NEW RANK), generic phylogeny of Eresidae, and asymmetric rates of change in spinning organ evolution (Araneae, Araneoidea, Entelegynae). Molecular Phylogenetics and Evolution 55(3):786–804 DOI 10.1016/j.ympev.2010.02.021.

Mirarab S, Reaz R, Bayzid MS, Zimmermann T, Swenson MS, Warnow T. 2014. ASTRAL: genome-scale coalescent-based species tree estimation. Bioinformatics 30(17):i541–i548 DOI 10.1093/bioinformatics/btu462.

Misof B, Liu S, Meusemann K, Peters RS, Donath A, Mayer C, Frandsen PB, Ware J, Flouri T, Beutel RG, Niehuis O, Petersen M, Izquierdo-Carrasco F, Wappler T, Rust J, Aberer AJ,

Aspock U, Aspock H, Bartel D, Blanke A, Berger S, Bohm A, Buckley TR, Calcott B, Chen J, Friedrich F, Fukui M, Fujita M, Greve C, Grobe P, Gu S, Huang Y, Jermiin LS, Kawahara AY, Krogmann L, Kubiak M, Lanfear R, Letsch H, Li Y, Li Z, Li J, Lu H, Machida R, Mashimo Y, Kapli P, McKenna DD,

Meng G, Nakagaki Y, Navarrete-Heredia JL, Ott M, Ou Y, Pass G, Podsiadlowski L, Pohl H, Von Reumont BM, Schutte K, Sekiya K, Shimizu S, Slipinski A, Stamatakis A, Song W, Su X, Szucsich NU, Tan M, Tan X, Tang M, Tang J, Timelthaler G, Tomizuka S, Trautwein M, Tong X, Uchifune T, Walzl MG, Wiegmann BM, Wilbrandt J, Wipfler B, Wong TKF, Wu Q, Wu G, Xie Y, Yang S, Yang Q, Yeates DK, Yoshizawa K, Zhang Q, Zhang R, Zhang W, Zhang Y, Zhao J, Zhou C, Zhou L, Ziesmann T, Zou S, Li Y, Xu X, Zhang Y, Yang H, Wang J, Wang J, Kjer KM, Zhou X. 2014. Phylogenomics resolves the timing and pattern of insect evolution. Science 346(6210):763–767 DOI 10.1126/science.1257570.

Misof B, Misof K. 2009. A monte carlo approach successfully identifies randomness in multiple sequence alignments: a more objective means of data exclusion. Systematic Biology 58(1):21–34 DOI 10.1093/sysbio/syp006.

Moreau CS, Bell CD, Vila R, Archibald SB, Pierce NE. 2006. Phylogeny of the ants: diversification in the age of angiosperms. Science 312(5770):101–104 DOI 10.1126/science.1124891.

Opell B. 1979. Revision of the genera and tropical American species of the spider family Uloboridae. Revisión de los géneros de las especies americanas tropicales de arañas de la familia Uloboridae. Bulletin of the Museum of Comparative Zoology 148(10):443–549.

Opell BD. 1982. Post-hatching development and web production of Hyptiotes cavatus (Hentz) (Araneae, Uloboridae). Journal of Arachnology 10:185–191.

Peñalver E. 2006. Early cretaceous spider web with its prey. Science 312(5781):1761–1761 DOI 10.1126/science.1126628.

Penney D, Ortuño VM. 2006. Oldest true orb-weaving spider (Araneae: Araneidae). Biology Letters 2(3):447–450 DOI 10.1098/rsbl.2006.0506.

Penney D, Wheater CP, Selden PA. 2003. Resistance of spiders to Cretaceous-Tertiary extinction events. Evolution 57(11):2599–2607.

Platnick NI, Coddington JA, Forster RR, Griswold CE. 1991. Spinneret morphology and the phylogeny of haplogyne spiders (Araneae, Araneomorphae). American Museum noviates 3016:1–76.

Plummer M, Best N, Cowles K, Vines K. 2006. CODA: Convergence diagnosis and output analysis for MCMC. R News 6(1):7–11.

Polotow D, Carmichael A, Griswold CE. 2015. Total evidence analysis of the phylo- genetic relationships of Lycosoidea spiders (Araneae, Entelegynae). Invertebrate Systematics 29(2):124 DOI 10.1071/IS14041.

Price MN, Dehal PS, Arkin AP, et al. 2010. FastTree 2-approximately maximum- likelihood trees for large alignments. PLoS ONE 5(3):e9490 DOI 10.1371/journal.pone.0009490.

Prum RO, Berv JS, Dornburg A, Field DJ, Townsend JP, Lemmon EM, Lemmon AR. 2015. A comprehensive phylogeny of birds (Aves) using targeted next-generation DNA sequencing. Nature 526(7574):569–573 DOI 10.1038/nature15697.

Rabosky DL, Donnellan SC, Grundler M, Lovette IJ. 2014. Analysis and Visualization of Complex Macroevolutionary Dynamics: an example from Australian Scincid Lizards. Systematic Biology 63(4):610–627 DOI 10.1093/sysbio/syu025.

Ramírez MJ. 2000. Respiratory system morphology and the phylogeny of haplogyne spiders (Araneae, Araneomorphae). Journal of Arachnology 28(2):149–157 DOI 10.1636/0161-8202(2000)028[0149:RSMATP]2.0.CO;2.

Ramírez MJ. 2014. The morphology and phylogeny of dionychan spiders (Araneae: Araneomorphae). Bulletin of the American Museum of Natural History 390(1):1–374 DOI 10.1206/821.1.

Raven RJ. 1985. The Spider Infraorder Mygalomorphae (Araneae): Cladistics and systematics. Bulletin of the American Museum of Natural History 182(1):1–184.

Rice P, Longden I, Bleasby A, et al. 2000. EMBOSS: the European molecular biology open software suite. Trends in genetics 16(6):276–277 DOI 10.1016/S0168-9525(00)02024-2.

Roure B, Baurain D, Philippe H. 2013. Impact of missing data on phylogenies inferred from empirical phylogenomic data sets. Molecular Biology and Evolution 30(1):197–214 DOI 10.1093/molbev/mss208.

Saez NJ, Senff S, Jensen JE, Er SY, Herzig V, Rash LD, King GF. 2010. Spider-venom peptides as therapeutics. Toxins 2(12):2851–2871 DOI 10.3390/toxins2122851.

Sanderson MJ. 2002. Estimating absolute rates of molecular evolution and diver- gence times: a penalized likelihood approach. Molecular Biology and Evolution 19(1):101–109 DOI 10.1093/oxfordjournals.molbev.a003974.

Sanggaard KW, Bechsgaard JS, Fang X, Duan J, Dyrlund TF, Gupta V, Jiang X, Cheng L, Fan D, Feng Y, Han L, Huang Z, Wu Z, Liao L, Settepani V, Thøgersen IB, Vanthournout B, Wang T, Zhu Y, Funch P, Enghild JJ, Schauser L, Andersen SU, Villesen P, Schierup MH, Bilde T, Wang J. 2014. Spider genomes provide insight into composition and evolution of venom and silk. Nature Communications 5(3765) DOI 10.1038/ncomms4765.

Schacht K, Scheibel T. 2014. Processing of recombinant spider silk proteins into tailor- made materials for biomaterials applications. Current Opinion in Biotechnology 29:62–69 DOI 10.1016/j.copbio.2014.02.015.

Scharff N, Coddington JA. 1997. A phylogenetic analysis of the orb-weaving spider family Araneidae (Arachnida, Araneae). Zoological Journal of the Linnean Society 120(4):355–434 DOI 10.1111/j.1096-3642.1997.tb01281.x.

Selden PA. 1996. First fossil mesothele spider, from the Carboniferous of France. Revue suisse de Zoologie 2:585–596.

Selden PA. 2002. First British Mesozoic spider, from Cretaceous amber of the Isle of Wight, southern England. Palaeontology 45:973–983 DOI 10.1111/1475-4983.00271.

Selden PA, Anderson JM, Anderson HM, Fraser NC. 1999. Fossil araneomorph spiders from the Triassic of South Africa and Virginia. Journal of Arachnology 27:401–414.

Selden PA, Gall J-C. 1992. A Triassic mygalomorph spider from the northern Vosges, France. Palaeontology 35:211–235.

Selden PA, Penney D. 2010. Fossil spiders. Biological Reviews 85(1):171–206. Selden PA, Ren D, Shih C. 2015. Mesozoic cribellate spiders (araneae: Deinopoidea) from china. Journal of Systematic Palaeontology 14:1–26.

Selden PA, Shih C, Ren D. 2013. A giant spider from the Jurassic of China reveals greater diversity of the orbicularian stem group. Naturwissenschaften 100(12):1171–1181 DOI 10.1007/s00114-013-1121-7.

Spagna JC, Crews SC, Gillespie RG. 2010. Patterns of habitat affinity and Austral/Hol- arctic parallelism in dictynoid spiders (Araneae:Entelegynae). Invertebrate Systematics 24(3):238–257 DOI 10.1071/IS10001.

Spagna JC, Gillespie RG. 2008. More data, fewer shifts: Molecular insights into the evo- lution of the spinning apparatus in non-orb-weaving spiders. Molecular Phylogenetics and Evolution 46(1):347–368 DOI 10.1016/j.ympev.2007.08.008.

Stamatakis A. 2014. RAxML version 8: a tool for phylogenetic analysis and post-analysis of large phylogenies. Bioinformatics 30(9):1312–1313 DOI 10.1093/bioinformatics/btu033.

Starrett J, Garb JE, Kuelbs A, Azubuike UO, Hayashi CY. 2012. Early events in the evolution of spider silk genes. PLoS ONE 7(6):e38084 DOI 10.1371/journal.pone.0038084.

Wahlberg N, Wheat CW, Peña C. 2013. Timing and patterns in the taxonomic di- versification of Lepidoptera (Butterflies and Moths). PLoS ONE 8(11):e80875 DOI 10.1371/journal.pone.0080875.

Wang B, Zhang H, Jarzembowski EA. 2013. Early Cretaceous angiosperms and beetle evolution. Frontiers in Plant Science 4(360):1–6 DOI 10.3389/fpls.2013.00360.

Ward PS. 2014. The phylogeny and evolution of ants. Annual Review of Ecology, Evolu- tion, and Systematics 45(1):23–43 DOI 10.1146/annurev-ecolsys-120213-091824.

Wood HM, Griswold CE, Gillespie RG. 2012a. Phylogenetic placement of pelican spiders (Archaeidae, Araneae), with insight into evolution of the ‘‘neck’’ and predatory behaviours of the superfamily Palpimanoidea. Cladistics 28(6):598–626 DOI 10.1111/j.1096-0031.2012.00411.x.

Wood HM, Matzke NJ, Gillespie RG, Griswold CE. 2012b. Treating fossils as terminal taxa in divergence time estimation reveals ancient vicariance patterns in the palpi- manoid spiders. Systematic Biology 62(2):264–284.

World Spider Catalog. 2015. World spider catalog . Version 17.0. Natural History Museum Bern. Available at http:// wsc.nmbe.ch.

World Spider Catalog. 2016. World spider catalog . Version 17.0. Natural History Museum Bern. Available at http:// wsc.nmbe.ch.

Xia X. 2014. Phylogenetic bias in the likelihood method caused by missing data coupled with among-site rate variation: an analytical approach. In: Hutchison D, Kanade, T, Kittler J, Kleinberg JM, Kobsa A, Mattern F, Mitchell JC, Naor M, Nierstrasz O, Pandu Rangan C, Steffen B, Terzopoulos D, Tygar D, Weikum G, Basu M, Pan Y, Wang J, eds. Bioinformatics research and applications. vol. 8492. Cham: Springer International Publishing, 12–23.

Table 1: Major spider lineages referenced throughout text. Superscripts (column 1) reference node labels in Fig. 1 (summary of family level relationships).

Lineage	Composition and placement	Description/characteristics
[1] Araneae	All spiders	Cosmopolitan; cheliceral venom glands, ability to produce silk from abdominal silk glands; male pedipalps modified for sperm transfer
[2] Mesothelae	Plesiomorphic sister group to all living spiders	SE Asia; mid ventrally positioned spinnerets; distinct dorsal abdominal tergites, very narrow sternum
[3] Opisthothelae	The two major spider lineages	Typical terminal spinneret placement and sternal morphology
[4] Mygalomorphae	Trapdoor, baboon and funnel spiders, tarantulas, and their kin	Paraxial chelicerae with venom glands; most lead sedentary lives in burrows; lack anterior median spinnerets; often large and hirsute; two pairs of book lungs
[5] Atypoidina	Sister group to remaining mygalomorphs	Most species with vestigial abdominal tergites and unique modifications to male pedipalp
[6] Avicularoidea	All remaining mygalomorph taxa	Includes major mygalomorph families, nearly half of which are likely not monophyletic
[7] Theraphosoidina	Comprises families Theraphosidae and Barychelidae	Includes the typically large and hirsute tarantulas and baboon spiders
[8] Araneomorphae	Over 90% of all spider diversity	Anterior median spinnerets fused to form a cribellum (later lost multiple times)
[9] Paleocribellatae	Comprises single family Hypochilidae; hypothesized sister group to all other araneomorphs	Hypochilid synapomorphies, e.g., cheliceral depression; also retain a number of primitive traits including two pairs of booklungs
Neocribellatae	Remaining spider lineages	Paracribellum (complimentary spinning field to cribellum); extension of venom gland into prosoma
Austrochiloidea	Families Austrochilidae and Gradungulidae; sister group to all other neocribellate lineages	Gondwanan taxa with notched tarsal organs; typically with two pairs of booklungs–posterior pair modified as tracheae in some taxa
[10] Haplogynae	Neocribellate lineage with simple genitalia; includes spitting spiders and cellar spiders	Spinnerets lack tartipores; mating with palps inserted simultaneously; in some taxa female genital opening lacks an epigynum; chelicerae fused at base, synspermia, male palpal organ simple
[11] Entelegynae	Comprises all remaining spider lineages with complex genitalia	Female genitalia with a flow through system of separate copulatory and fertilization ducts; male palpal organ typically under hydraulic control
Palpimanoidea	Comprises a number of enigmatic families	Araneophages with lateral scopulae on anterior legs
Eresoidea	Includes 3 families: Eresidae, Hersiliidae, Oecobiidae; sister to remaining entelegynes	Controversial superfamily; oecobiids and hersiliids share a unique attack behavior
Orbiculariae	Comprises the Deinopoidea and Araneoidea	Members of this lineage include cribellate and ecribellate orb-web weavers as well as derived araneoids that use adhesive threads to construct sheet and cob-webs
Deinopoidea	Includes the cribellate orbicularian families Uloboridae and Deinopidae	Construct cribellate orb web; long considered sister group to adhesive orb web weavers on basis of behavioral web construction data
[12] Araneoidea	Spider superfamily that includes adhesive orb web weaving taxa and others	Members of this lineage all use adhesive threads; monophyly supported by a number of spinning and other morphological characteristics
[13] RTA	Large diverse lineage of spiders that includes wolf, jumping, running, fishing, and crab spiders	Defined primarily by the presence of a projection on the male palp–the retrolateral tibial apophysis (RTA)
[14] Dionycha	Subclade of the RTA lineage, comprises about 1/3 of all spider diversity	Defined as a group based on their two clawed condition with flanking tufts of setae for adhesion to smooth surfaces
Lycosoidea	Large superfamily comprising 10 families including fishing and wolf spiders	Monophyly of this superfamily is based on a number of morphological features (not universal) including a grate-shaped tapetum, an oval-shaped calamistrum, and male palpal features

Table 2: Summary of all phylogenomic analyses. Data matrix numbers correspond to Fig. 2, inset.

Data set	#OGs	#AAs	% missing	#reps	Log likelihood	Notes
(1) All genes	3,398	696,652	38.5%	225	−20949310.821967	ExaML AUTOF
(2) 1st reduce	1,699	410,717	26.0%	300	−14297508.033111	ExaML AUTOF
(3) 2nd reduce	850	230,582	19.6%	300	−8098715.107390	ExaML AUTOF
(4) BCC	1,699	311,756	33.6%	300	−10017456.343941	ExaML AUTOF
(5) Arthropod core OG	549	107,307	33.0%	1,000	−2729523.038858	ExaML AUTOF bs in RAxML
(6) 74 taxa (-Stegodyphus)	3,398	629,566	38.8%	300	−20569138.970981	ExaML AUTOF
(7) MARE (58 taxa, 55 ingroup)	1,488	351,333	19.6%	295	−9227466.065087	ExaML AUTOF
(8) ASTRAL	3,398			100		100 bootstrap reps per partition

Table 3: Posterior probabilities (PP), ages (Ma), and 95% confidence intervals (CI) for the highest posterior density (HPD) recovered by the BEAST analysis. Node numbers correspond to Fig. 5. Node numbers in bold correspond to numbers in Fig. 1 and Table 1.

Node	Age	HPD 95% CI	Taxonomic group
1	340	287–398	Araneae
3	309	258–365	Opistothele
4	261	218–307	Mygalomorphae
5	108	49–192	Atypoidina
6	114	57–197	Avicularoidea
7	47	2–125	Theraphosoidina
8	276	223–330	Opistothelae
10	190	121–262	Haplogynae
11	214	154–280	Entelegynae
12	170	114–233	Araneoidea
13	139	83–201	RTA
14	86	40–139	Dionycha
15	218	53–389	
16	37	2–109	
17	79	18–163	
18	162	85–257	
19	93	47–151	
20	71	25–127	
21	48	35–217	Ctenizidae
22	232	165–299	
23	160	49–254	
24	158	85–232	
25	101	28–179	
26	81	23–148	Pholcidae
27	197	137–263	
28	92	26–172	Theridiidae
29	148	96–208	
30	127	75–186	
31	100	44–160	
32	64	15–123	Tetragnathidae
33	130	81–186	
34	107	52–165	
35	76	25–131	
36	94	49–149	
37	61	22–116	Araneidae
38	33	29–312	
39	41	33–420	
40	191	134–258	
41	152	64–228	

Table 3: continued

42	21	28–126	Uloboridae
43	174	117–242	
44	112	60–174	
45	44	4–113	
46	92	44–149	
47	74	29–126	
48	47	34–243	
49	120	68–182	
50	104	57–160	
51	71	28–121	
52	52	36–130	
53	70	28–120	Lycosoidea
54	50	35–735	
55	49	15–93	
56	37	27–211	

Figure 1: Summary, preferred tree, of spider relationships based on phylogenomic analyses shown in Figure 2. Numbers at nodes correspond to superscripts in Table 1. Images in descending order: Scorpion, Mesothelae, Antrodiaetidae, Paratropopididae, Ctenizidae, Pholcidae, Scytodidae, Theridiidae, Tetragnathidae, Nephilidae (male and female), Uloboridae, Oecobiidae, Agelenidae, Salticidae, Lycosidae, Oxyopidae.)

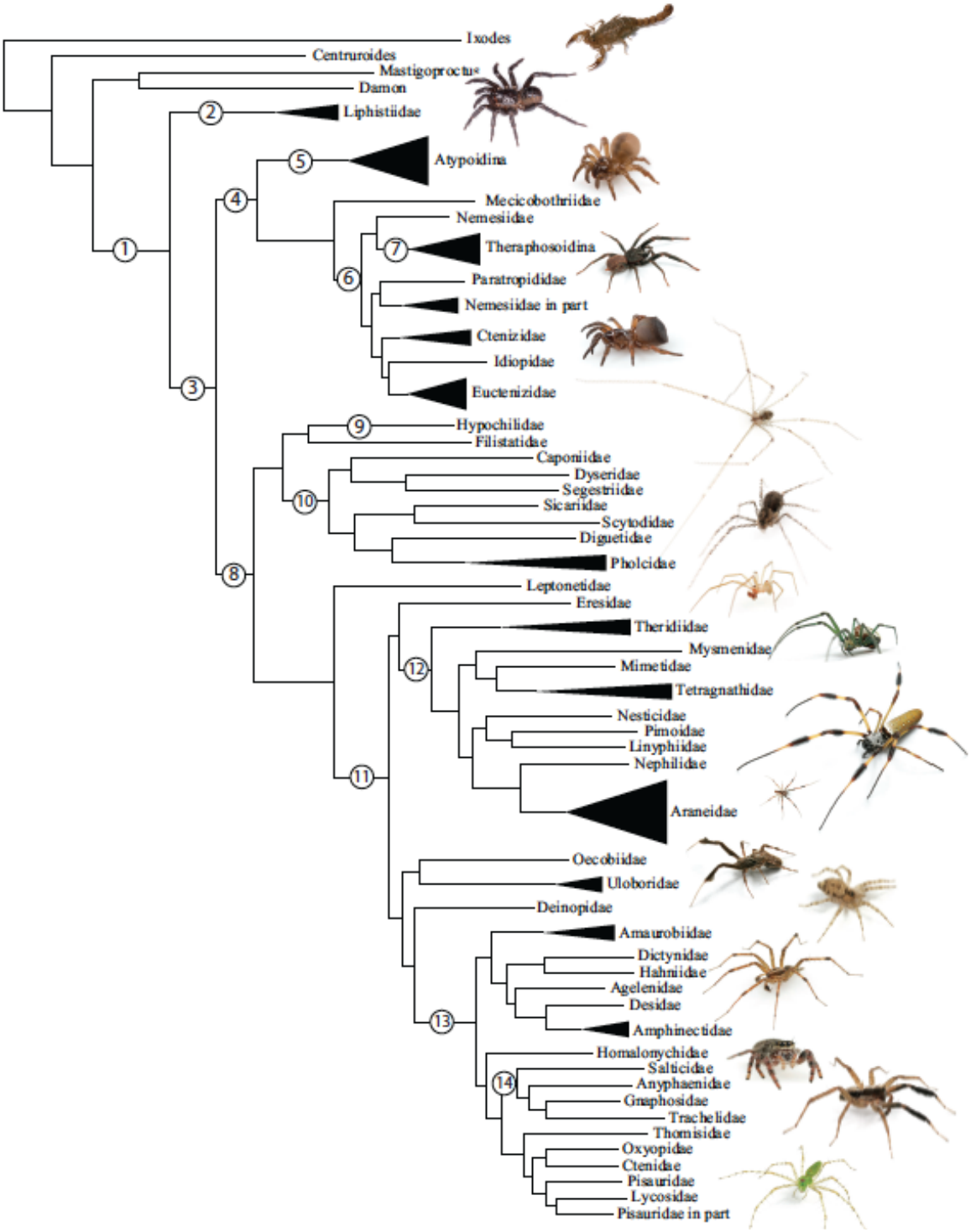

Figure 2: Summary of phylogenomic analyses (different matrices outlined in Table 2) on the phylogenetic hypothesis based on ExaML analysis of dataset 1 (3,398 OGs). Box plots indicate bootstrap value ranges for each node across matrices 1-7; single solid blocks indicate bootstrap
values of 100 % in all analyses.)

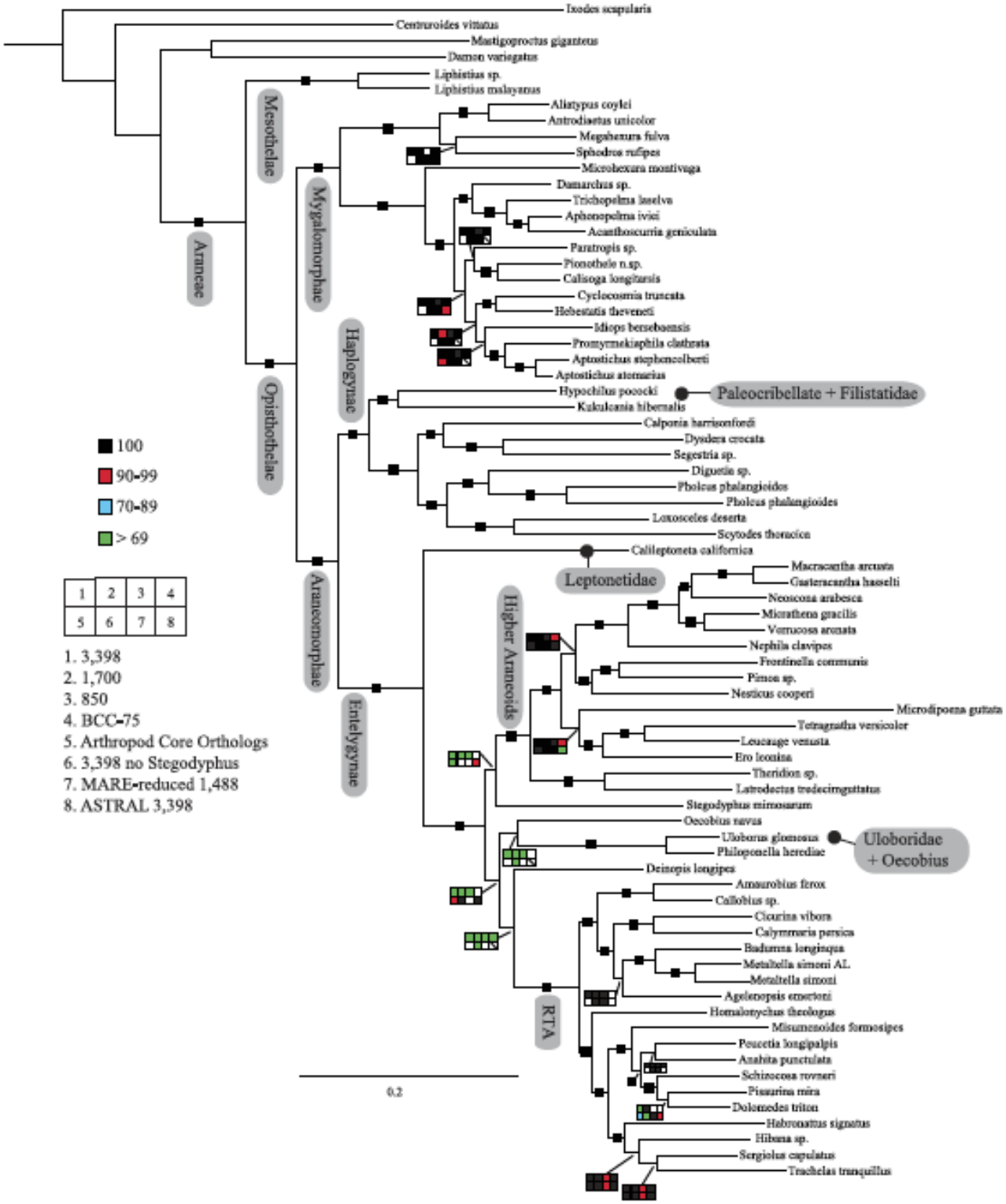

Figure 3: ASTRAL gene tree analysis of spider relationships based on 3,398 genes. Relative support value ranges reported at each node (inset legend); red stars indicate branches not congruent with tree shown in Figs. 1, 2.

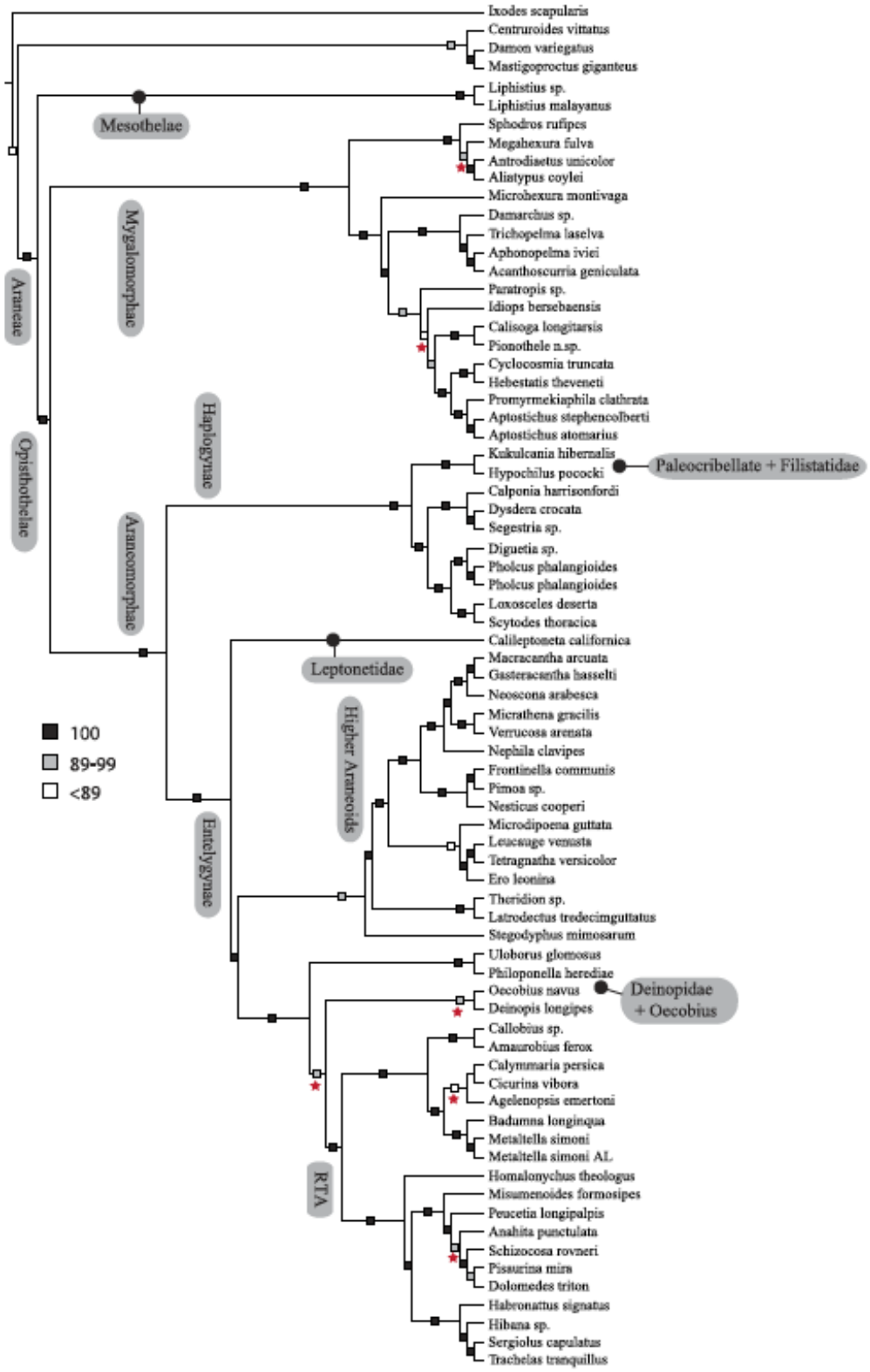

Figure 4: Chronogram resulting from two Bayesian MCMC runs performed in BEAST showing estimated divergence time for major spider lineages. Time scale on x axis; node point estimates and 95 % confidence intervals (blue bars) are reported in Table 2.

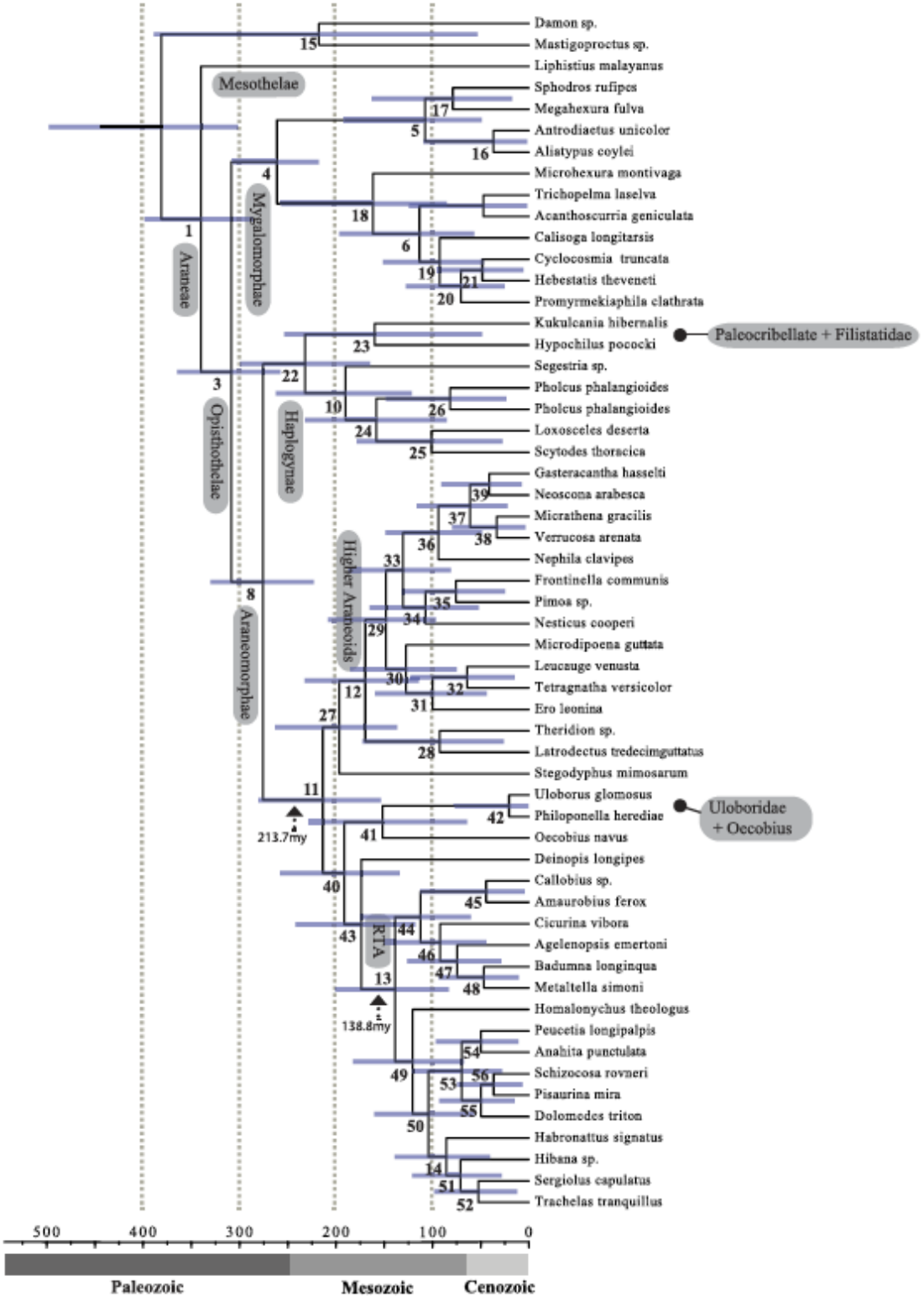

Figure 5: Time-calibrated phylogeny of spiders with branches colored by reconstructed net diversification rates (left). Rates on branches are means of the marginal densities of branch-specific rates. Inset histogram (lower left) shows posterior density of speciation rates. Smaller phylogenies (top right) show the four distinct shift configurations with the highest posterior probability. For each distinct shift configuration, the locations of rate shifts are shown as red (rate increases) and blue (rate decreases) circles, with circle size proportional to the marginal probability of the shift. The macroevolutionary cohort analysis (lower right) displays the pairwise probability that any two species share a common macroevolutionary rate dynamic. Dashed arrow indicates position of RTA clade.

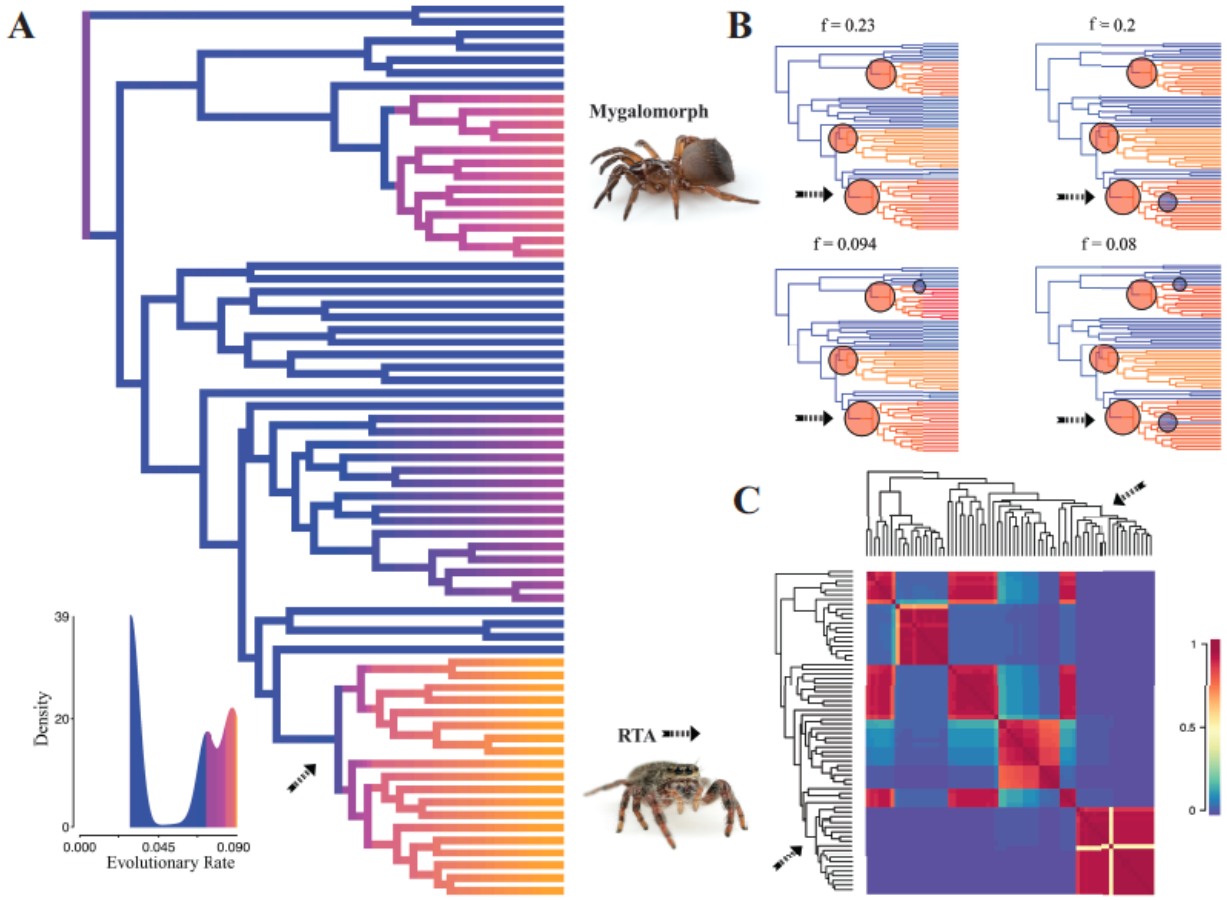

Figure 6: ML ancestral state reconstructions of web type on the time-calibrated phylogeny of spiders. Circle areas correspond to probability of ancestral states. The arrow points to one of the main diversification rate shifts reconstructed by BAMM at the MRCA of Entelegynae excluding Leptonetidae

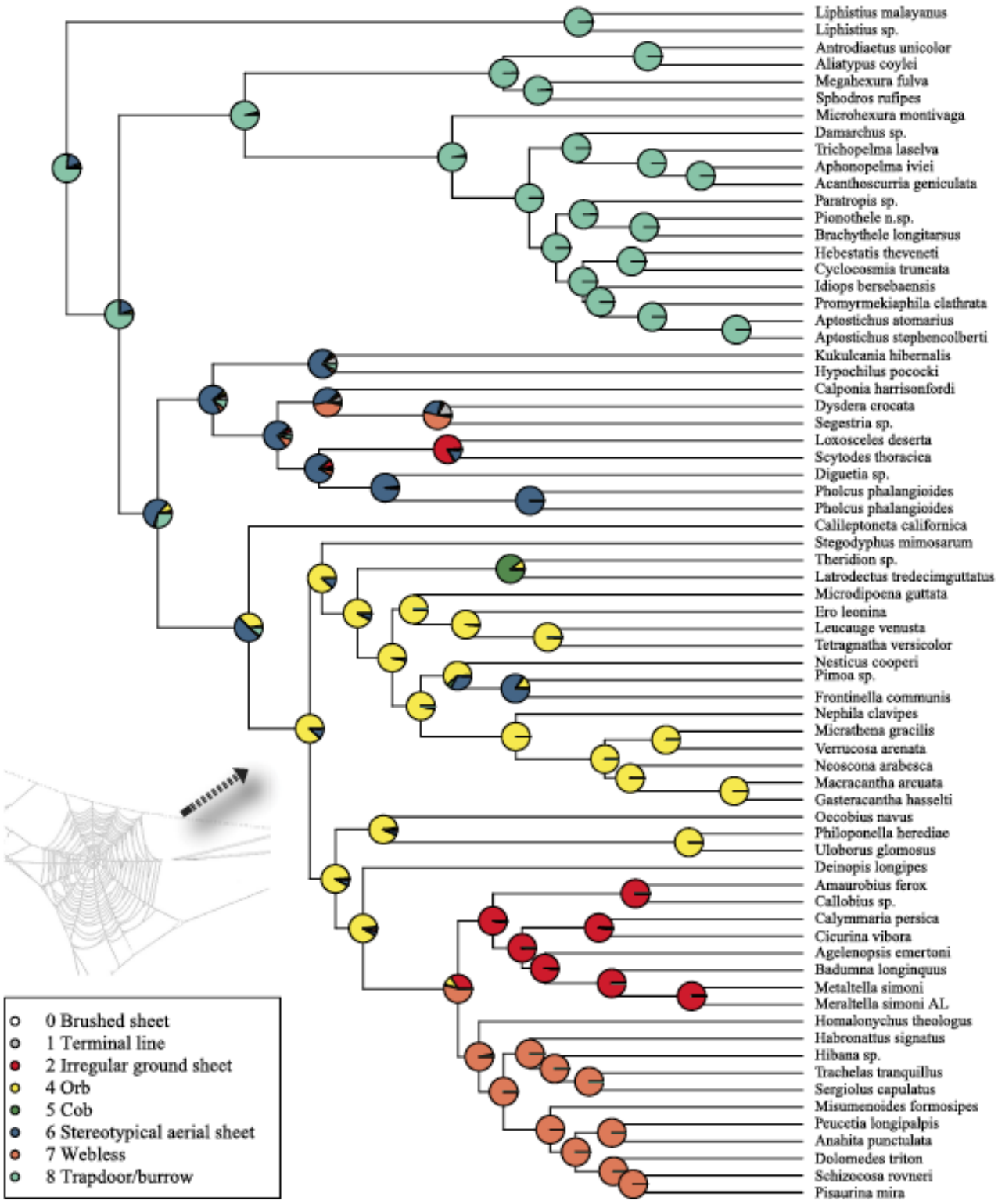

Chapter II

Evaluating Species Boundaries in the *Aptostichus atomarius* species complex

Introduction:

The trapdoor spider genus *Aptostichus* currently comprises 41 species, distributed widely throughout the California Floristic Province (CFP) with disjunct populations in Nevada, Arizona and Mexico (Bond, 2012; Valdez & Roldan, 2016). Like other spiders in the suborder Mygalomorphae *Aptostichus* are long-lived predators (15-30 years, 5 to reach maturity) that construct and inhabit silk lined burrows. *Aptostichus* species form a cryptic trapdoor from layers of silk and substrate, which covers the burrow entrance – providing protection as well as a predatory advantage. This engineering feat allows *Aptostichus* to occupy a diversity of habitats. These species occur on roadside slopes, ravines, and hillsides with variable substrate types in ecosystems ranging from alpine forests to coastal dunes. When undisturbed, these sedentary spiders leave their burrow at most twice; adult males venture out to find female burrows during seasonal reproductive periods and juvenile spiders disperse from their mothers' burrow. When present at a locality, they can form dense colonies (multiple conspecific burrows per square foot), and are often syntopic with other Mygalomorph genera.

Within the genus, the *Aptostichus atomarius* species complex exemplifies the kind of cryptic diversity found with increasing regularity in Mygalomorph spiders (e.g., Hendrixson & Bond, 2005; Hamilton, Formanowicz & Bond, 2011; Starrett et al., 2018), other arthropod systems (Bickford et al., 2007; Daniels et al., 2009; Nicholls et al., 2010), and other genera subject to the CFP's complex geologic history (Calsbeek et al.,2003; Myers et al., 2014). Current members of the complex (*A. atomarius*, *A. stanfordianus*, *A. stephencolberti*, *A. miwok*, *A.*

angelinajolieae, and *A. dantrippi*) have been established through an integrative delimitation method, which incorporated geographic and ecological aspects of the system with genetic structure (Bond &Stockman, 2008; Bond, 2012). Despite any discernable divergence in morphological characters traditionally used to define mygalomorph spider species (e.g. sexual and secondary sexual characters), this group displays very high levels of pairwise mtDNA genetic divergence (Bond & Stockman, 2008). Mitochondrial genetic structuring is unambiguous, largely tracking geographic boundaries as would be expected of organisms with low female vagility. Though compelling evidence for the independence of these lineages has been established, support for phylogenetic relationships between *atomarius* complex species is still weak at deeper nodes (Bond, 2012). Current delimitation within the group relies heavily on mitochondrial gene tree topology (12S-16S region); though supplemented with limited sampling of the nuclear rRNA Internal Transcribed Spacer unit (Bond & Stockman, 2008) and later improved with broader sampling across the distribution (Bond, 2012) species diagnoses within the complex primarily reflect patterns of mitochondrial inheritance and evolution. The extent to which single gene trees, particularly those derived from mitochondrial DNA, reflect the broader genomic history of this complex remains unclear.

Increasing efficiency and availability of genomic approaches has created a pathway for researchers of non-model organisms to overcome limitations of mitochondrial only or single gene tree analyses (Ellegren, 2014). For a fraction of the time and capital required to generate individual gene trees via traditional sequencing methods, high-throughput driven, multi-locus datasets can be obtained and used to estimate a species tree. Both higher-level systematic analyses (Misof et al., 2014, Prum et al., 2015) and delimitation efforts at the species/population level have benefited (Pease et al., 2016, Domingos et al., 2017). The two loci-generating

methods employed here, genotyping-by-sequencing (GBS; Elshire et al., 2011) and Anchored Hybrid Enrichment (AHE; Lemmon, Emme & Lemmon, 2012), sample from different, independent, genomic constituents. GBS applies a restriction enzyme based method to digest genomic DNA and sample single nucleotide polymorphisms (SNPs) from across the genome. These data are particularly useful for initial detection of genetic structure via unguided clustering analysis and the generation of species hypotheses (discovery), which can be validated through independent analyses. AHE leverages taxon specific probes to sequence highly conserved regions of genomic sequence and variably divergent flanking regions. This method can generate hundreds of deeply sequenced loci for large numbers of samples, useful when resolving relationships at multiple phylogenetic scales (e.g. Brandley et al., 2015; Young et al., 2016). In this study, AHE loci form the basis of phylogenomic reconstruction, validation via BPP (Bayesian Phylogenetics and Phylogeography; Yang, 2015), and refinement of species boundaries – specifically, model-based exploration of contemporary and historic gene flow between species using PHRAPL (Phylogeographic Inference using Approximate Likelihoods; Jackson et al., 2017).

Though providing an enormous amount of raw material for establishing the existence and extent of genetic lineages, these data have their own limitations and considerations. Single gene trees disagree, sometimes in remarkable ways, with the estimated species tree reflecting the complex interaction of micro and macroevolutionary forces (Degnan & Rosenberg, 2009). Consolidation of divergent gene histories under the multi-species coalescent can require substantial computational power when many species and large numbers of loci are considered; as a result, many heuristic approaches have been developed (Nakleh, 2013). Striking a balance between analyses of additional loci, adequate population/species sampling, and independent lines

of evidence (e.g. geography, ecology, behavior) can be challenging, but it is crucial if a truly integrative approach to species delimitation is to be achieved. In pursuit of this ideal, we take a discovery/validation approach to molecular delimitation building upon integrative systematic strategies employed elsewhere (Hedin, Carlson & Coyle, 2015; Wachter et al., 2015) which combine independent methods for 1) generating species hypotheses (through clustering or phylogenetic analysis) and 2) validating species hypotheses (using spedeSTEM, BPP or other statistical evaluation of competing hypotheses). We employ genetic methods of clustering and multi-locus phylogenetic analysis from a broader sample of the *Aptostichus* genome, evaluating the concordance (or lack thereof) between nuclear loci and the previously resolved mitochondrial gene tree and validate our species hypotheses using BPP. Lastly, we attempt to expand the integrative approach to include the possibility of male-dispersal mediated gene flow using the program PHRAPL, refining the extent and permeability of species boundaries within the *A. atomarius* complex.

Materials and Methods:

Samples were selected such that each species in the atomarius complex had representatives spanning its known distribution (Fig 1). Geographic considerations were balanced with sample availability and minimum requirements (sample number/population and DNA quality) for each type of genetic analysis performed. Given the multi-step integrative approach applied, initial sampling was foundational to later genomic analysis; the samples used in the GBS protocol guided the sampling scheme used in the AHE analysis. When possible, the same samples, or individuals collected at the same localities, were used for both the GBS and AHE sequencing protocols to allow

for comparison of the two approaches. Additionally, many of the same individuals used in Bond and Stockman (2008) were included when preserved tissue was available. Overlap between the two genomic data types detailed herein can be found in Table 1.

DNA was extracted from preserved leg tissue (90% Ethanol or RNAlater) using the Qiagen DNeasy Kit, and assessed for sufficient yield and quality. High molecular weight genomic DNA was sent either to the Institute for Genomic Diversity at Cornell University (GBS protocol, n=47) or the Center for Anchored Phylogenomics at Florida State University (AHE protocol, n=40 + 3 outgroup taxa) for library preparation and sequencing. Details of the specific genomic sequencing methods are as follows.

GBS Sequencing and Filtering

GBS for non-model organisms such as *Aptostichus* requires an initial optimization of a single sample to select an appropriate restriction enzyme set. In this case a single enzyme, EcoT22I, was chosen as sample digestion with this 6-base cutter yielded a distribution of fragment sizes suitable for Illumina sequencing (<500bp). Samples were plated in a 48-plex design (47 individuals in duplicate on a 96 well plate) and digested. Unique barcode adapters were ligated to each sample to allow for pooling during sequencing and downstream demultiplexing. Illumina sequencing adapters were annealed to DNA fragments, and the pooled samples were sequenced on a single flowcell lane of the Illumina HiSeq 2000 platform (50 bp, SE reads). Since no suitable reference genome was available for mygalomorph spiders, raw sequences were processed using the Universal Network Enabled Analysis Kit (UNEAK; Lu et al., 2013), an analysis pipeline for non-model organisms implemented in TASSEL v3.0 (Bradbury, 2007). In lieu of a reference genome, the UNEAK pipeline first trims and aligns reads to each other, collapsing them into sequence tags. Tags differing at only one site are then

identified and those forming complex networks with each other are filtered out as they likely represent sequencing errors, paralogs, or repetitive sequences. Importantly, UNEAK employs an error tolerance rate parameter of 0.3 during the network analysis phase to account for the expected Illumina sequencing error rate, allowing only highly covered reciprocal tag pairs to remain. This process results in a series of file types representing different filtering levels and merge methods, specifically vcf and HapMap files that have either been merged by taxon and/or by SNP site. The unfiltered SNP and taxon merged HapMap file from this output was subjected to filtering prior to analysis; TASSEL (v5.2.27) was used to further minimize missing sites in the data. Three filtered datasets, varying in proportion of missing sites (10, 20, and 30%) were generated and converted into the STRUCTURE input file format in preparation for downstream analyses.

Species/Population Discovery

GBS derived SNPs were used in two similar clustering analyses – a Bayesian admixture analysis in STRUCTURE (Pritchard, 2000, Falush et al., 2003) and an analysis in the R package LEA (Frichot & François, 2015) that uses a cross-entropy criterion to estimate the number of ancestral populations given a genomic matrix. An admixture model with correlated allele frequencies was selected in STRUCTURE. For each filtered dataset, twenty replicate runs were generated (100,000 burn-in generations followed by 1,000,000 MCMC runs) for values of K ranging from 2 to 8. The replicated runs for each dataset were then evaluated using the program StructureHarvester (Earl, 2012) to determine the optimal value for K. Alignment and summary of clusters across replicates for the optimal K value was determined by the program CLUMPP (Jakobsson, 2007) and visualized using STRUCTURE PLOT (Ramasamay, 2014, v2.0). STRUCTURE input files were converted to the appropriate file type in LEA using the

struct2geno function and the snmf function was used to generate 30 replicates of population structure analyses for values of K ranging from 1 to 8. The number of clusters was chosen using the minimal cross-entropy criterion output; the value of K displaying a plateau in this curve was selected. Within the 30 replicates of the appropriate K value, the run with the lowest cross-entropy estimate was retained for generation of a STRUCTURE-like ancestry coefficient plot.

AHE Loci Capture and Processing

Genomic DNA from 43 *Aptostichus* (40 ingroup, 3 outgroup) representing geographic clades recovered in previous phylogenetic analyses, overlapping with GBS samples where possible and with an increased focus on groups underrepresented in the GBS analyses was sent to the Center for Anchored Phylogenomics at Florida State University to undergo anchored hybrid enrichment (www.anchoredphylogeny.com). Library preparation, sequencing, and bioinformatic processing of raw Illumina data follow methods outlined in Lemmon et al., (2012) and Hamilton et al., (2016). Hamilton details the design of the Spider Probe Kit utilized as well as the methods that led to sequence alignments analyzed in the current work. Briefly, sonication of up to 500ng genomic DNA for each sample was followed by addition of sample indices, blunt end repair, and size selection (300-800bp fragments). Indexed samples were pooled at equal quantities before being enriched using the AHE Spider Probe Kit (v1). This kit was designed to target 585 conserved regions of spider genomic and transcriptomic sequences. Following enrichment, reactions were pooled again and sequenced on a single Illumina HiSeq 2500 lane (150bp, PE reads) at the Florida State University Translational Science Laboratory. Prior to sequence assembly, overlapping paired reads were merged following Rokyta et al. (2012). Read pairs failing to merge were utilized but left unmerged during assembly. Divergent reference assembly was used to map reads to the probe regions and extend the assembly into the flanking

regions (see Prum et al., 2015 and Hamilton et al., 2016 for details). Orthology was determined among the homologous consensus sequences at each locus following Prum et al. (2015) and Hamilton et al. (2016). Sequences in each orthologous cluster were aligned using MAFFT v7.023b (Katoh & Standley, 2013), using the --genafpair and --maxiterate 1000 flags. Since the spider AHE loci probe design was heavily influenced by conserved sequence regions present in reference transcriptome sequences, AHE alignments were mapped back to reference *Aptostichus* transcriptome contigs for annotation of protein coding components within the AHE sequences. First, a BLAST search using a fasta file containing a single representative sequence from each AHE locus as the query and five previously derived transcriptome assemblies for *Aptostichus* species within the complex (*A. atomarius*, *A. angelinajolieae*, *A. stanfordianus*, *A. stephencolberti*, and *A. miwok*) as the database was used to identify relevant contigs for mapping. Each locus was then assigned a "transcriptome group" identification based on the reference sequence to which it hit. At this taxonomic level, individual AHE loci represent fragments of conserved genomic regions also represented in aligned transcriptomes. Flanking regions in this case represent introns rather than variable protein coding regions.

Phylogenomic Analyses

The recovered AHE loci were analyzed in a phylogenetic framework. First, prior to any additional trimming or filtering of alignments, all loci recovered (644) were concatenated and the program IQ-TREE (Nguyen et al., 2014) was used to perform a maximum likelihood analysis of the resulting supermatrix. The built-in model selection feature of IQ-TREE, ModelFinder (Kaylaanamoorthy et al., 2017), was used to select the optimal model and partitioning scheme for each locus in the supermatrix; confidence estimates were generated using the ultrafast bootstrap (Hoang et al., 2017) and SH-aLRT (Guindon et al., 2010) methods (1000 replicates

each). Due to the redundant nature of the AHE loci, the full dataset was reduced via selection of a single AHE locus per transcript group (n=428) and further filtered to remove loci for which there were less than 5 representative samples from each putative species group (all currently described species and *A. stanfordianus* North/South clades). The resulting dataset contained 141 loci and is the preferred focus of phylogenomic analysis, as it is small enough to be used for downstream, computationally intensive species delimitation methods. A fully concatenated analysis of this subset was performed with settings identical to the 644 locus analysis to assess consistency of topology and support. IQ-TREE was then used to generate individual gene trees for the 141 set of loci (-m TESTNEW, 1000 UFboot, 1000 SH-aLRT), which served as input for the coalescent-based species tree analysis in ASTRAL II (Mirarab & Warnow 2015). Both bootstrap and gene-resampling only assessments of nodal support available in ASTRAL were performed using individual gene tree input from IQ-TREE. Additionally, to evaluate gene tree bias in our 141 loci subset, an ASTRAL species tree was generated for all 644 loci using IQ-TREE inputs as described previously.

Species Validation

Using the coalescent species delimitation approach available in the software package Bayesian Phylogeography and Phylogenomics (BPP version 3, Rannala & Yang, 2015; Yang & Rannala, 2014) species hypotheses as recovered in the discovery and phylogenomic methods were further evaluated. Three different types of analyses were performed with alignments of the 141-gene subset utilized in phylogenomic reconstructions as input. First, a joint estimation of the species tree and species delimitation (unguided analysis type 'A11'; Yang, 2015) was executed to independently evaluate tree topology and individual group assignments. Priors reflecting an assumption of small ancestral population size (2,2000) and relatively deep divergence (1,10)

were chosen based on the biology of the group and previous BPP analyses of other mygalomorph spiders (Hedin, Carlson & Coyle, 2013). The clean data option, which removes ambiguities and gap positions in the alignments, was chosen for all analyses. Each BPP run included $1x10^5$ MCMC generations (burn-in of 5000) sampled every 5 generations and was performed in triplicate. Following the A11 analysis, two additional species delimitation analyses with identical parameters but with fixed guide trees (type 'A10'; Yang, 2015) reflecting alternate topologies recovered in phylogenomic analyses (concatenation vs. species tree topologies) were executed.

Species Boundary Refinement

To assess the presence, magnitude and direction of gene flow between putative species of the *atomarius* complex with abutting ranges, the program PHRAPL was employed. PHRAPL is written in R and allows for the generation and evaluation of demographic models (migration, coalescent events, demographic events) under the assumptions of the multispecies coalescent. This tool evaluates the probability of a set of empirically derived gene trees, calculating the proportion of topologies simulated under a range of demographic parameters matching observed topologies, ultimately ranking fit of all demographic models tested using the Akaike information criterion (AIC) framework. To make this type of exploratory analysis possible, PHRAPL implements several strategies including subsampling of tree tips and calculating tree degeneracy weights to reduce the influence of intra-population-only discord. Models must be generated first, given a specified number of free parameters (K), followed by creation of an appropriately subsampled dataset. For this dataset, species comparisons were divided into geographic regions of interest (e.g. North, Central, South) due to the computational challenges posed by testing model sets containing more than 3 species/populations at a time (Jackson et al., 2017). Gene trees generated by IQ-TREE for the 141 AHE loci subset were used as input along with a

population assignment file. Population assignments were based on the consensus of previous analyses. Gene trees included only the focal species for each subset and two outgroup taxa, *A. hesperus* and *A. madera*, which served as the root taxa and were subsequently trimmed by PHRAPL. Since parameter space can quickly overwhelm computational power, initial analyses were limited to 3 population models with only tree-like topologies (all populations coalesce), a single free parameter for migration (all migration rates equal), and only symmetrical migration (48 models). After evaluating the limited model space generated with these parameters, a more complex set of models allowing asymmetric migration rates while limiting tree topology to the three-taxon relationships derived from phylogenomic analyses was explored (256 models). PHRAPL was executed on the Auburn University high performance computing resource, Hopper, using R version 3.3.0. Each population subsampling size was set to 3, with 200 subsamples per gene; 10,000 trees were simulated for each model using default collapse start (0.3, 0.58, 1.11, 2.12, 4.07, 7.81, 15) and migration start (0.1, 0.22, 0.46, 1, 2.15, 4.64) grid search parameters. Two replicates of each analysis were performed to evaluate consistency of results.

Results:

The GBS protocol yielded 190,873,287 reads for 47 individuals, which were assembled into 29,967,018 sequence tags. From these tags, 33,934 SNPs were called and additional filtering of these sites based on missingness resulted in three files containing 412 (D1, 10% missing sites), 990 (D2, 20% missing sites), and 1628 (D3, 30% missing sites). The AHE protocol resulted in a total of 644 multiple sequence alignments varying in length (100-2251 bp), sequence similarity (68.6-99.3% pairwise identity), and taxon occupancy (41.86-100%). In total,

there were 48,7882 sites (18,160,824 nucleotides) in the fully concatenated AHE supermatrix. Summary statistics for individual loci can be found in Supplementary Table 2. When mapped back to transcripts of *Aptostichus atomarius*, the centralized probe region of these loci was found to be associated with only 428 unique contigs; that is, AHE probes displayed a one to many relationship with resulting AHE loci. Classifying these loci by which "transcript group" they belong to (membership ranging in size from 1-8), allowing only one representative locus per group, and setting a minimum criterion for species representation (at least 5 individuals/previously identified clade) the data was reduced to 141 loci. In the 124 cases where more than one AHE alignment mapped to the same transcript, the longest alignment was chosen.

GBS Data Clustering Analyses

Most analyses detected an optimal K of five, with clusters corresponding largely to mitochondrial clades. STRUCTURE analysis of the most conservatively filtered SNP dataset (D1, 10% missing sites) recovered six distinct clusters within the sequenced samples (Fig 2a). Several clades previously identified primarily on the basis of mitochondrial divergence were found to be exclusive – *A. stephencolberti*, *A. angelinajolieae*, and individuals from the southern half of the *A. stanfordianus* range formed a distinct cluster. Individuals from the southern part of the *A. atomarius* range were distinct in the preferred output from those in the northern portion, which clustered with the *A. dantrippi* specimen from that area (MY0730). In solutions where *A. atomarius* and *A. dantrippi* were not collapsed as one (all LEA analyses see Figures 2b,3b,4b and STRUCTURE for D2, Figure 3a) this *A. dantrippi* singleton showed very high levels of admixture and more shared ancestry with *A. stanfordianus* South than *A. atomarius*. The second *A. dantrippi* specimen consistently clustered with *A. angelinajolieae*; to account for the possibility of experimental error or misidentification, this individual was intentionally re-

extracted for the AHE analyses. The northern dune species, *A. miwok*, and individuals from the northern portion of the *A. stanfordianus* range were collapsed into one population in all analyses; SNP markers alone were not sufficient to distinguish these two species.

Phylogenomic Relationships

Concatenated analyses of the AHE loci were congruent between the full set (644 loci, Figure 5) and the filtered set (141 loci, Figure 6). Mitochondrial clades from Bond and Stockman (2008) and Bond (2012) were recovered with high support, though the arrangement differed from the 2008 mtDNA-based topology. *A. miwok* is nested within the northern clade of *A. stanfordianus* and the southern *A. stanfordianus* are found sister to the southern dune species *A. stephencolberti* as previously found, but *A. angelinajolieae* is placed sister to the *A. stanfordianus* North + *A. miwok* clade and *A. atomarius* is sister to *A. dantrippi*. The ASTRAL II species tree for all 644 loci had the same topology as concatenated analyses, with high support (>90 local posterior probability) for most deep nodes in the tree, falling below that level only at some inter-population level splits near the tips of the tree and for the *A. stanfordianus* South/*A. stephencolberti* node (Fig 7). The species tree based on the 141 loci subset generated by ASTRAL II resembled the concatenated tree apart from the placement of *A. angelinajolieae*, found to be sister to a clade containing all other species (Fig 8).

The two primary topologies recovered – *A. angelinajolieae* + northern species and *A. angelinajolieae* sister to all other complex members – were used in BPP species delimitation in analyses requiring guide tree input. A single case of species mis-assignment was confirmed; sample MY3809, originally considered *A. dantrippi* based on its sampling locality was consistently placed within the *A. angelinajolieae* clade with high support as found in the GBS

clustering analyses. A second individual sampled from the same locality, MY3807, was placed within the *A. dantrippi* clade indicating possible sympatry.

Species Delimitation and Refinement

The joint estimation of species tree topology and species delimitation analysis in BPP consistently generated high support for most relationships recovered in phylogenomic and clustering analyses (Fig 9). The unguided analysis recovered a species tree topology matching that of the concatenated phylogenomic analyses; *A. angelinajolieae* was sister to the *A. miwok*/*A. stanfordianus* (North) grouping but with variable support (0.87-0.99) as the top model. Five of the currently delimited species were fully supported in the A11 analysis; the sixth member of the *atomarius* complex, *A. stanfordianus*, was once again found to contain two distinct genetic lineages with full support. When the guide tree was fixed to match the concatenated topology (*A. angelinajolieae* sister to northern species) the *A. atomarius*/*A. dantrippi* split became the focus of uncertainty with posterior support ranging from 0.46-1 across replicates for the two species delimitation. Alternatively, fixing the guide tree to match the 141 loci based ASTRAL species tree resulted in full support for (>0.96) all seven groups.

PHRAPL analysis of geographic subsets within this tree revealed some indication of contemporary migration and historical contact between sister species, migration rate parameters were high in the asymmetric models, fixed at ~2.15 in all top ranked models (Fig 10a-c). The highest ranking model for the northern species group, as taken from the concatenated tree topologies (*A. angelinajolieae*, *A. miwok/A. stanfordianus* North), included asymmetric migration between the dune endemic *A. miwok* and its inland sister *A. stanfordianus* and historical migration between *A. angelinajolieae* and the ancestor of the other two species (Fig 10a). Species in the central part of the *atomarius* complex range displayed only ancestral

migration from the *A. stephencolberti/A. stanfordianus* South sister grouping into A. angelinajolieae (Fig 10b). In the southern ranges, contemporary migration from *A. dantrippi* into *A. atomarius* and historical migration from the *A. dantrippi/A. atomarius* sister grouping into *A. angelinajolieae* were both detected (Fig 10c). Alternatively, PHRAPL analyses which were not constrained to match the species tree topology revealed a tendency for disruption of sister species, lower migration rate estimates, and symmetrical contemporary migration between geographically adjacent species groups (Fig 11a-c). In the northern comparison, the topology matches that of the species tree, with *A. angelinajolieae* sister to an *A. miwok/A. stanfordianus* grouping with low estimated migration between the northern dune species and its inland sister (Fig 11A). In the central region comparison, *A. angelinajolieae* coalesces with *A. stanfordianus* South and there is moderate migration between the dune endemic species and the inland species (Fig 11B). A similar situation appears in the comparison of southern species, where *A. angelinajolieae* coalesces first with *A. atomarius* to the exclusion of *A. dantrippi,* found to be the strongly supported sister of *A. atomarius* in all other analyses, with moderate migration estimates (11C).

Discussion:

We have applied two independent, genomic-scale datasets (GBS and AHE) to thoroughly evaluate genetic boundaries between the six currently described members of the *Aptostichus atomarius* species complex, validating all but *Aptostichus stanfordianus* and resolving divergences within a coalescent species tree framework. Herein we apply a three stage, integrative approach with phases of SNP-based discovery, independent genomic validation, and refinement of sister species relationships. Previous delimitations in this group of morphologically

homogeneous trapdoor spiders have depended heavily upon a handful of divergent mitochondrial sites and the assumption of geographic exclusivity within the complex. Our findings indicate that although previously utilized mitochondrial markers do, in part, reflect species boundaries in the *A. atomarius* complex, they fail to accurately recover relationships between species and obscure the potential effects of male dispersal mediated gene flow between sister species.

Cryptic Speciation

Both GBS and AHE markers revealed striking divergence between northern and southern populations of what is currently known as *Aptostichus stanfordianus*. Despite an apparently contiguous geographic distribution throughout the central California Coast Ranges, the two distinct genetic lineages sampled from this region are most closely associated with adjacent dune species (*A. miwok* in the north, *A. stephencolberti* in the south) rather than each other. This divergence was hinted at by previous works (Bond & Stockman, 2008; Bond, 2012), however, ambiguity of clade placement resulted in a conservative delimitation that did not include splitting *A. stanfordianus*. Given the apparent deep divergence within this species, with clades representing independently evolving lineages and displaying properties of phylogenetic species (i.e. secondary species criteria sensu DeQuieroz, 2007) such as reciprocal monophyly and diagnosability, we propose that the southern *A. stanfordianus* individuals constitute a new species. There appears to be some degree of north/south geographic partitioning in the region, though the current sampling is insufficient to clearly delimit the physical boundary between species ranges. Combining individuals sampled in this study with previous works, the range of *A. stanfordianus* South appears to extend from the gap between the Santa Cruz Mountains and the Gabilan Range eastward into the Diablo Range (Figure 11). Bordered to the west by the Salinas Valley and to the east by the Central Valley, this distribution as currently understood appears to

wrap around the Eastern Diablo Range where *A. stanfordianus* North individuals are found exclusively. *A. stanfordianus* North also predominates in the Santa Clara Valley, sweeping into foothills north of the San Francisco Bay near Clear Lake. This Santa Clara Valley/Diablo Range intersection is one of many regions within the complex range that would benefit from denser sampling and investigation of potential reproductive barriers, as it seems likely that individuals from *A. stanfordianus* and the cryptic *A. stanfordianus* South might coexist near the edges of their respective ranges with no clear geographic barriers to close range dispersal and male migration.

Sympatry and Species Diagnosis

In both the discovery and validation phases of analysis, we detected further evidence of sympatry between *A. angelinajolieae* and *A. dantrippi* at a locality in the western portion of the *A. dantrippi* range. In isolation, this finding would most parsimoniously indicate sample mislabeling at some stage of sample collection, processing or analysis. However, coupled with previous findings of mismatch between geographic assignments to species and mitochondrial haplotypes, a pattern of sympatry between *A. angelinajolieae* and three adjacent southern species (*A. atomarius*, *A. dantrippi*, *A. stanfordianus* South) is evident. Several localities have sampled individuals that represent more than one lineage. This finding has a couple of implications; the *A. angelinajolieae* range is much larger than previously known, the Salinas River valley may not represent an impermeable barrier to *Aptostichus* dispersal, and the potential for mitochondrial introgression between species cannot be entirely dismissed when interpreting sampled haplotypes near range borders.

We hypothesize that the sampling gap south of *A. angelinajolieae*'s current range conceals the true extent of the distribution, south from the Monterey area through the Santa

Lucia Range to San Luis Obispo and west to the edge of the Central Valley. This region remains underrepresented in trapdoor phylogeography studies, either representing sampling bias due to lack of road access or a real gap in mygalomorph distribution due to geologic events or other forces. There is precedent for genetic connection between trapdoor spider populations spanning, but not including, the Salinas Valley, however. This pattern has also been observed in the trapdoor spider genera *Aliatypus* (Hedin & Carlson, 2011) and *Antrodiaetus* (Hedin, Starrett & Hayashi, 2012). Because fixed mitochondrial differences and geographic locality are the primary means of diagnosing species in this complex, individuals occurring in sympatry may always represent a challenge to subsequent analysis unless lack of mitochondrial introgression is established or another metric for identifying species is developed. In all analyses, the single specimen representing this potential sympatry was unambiguously placed within the *A. angelinajolieae* clade, providing limited evidence that in cases of sympatry mitochondrial and nuclear genomic signatures of divergence are in accord.

Sister Species or Metapopulations?

Anchored enrichment loci also revealed strongly supported sister species relationships between several pairs of complex members. Both dune species have inland sister species – *A. miwok* pairing with *A. stanfordianus* North and *A. stanfordianus* South with *A. stephencolberti*. The southernmost species, *A. atomarius* and *A. dantrippi*, also have a well-supported sister relationship. Placement of *A. angelinajolieae* remains somewhat ambiguous, alternatively found sister to the northern species and at the base of the species tree. The most well supported phylogenetic analyses are in congruence with the coalescent tree topology recovered in the unguided BPP analysis, lending credence to the northern association of *A. angelinajolieae*. In each phase of the analysis there was some tendency for sister species collapse, particularly at the

A. stanfordianus North/*A. miwok* and *A. atomarius*/*A. dantrippi* splits. This pattern was subtle in the discovery and validation stages and could be attributed to weaknesses of experimental design (not enough sites, not enough individuals per population) or appeared only in secondary analyses and given less weight when results were evaluated holistically.

Relative to the other analyses, PHRAPL results indicate that there is a moderate amount of contemporary migration between these two sister species pairs that might play a role in generating the patterns of divergence we observed. Gene flow between species need not ultimately lead to the collapse of established independent lineages, or change the fact that these lineages are currently diagnosable, but its occurrence here challenges our understanding of mygalomorph dispersal and the *atomarius* complex distribution. For gene flow to occur between these sister species pairs, males would have to be moving much farther (or range borders are much closer) than expected over increasingly fragmented habitats to successfully find and mate with females of adjacent species. Additionally, successful mating would depend on the absence of species-specific mating cues – chemical, behavioral, or temporal – not likely given the role of sex pheromones and intricate pre/post mating behaviors of trapdoor and other mygalomorph spiders (Ferretti et al., 2013).

Considering the above, we regard the PHRAPL results with some suspicion, particularly because incomplete lineage sorting between sister species seems to be a more valid explanation of the data given our current understanding of the system. Divergences are likely quite deep within the *atomarius* complex; one estimate of the split between two members (*A. atomarius* and *A. stephencolberti*) in the context of transcriptome ortholog divergence was around 3-8 Mya (Bond et al., 2014). For this group, "contemporary" migration may reflect gene flow nearer the species coalescent point than present day. If migration were currently happening at the level

suggested by PHRAPL analyses, we would expect much more discordance across the tree and higher levels of admixture in the discovery analyses with STRUCTURE. The inability of PHRAPL to recover the three-taxon topology that is compatible with the species tree in the unconstrained model exploration was unexpected, but may indeed indicate that migration is providing signal in the data that is leading to incorrect phylogenetic reconstructions. More complete model explorations that include all species without assumptions about the species tree topology, though computationally taxing, may be necessary to understand the patterns of migration in this group.

Conclusions:

There is no single perfect species delimitation method, many require significant input from the researcher (e.g. population parameter estimates, species guide tree, species/population assignments, estimated gene trees etc.) and like any statistical method they make simplifying assumptions (Carstens et al., 2013). Similarly, the emergence of varied genome-wide sequencing methods has resulted in data types with application at different phylogenetic scales having different considerations at the sampling, processing, and analysis stages (Matz, 2017; da Fonesca et al, 2015). AHE and other enrichment approaches offer versatility, repeatability, and a wealth of information for phylogenetic reconstruction, particularly valuable for non-model organisms with no genomic resources. With this flood of information comes a host of incompatible gene histories that must be reconciled, sometimes at a significant computational cost, but may also reveal hidden associations between species. GBS and SNP-based methods have advantages of a well-established suite of analysis tools, though they are perhaps best employed at a shallow phylogenetic scale ideally in system with some pre-existing genomic resources. Deeply divergent

lineages can reduce GBS SNP recovery rates, as we saw here, and low sample sizes may also contribute to inconsistent results during analysis. In future iterations of integrative systematic work in the *A. atomarius* complex, sister species boundaries might be better suited for a focused GBS or RADseq-type analysis, where thorough assessment of shared ancestry might yield more robust results.

Integrative taxonomy is a highly iterative process; here we have clarified our understanding of relationships within the *A. atomarius* sister species complex and generated a testable species tree hypothesis supported by a wide swath of nuclear genomic loci while also revealing areas in need of further examination. The integration of multiple genomic datasets and analyses with complementary statistical tendencies has generated a more refined view of species boundaries; however true integration across disciplines, e.g. behavior, ecology, physiology, might inform our models of trapdoor spider population dynamics while simultaneously providing lines of evidence for species boundaries outside of genetic markers. The genomic resources developed here and elsewhere may provide the raw material for directing studies in other disciplines. Which chemosensory genes and pathways are present in trapdoor spiders? Are there species-specific changes in odorant binding proteins or receptors that might lead to species recognition? What are the differences between courtship behaviors (drumming, tapping, vibrating etc.) between species within the *atomarius* complex? There are gaps in our genetic sampling of the complex and in our knowledge of aspects of *Aptostichus* natural history. A large portion of the *A. angelinajolieae* range may still be left unsampled, there are disjunct populations of the widely distributed *A. atomarius* that have not been included in any genetic analyses to date, and while our study shows that *A. stanfordianus* is a composite of two deeply divergent independent lineages our understanding of where they overlap and how they might interact

remains incomplete. Rectifying these gaps should increase the resolution of species boundaries and allow for increasingly more accurate interpretations of the *A. atomarius* complex genetic landscape.

References:

Bickford, D., Lohman, D. J., Sodhi, N. S., Ng, P. K., Meier, R., Winker, K., Ingram K., & Das, I. (2007). Cryptic species as a window on diversity and conservation. *Trends in Ecology & Evolution*, 22(3), 148-155.

Bradbury, P. J., Z. Zhang, D. E. Kroon, T. M. Casstevens, Y. Ramdoss, and E. S. Buckler. 2007. Tassel: software for association mapping of complex traits in diverse samples. *Bioinformatics,* 23, 2633–2635.

Brandley, M. C., Bragg, J. G., Singhal, S., Chapple, D. G., Jennings, C. K., Lemmon, A. R., Lemmon, E.M., Thomposon M.B., & Moritz, C. (2015). Evaluating the performance of anchored hybrid enrichment at the tips of the tree of life: a phylogenetic analysis of Australian Eugongylus group scincid lizards. *BMC Evolutionary Biology*, 15(1), 62.

Bond, J. E. (2012). Phylogenetic treatment and taxonomic revision of the trapdoor spider genus *Aptostichus* Simon (Araneae, Mygalomorphae, Euctenizidae). ZooKeys, (252), 1.

Bond, J. E., Garrison, N. L., Hamilton, C. A., Godwin, R. L., Hedin, M., & Agnarsson, I. (2014). Phylogenomics resolves a spider backbone phylogeny and rejects a prevailing paradigm for orb web evolution. *Current Biology*, 24(15): 1765-1771.

Bond, J. E., & Stockman, A. K. (2008). An integrative method for delimiting cohesion species: finding the population-species interface in a group of Californian trapdoor spiders with extreme genetic divergence and geographic structuring. *Systematic Biology*, 57(4), 628-646.

Carstens, B. C., Pelletier, T. A., Reid, N. M., & Satler, J. D. (2013). How to fail at species delimitation. *Molecular Ecology*, 22(17), 4369-4383.

da Fonseca, R. R., Albrechtsen, A., Themudo, G. E., Ramos-Madrigal, J., Sibbesen, J. A., Maretty, L., & Pereira, R. J. (2016). Next-generation biology: sequencing and data analysis approaches for non-model organisms. *Marine Genomics*, 30, 3-13.

Daniels, S. R., Picker, M. D., Cowlin, R. M., & Hamer, M. L. (2009). Unravelling evolutionary lineages among South African velvet worms (Onychophora: Peripatopsis) provides evidence for widespread cryptic speciation. *Biological Journal of the Linnean Society*, *97*(1), 200-216.

Degnan, J. H., & Rosenberg, N. A. (2009). Gene tree discordance, phylogenetic inference and the multispecies coalescent. *Trends in Ecology & Evolution*, 24(6), 332-340.

Domingos, F. M., Colli, G. R., Lemmon, A., Lemmon, E. M., & Beheregaray, L. B. (2017). In the shadows: Phylogenomics and coalescent species delimitation unveil cryptic diversity in a Cerrado endemic lizard (Squamata: Tropidurus). *Molecular Phylogenetics and Evolution*, 107, 455-465.

Earl, D. A. & vonHoldt, B.M. (2012). Structure harvester: a website and program for visualizing structure output and implementing the evanno method. *Conservation*

Genetics Resources, 4 (2), 359–361.

Ellegren, H. (2014). Genome sequencing and population genomics in non-model organisms. *Trends in Ecology & Evolution*, *29*(1): 51-63.

Elshire R.J., Glaubitz J.C., Sun Q., Poland J.A., Kawamoto K., Buckler E.S., & Mitchell, S.E. (2011). A Robust, Simple Genotyping-by-Sequencing (GBS) Approach for High Diversity Species. *PLoS ONE,* 6(5): e19379. https://doi.org/10.1371/journal.pone.0019379

Falush, D., Stephens, M., and Pritchard, J.K. (2003). Inference of population structure using multilocus genotype data: linked loci and correlated allele frequencies. *Genetics,*164, 1567–1587.

Ferretti, N., Pompozzi, G., Copperi, S., González, A., & Pérez-Miles, F. (2013). Sexual behaviour of mygalomorph spiders: when simplicity becomes complex; an update of the last 21 years. *Arachnology*, 16(3), 85-93.

Frichot, E. & Francois, O. (2015). Lea: an r package for landscape and ecological association studies. *Methods in Ecology and Evolution*, 6, 925–929.

Guindon, S., Dufayard , F., Lefort, V., Anisimova, M., Hordijk, W., & Gascuel, O. (2010). New algorithms and methods to estimate maximum-likelihood phylogenies: assessing the performance of phyml 3.0. *Systematic Biology,* 59, 307–321.

Hamilton, C.A., Formanowicz, D.R., & Bond, J.E. (2011). Species delimitation and phylogeography of Aphonopelma hentzi (Araneae, Mygalomorphae, Theraphosidae): cryptic diversity in North American tarantulas. *PloS one,* 6(10), e26207.

Hamilton, C.A., Lemmon, A.R., Lemmon, E.M., & Bond, J.E. (2016). Expanding anchored hybrid enrichment to resolve both deep and shallow relationships within the spider tree of life. *BMC Evolutionary Biology*, 16(1), 212.

Hedin, M., & Carlson, D. (2011). A new trapdoor spider species from the southern Coast Ranges of California (Mygalomorphae, Antrodiaetidae, Aliatypus coylei, sp. nov,), including consideration of mitochondrial phylogeographic structuring. *Zootaxa*, 2963(1), 55-68.

Hedin, M., Carlson, D., & Coyle, F. (2015). Sky island diversification meets the multispecies coalescent–divergence in the spruce fir moss spider (Microhexura montivaga, Araneae, Mygalomorphae) on the highest peaks of southern Appalachia. *Molecular Ecology*, 24(13), 3467-3484.

Hedin, M., Starrett, J., & Hayashi, C. (2013). Crossing the uncrossable: novel trans-valley biogeographic patterns revealed in the genetic history of low dispersal mygalomorph spiders (Antrodiaetidae, Antrodiaetus) from California. *Molecular Ecology*, 22(2), 508-526.

Hendrixson, Brent E., and Jason E. Bond. (2005). Testing species boundaries in the

Antrodiaetus unicolor complex (Araneae: Mygalomorphae: Antrodiaetidae):“paraphyly” and cryptic diversity. *Molecular Phylogenetics and Evolution*, 36(2), 405-416.

Hoang, D.T., Chernomor, O., von Haeseler, A., Minh, B.Q., & Le, S.V. (2017). Ufboot2: Improving the ultrafast bootstrap approximation. *Molecular Biology and Evolution*, 35(2), 518-522.

Jackson, N.D., Morales, A.E., Carstens, B.C., & O’Meara, B.C. (2017). PHRAPL: Phylogeographic inference using approximate likelihoods. *Systematic Biology*, 66(6), 1045-1053.

Jakobsson, M. & Rosenberg N.A. (2007). Clumpp: a cluster matching and permutation program for dealing with label switching and multimodality in analysis of population structure. *Bioinformatics*, 23, 1801–1806.

Kalyaanamoorthy, S., Minh, B.Q., Wong, T.K., von Haeseler, A., &. Jermiin, L.S. (2017). Modelfinder: fast model selection for accurate phylogenetic estimates. *Nature Methods*, 14, 587-589.

Katoh, K. & Standley, D.M. (2013). Mafft multiple sequence alignment software version 7: improvements in performance and usability. *Molecular Biology and Evolution,* 30, 772–780.

Lemmon, A.R., Emme, S.A., & Lemmon, E.M. (2012). Anchored hybrid enrichment for massively high-throughput phylogenomics. *Systematic Biology*, 61(5), 727-744.

Lu, F., Lipka, A.E., Glaubitz, J., Elshire, R., Cherney, J.H., Casler, M.D., Buckler, E.S., & Costich, D.E. (2013). Switchgrass genomic diversity, ploidy, and evolution: novel insights from a network-based snp discovery protocol. *PLoS Genetics,* 9(1), e1003215.

Matz, M.V. (2017). Fantastic Beasts and How To Sequence Them: Ecological Genomics for Obscure Model Organisms. *Trends in Genetics*. 34(2), 121-132.

Mirarab, S. & Warnow, T. (2015). Astral-ii: coalescent-based species tree estimation with many hundreds of taxa and thousands of genes. *Bioinformatics* 31, i44–i52.

Misof, B., Liu, S., Meusemann, K., Peters, R. S., Donath, A., Mayer, C., Niehuis, O., et al. (2014). Phylogenomics resolves the timing and pattern of insect evolution. *Science*, *346*(6210), 763-767.

Nguyen, L.T., Schmidt, H.A., von Haeseler, A., & Minh, B.Q. (2014). Iq-tree: a fast and effective stochastic algorithm for estimating maximum-likelihood phylogenies. *Molecular Biology and Evolution,* 32, 268–274.

Nicholls, J.A., Preuss, S., Hayward, A., Melika, G., Csoka, G., Nieves‐Aldrey, J.L., Askew R.R., Tavakoli, M., Schonrogge, K., & Stone, G.N. (2010). Concordant phylogeography and cryptic speciation in two Western Palaearctic oak gall parasitoid species complexes.

Molecular Ecology, *19*(3), 592-609.

Pease, J.B., Haak, D.C., Hahn, M.W., & Moyle, L.C. (2016). Phylogenomics reveals three sources of adaptive variation during a rapid radiation. *PLoS Biology*, *14*(2), e1002379.

Pritchard, J.K., Stephens, M., & Donnelly, P. (2000). Inference of population structure using multilocus genotype data. *Genetics,* 155, 945–959.

Prum, R.O., Berv, J.S., Dornburg, A., Field, D.J., Townsend, J.P., Lemmon, E.M., & Lemmon, A.R. (2015). A comprehensive phylogeny of birds (aves) using targeted next generation dna sequencing. *Nature,* 526, 569–573.

Ramasamy, R.K., Ramasamy, S., Bindroo, B.B., & Naik, V.K. (2014). Structure plot: a program for drawing elegant structure bar plots in user friendly interface. *SpringerPlus*, 3, 431.

Myers, E.A., Rodríguez-Robles, J.A., Denardo, D.F., Staub, R.E., Stropoli, A., Ruane, S., & Burbrink, F.T. (2013). Multilocus phylogeographic assessment of the California Mountain Kingsnake (Lampropeltis zonata) suggests alternative patterns of diversification for the California Floristic Province. *Molecular Ecology*, *22*(21), 5418-5429.

Nakhleh, L. (2013). Computational approaches to species phylogeny inference and gene tree reconciliation. *Trends in Ecology & Evolution*, 28(12), 719-728.

Starrett, J., Hayashi, C.Y., Derkarabetian, S., & Hedin, M. (2018). Cryptic elevational zonation in trapdoor spiders (Araneae, Antrodiaetidae, Aliatypus janus complex) from the California southern Sierra Nevada. *Molecular Phylogenetics and Evolution*, *118*, 403-413.

Yang, Z. (2015). The BPP program for species tree estimation and species delimitation. *Current Zoology*, 61(5), 854-865.

Young, A.D., Lemmon, A.R., Skevington, J.H., Mengual, X., Ståhls, G., Reemer, M., Jordaens, K., Kelso, S., Lemmon, E.M., Hauser, M., De Meyer M., Misof, B., & Wiegman B.M. (2016). Anchored enrichment dataset for true flies (order Diptera) reveals insights into the phylogeny of flower flies (family Syrphidae). *BMC evolutionary biology*, 16(1), 143.

Valdez-Mondragón, A., & Cortez-Roldán, M.R. (2016). On the trapdoor spiders of Mexico: description of the first new species of the spider genus *Aptostichus* from Mexico and the description of the female of Eucteniza zapatista (Araneae, Mygalomorphae, Euctenizidae). *ZooKeys*, (641), 81.

Wachter, G.A., Muster, C., Arthofer, W., Raspotnig, G., Föttinger, P., Komposch, C., Steiner, F.M., & Schlick-Steiner, B.C. (2015). Taking the discovery approach in integrative taxonomy: decrypting a complex of narrow-endemic Alpine harvestmen (Opiliones: Phalangiidae: Megabunus). *Molecular Ecology*, 24(4), 863-889.

Table1: Specimen localities and dataset inclusion. AE = Anchored Hybrid Enrichment, GBS = Genotyping by Sequencing, BOTH = specimen tissue used in both analyses.

NAME	GBS/AE	LAT	LONG	SPECIES	COUNTY
MY03057	BOTH	36.3997	-121.8914	*angelinajolieae*	Monterey
MY03130	GBS	36.45118	-121.69199	*angelinajolieae*	Monterey
MY03309	GBS	36.29045	-121.46594	*angelinajolieae*	Monterey
MY03310	AE	36.29045	-121.46594	*angelinajolieae*	Monterey
MY03311	GBS	36.44555	-121.68272	*angelinajolieae*	Monterey
MY03312	AE	36.44555	-121.68272	*angelinajolieae*	
MY03315	GBS	36.392	-121.62524	angelinajolieae	Monterey
MY03317	GBS	36.57537	-121.87376	angelinajolieae	Monterey
MY03318	AE	36.57537	-121.87376	angelinajolieae	Monterey
MY03321	GBS	36.53836	-121.73766	angelinajolieae	Monterey
MY03630	BOTH	36.44477	-121.68555	*angelinajolieae*	Monterey
MY03631	AE	36.44477	-121.68555	*angelinajolieae*	Monterey
MY00741	BOTH	35.41695	-120.55722	atomarius	San Luis Obispo
MY02268	AE	34.4463	-119.6303	atomarius	Santa Barbara
MY02595	BOTH	33.67712	-117.11578	atomarius	Riverside
MY02610	GBS	34.16372	-117.83891	atomarius	Los Angeles
MY02673	GBS	33.51366	-117.58231	atomarius	Orange
MY02980	GBS	34.7422	-120.5974	atomarius	Santa Barbara
MY03632	GBS	32.88369	-116.82239	*atomarius*	San Diego
MY03633	AE	32.88369	-116.82239	*atomarius*	San Diego
MY03711	GBS	34.49277	-120.0658	*atomarius*	Santa Barbara
MY03767	GBS	34.702	-118.8016	*atomarius*	Los Angeles
MY03769	AE	34.702	-118.8016	*atomarius*	Los Angeles
MY00730	BOTH	35.66343	-118.02767	dantrippi	Kern

MY03806	AE	34.8624	-119.1275	*dantrippi*	Kern
MY03807	AE	35.3452	-119.8107	*dantrippi*	San Luis Obispo
MY03808	AE	34.8624	-119.1275	*dantrippi*	Kern
MY03809	BOTH	35.3452	-119.8107	*dantrippi*	San Luis Obispo
My03817	AE	35.4843	-118.6477	*dantrippi*	Kern
MY00290	BOTH	41.86952	-124.20733	miwok	Del Norte
MY00301	GBS	41.01333	-124.10923	miwok	Humboldt
MY00304	GBS	41.01333	-124.10923	miwok	Humboldt
MY00702	GBS	40.69792	-124.27255	miwok	Humboldt
MY03052	AE	41.0096	-123.64559	miwok	Humboldt
MY03522	GBS	38.02626	-122.88313	*miwok*	Marin
MY03524	BOTH	38.15538	-122.94839	*miwok*	Marin
MY03527	GBS	38.15538	-122.94839	*miwok*	Marin
MY03531	GBS	38.33898	-123.06149	*miwok*	Sonoma
MY03540	AE	39.54767	-123.76315	*miwok*	Mendocino
MY03541	BOTH	39.54767	-123.76315	*miwok*	Mendocino
MY03542	BOTH	40.69925	-124.2738	*miwok*	Humboldt
MY03546	AE	40.69925	-124.2738	*miwok*	Humboldt
MY00282	GBS	39.02042	-122.38972	stanfordianus	Colusa
MY03121	GBS	37.03099	-122.06482	stanfordianus	Santa Cruz
MY03267	AE	37.47373	-121.236	stanfordianus	Stanislaus
MY03275	GBS	37.42459	-121.34256	stanfordianus	Stanislaus
My03279	BOTH	37.06702	-121.1941	stanfordianus	Merced
MY03284	AE	37.06493	-121.21024	stanfordianus	Merced
MY03293	GBS	36.78522	-121.46323	stanfordianus	San Benito
MY03297	AE	36.8166	-121.52642	stanfordianus	San Benito
MY03301	BOTH	36.57962	-121.19069	stanfordianus	San Benito

MY03305	GBS	36.09625	-120.52497	stanfordianus	Fresno
MY03308	AE	36.19888	-120.73813	stanfordianus	Monterey
MY03329	GBS	37.05991	-121.67788	stanfordianus	Santa Clara
MY03342	GBS	38.49525	-122.12369	stanfordianus	Napa
MY03353	AE	38.41631	-122.66103	stanfordianus	Sonoma
MY03357	GBS	37.99741	-122.45714	stanfordianus	Marin
MY03358	AE	37.99741	-122.45714	stanfordianus	Marin
MY03481	BOTH	37.39347	-121.81573	stanfordianus	Santa Clara
MY03482	AE	37.39347	-121.81573	stanfordianus	Santa Clara
MY03486	BOTH	37.15198	-121.58653	stanfordianus	Santa Clara
MY00700	GBS	36.30625	-121.89718	stephencolberti	Monterey
MY03070	BOTH	36.6905	-121.8105	stephencolberti	Monterey
MY03489	GBS	36.78551	-121.79454	stephencolberti	Monterey
MY03491	AE	36.78551	-121.79454	stephencolberti	Monterey
MY03492	BOTH	36.87809	-121.82616	stephencolberti	Santa Cruz
MY03498	AE	36.96683	-122.12281	stephencolberti	Santa Cruz
MY03499	GBS	36.96683	-122.12281	*stephencolberti*	Santa Cruz
MY03510	GBS	37.15513	-122.3555	*stephencolberti*	San Mateo
MY03513	AE	37.26598	-122.41219	*stephencolberti*	San Mateo
MY03517	GBS	37.71219	-122.50141	*stephencolberti*	San Francisco

Figure 1: Map of sampling localities for different genomic sequencing approaches

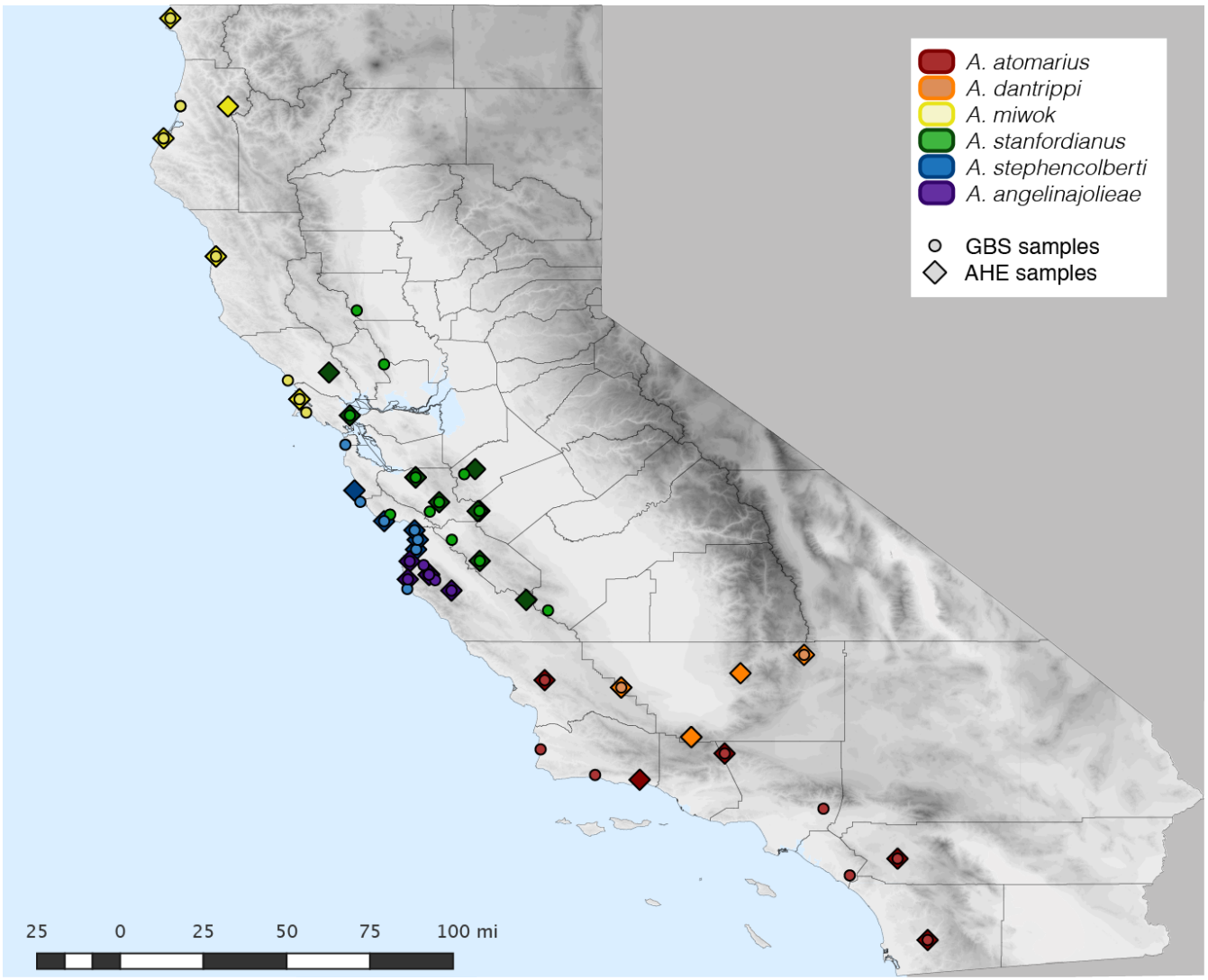

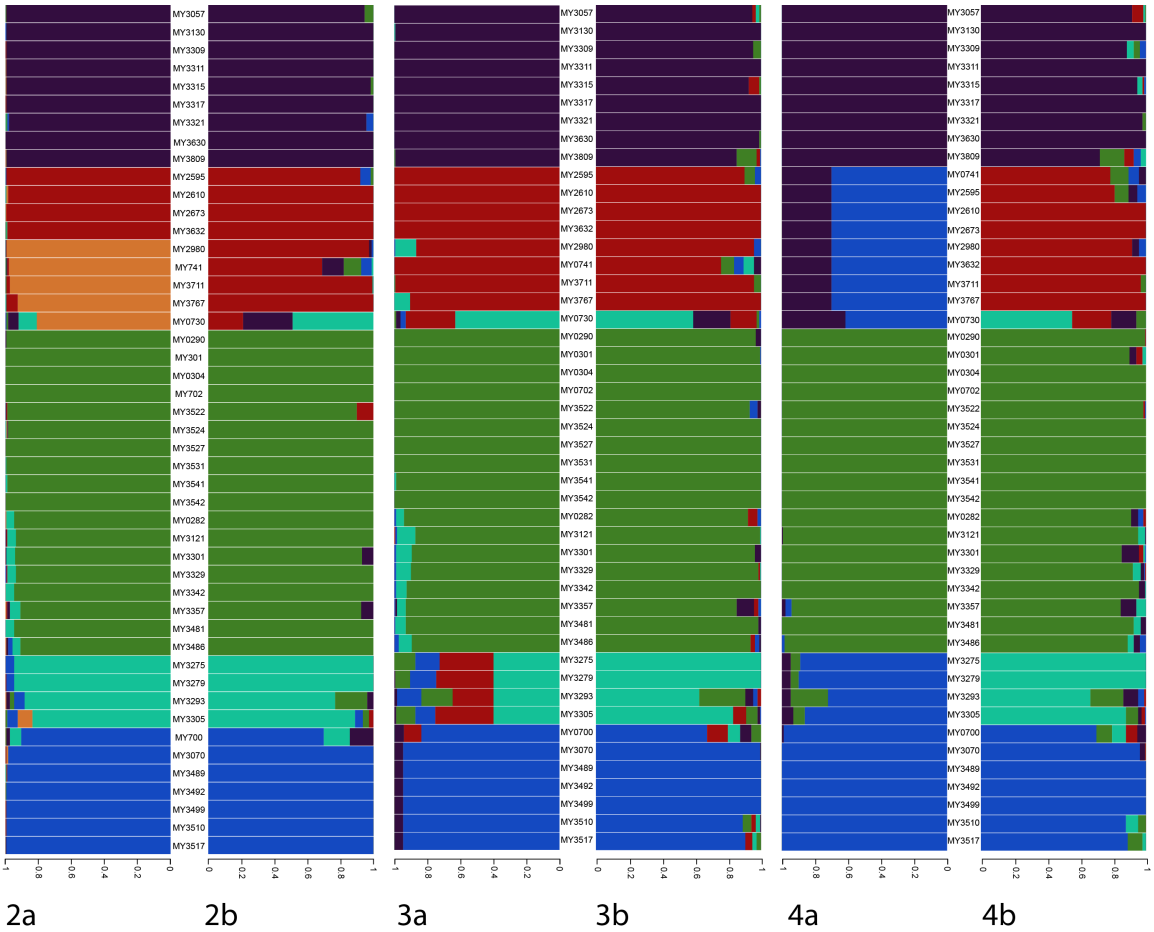

Figures 2-4: STRUCTURE (2a,3a,4a) and LEA (2b,3b,4b) admixture plots for the 10, 20 and 30% missing site filtered datasets. Purple = angelinajolieae, Red = atomarius, Orange = dantrippi, Green = stanfordianus North + miwok, Teal = stanfordianus South, Blue = stephencolberti.

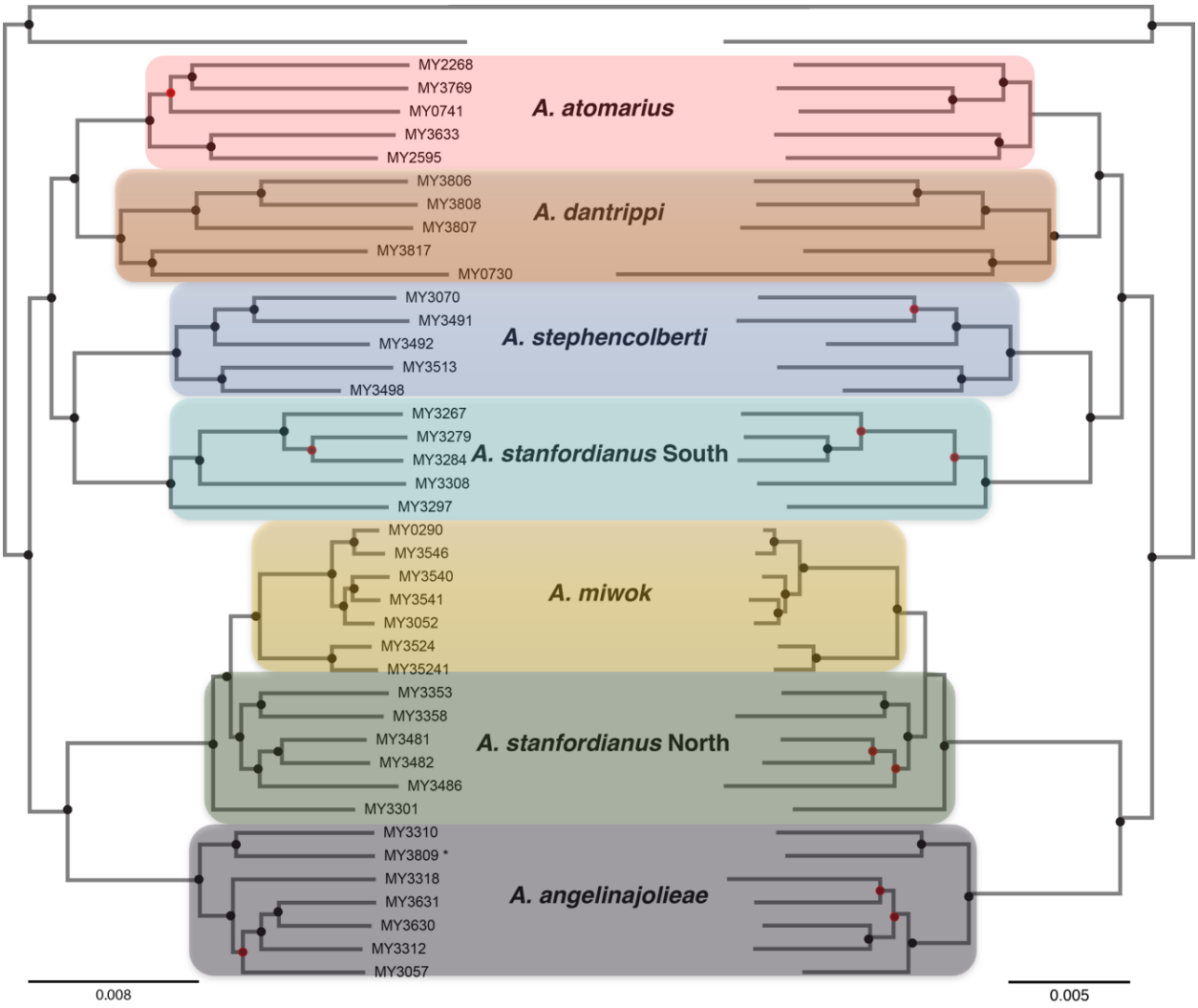

Figure 5 and 6: Left: Maximum likelihood (IQTREE) analysis of concatenated matrix of 644 AHE loci. Full support (SH-aLRT >80/UFboot >95) unless otherwise shown. Right: Maximum likelihood (IQTREE) analysis of concatenated matrix of 141 AHE loci. Full support (SH-aLRT >80/UFboot >95) indicated by black dots, red indicate less than full.

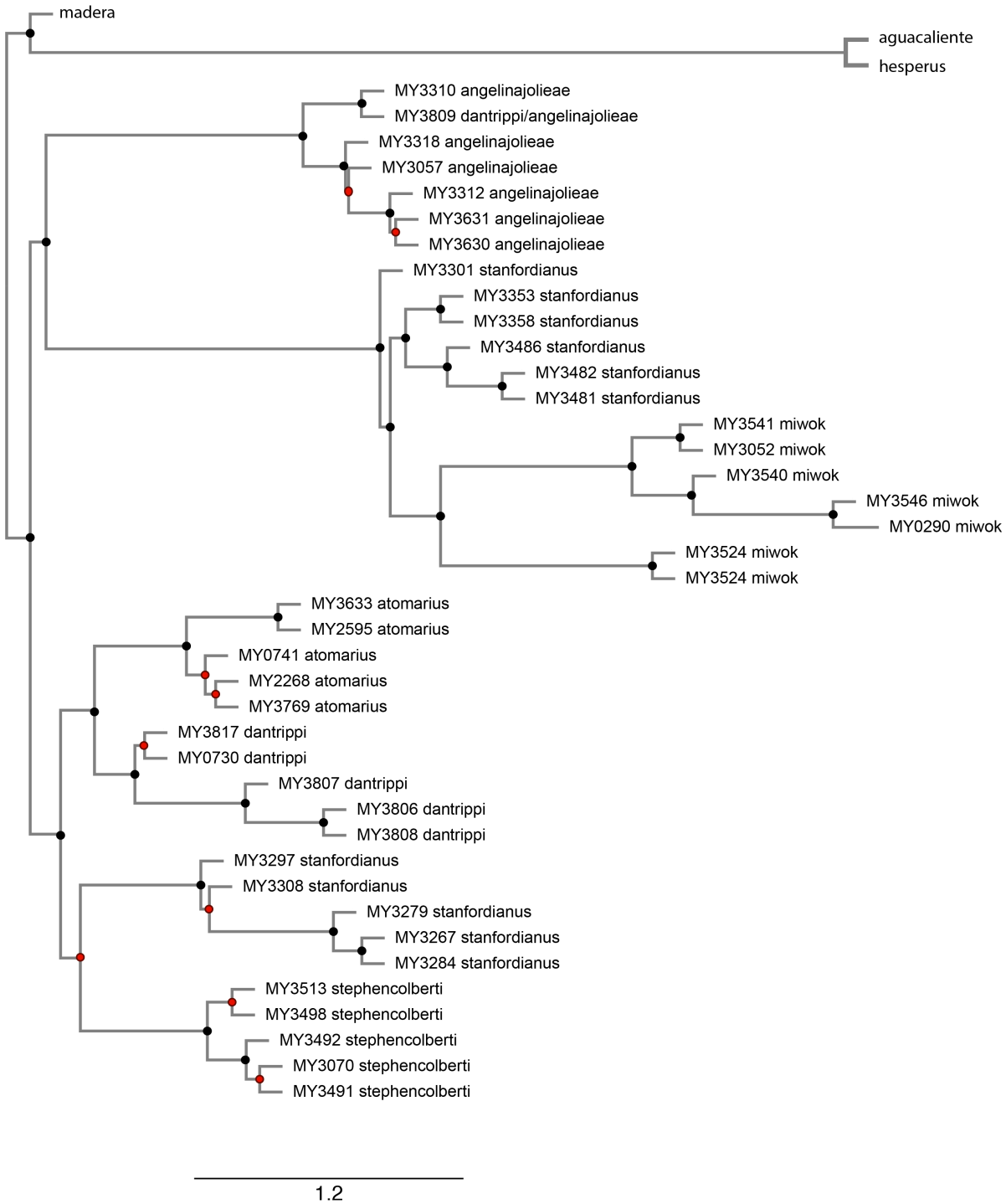

Figure 7: ASTRALII analysis of the full 644 AHE loci set, gene-resampling method; branch supports represent local posterior probabilities. Black dots represent full support (>90 lpp), red less than 90.

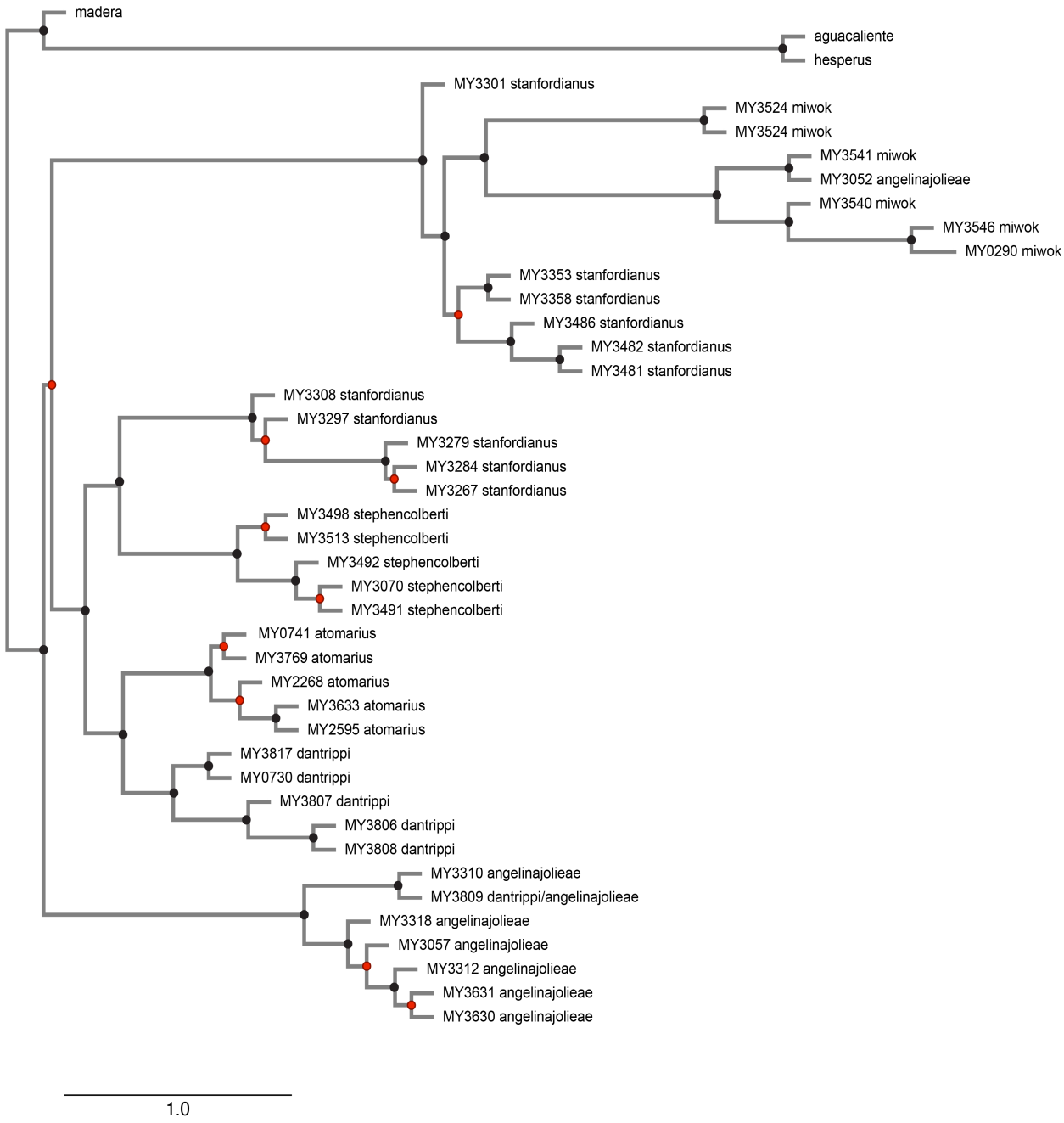

Figure 8: ASTRALII analysis of 144 AHE loci set, gene-resampling method; branch supports represent local posterior probabilities. Black dots represent full support (>90 lpp), red less than 90.

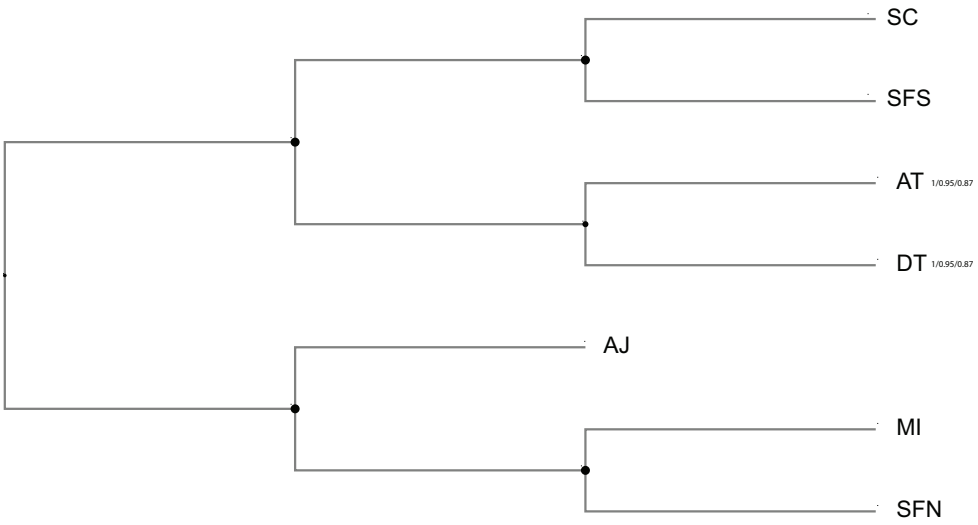

Figure 9: Summarized BPP3 topology with fully supported delimited species. Replicate variation in the guided analysis noted to the right of species abbreviations. SC=stephencolberti, SFS=stanfordianus South, AT=atomarius, DT=dantrippi, AJ=angelinajolieae, MI=miwok, SFN=stanfordianus North.

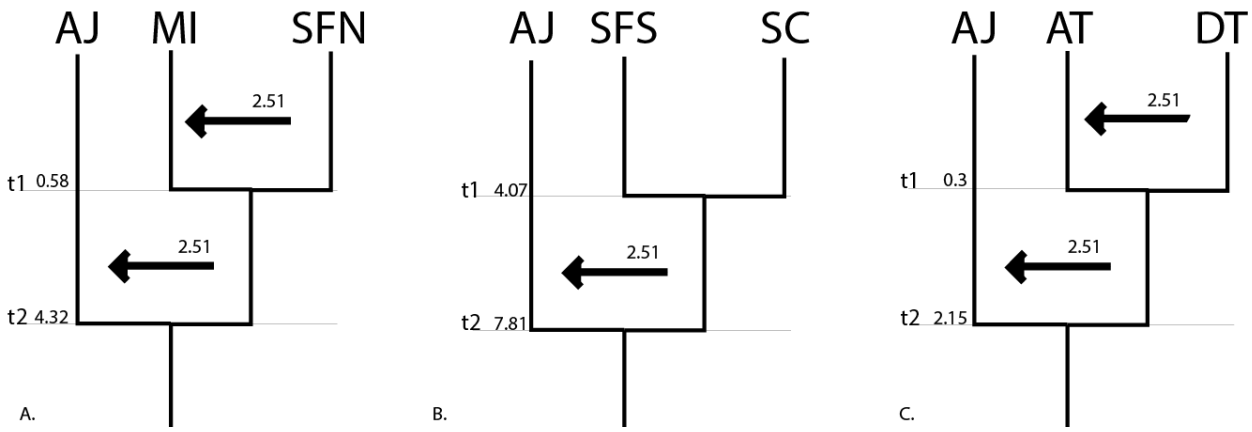

Figure 10: Summary of PHRAPL analyses for three geographic subsets of data. Top assymetric models for North (A), Middle (B), and Southern (C) subsets of species. t values indicate coalescent times, arrows indicate direction of migration. AJ=angelinajolieae, SFS= stanfordianus South, MI=miwok, SC=stephencolberti, AT=atomarius, DT=dantrippi.

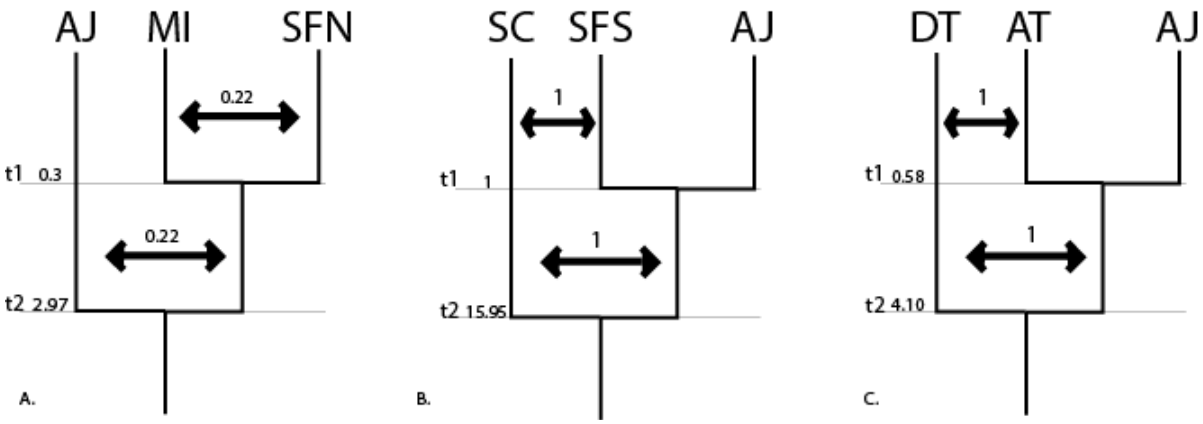

Figure 11: Unconstrained PHRAPL analysis for geographic subsets A) North B)Mid and C) South

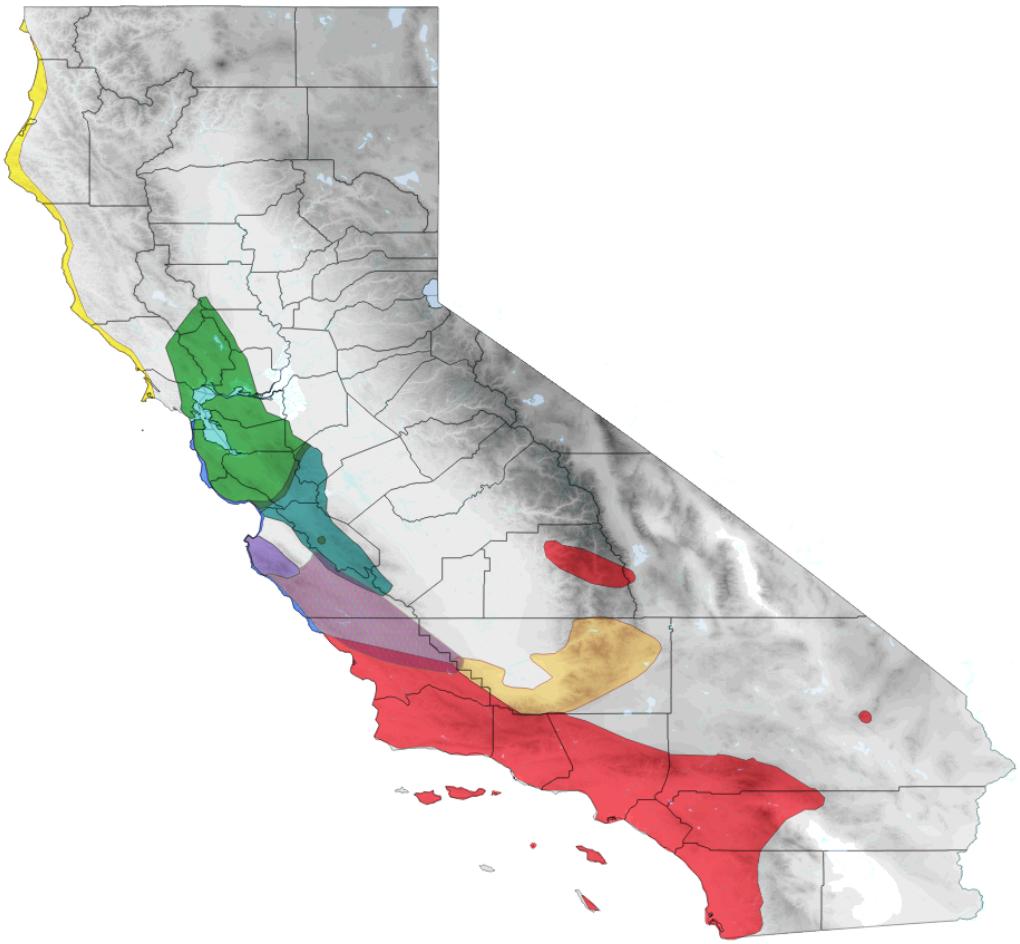

Figure12: Map with refined species distributions. Red=atomarius, Orange=dantrippi, Yellow=miwok, Green=stanfordianus North, Teal=stanfordianus South, Blue=stephencolberti, Purple=angelinajolieae, Purple Hatching= potential anjelinajoliea range

Chapter III
Transcriptome characterization of the atomarius species complex: detecting signals of selection in dune endemic species

Background:

Trapdoor spiders belong to an ancient lineage of chelicerate arthropods, the spider suborder Mygalomorphae, which includes charismatic fauna such as tarantulas and Australian funnel-web spiders. These spiders are sedentary, fossorial predators, which build silk-lined burrows; females are non-vagile and mature males emerge seasonally to search for females (Bond et al., 2012). Mygalomorph spiders contain considerably less extant species diversity (348 genera, 3846 species) than their Araneomorph relatives (3,732 genera, 44,534 species) (WSC, 2018), and have historically received less attention in the scientific literature. They present several challenges to researchers interested in performing rigorous experimental studies; they can be difficult to collect in large numbers from across their ranges, they are remarkably long lived and take years to reach sexual maturity (Main, 1978; Bond et al., 2001), and until recently very few genetic markers and no genomic resources were available for the suborder (but see Sanggaard et al., 2014; Hamilton et al., 2016). At the same time, they pose considerable appeal in terms of investigating physiological adaptation to harsh environments (Mason et al., 2013), longevity (Criscuolo et al., 2010), evolution and application of novel venom peptides (Diego-Garcia et al., 2016), chemosensory systems (Perez-Miles et al., 2017), genome size evolution (Gregory & Shorthouse, 2003), and historical biogeography to name a few.

With technological advances in sequencing, opportunities to begin generating genomic resources for non-model arthropods have increased substantially, from only 3 genomes in 2002 to over 540 at varying levels of completeness (27 at the chromosome level, 63 at the contig level, 458 at the scaffold level; https://www.ncbi.nlm.nih.gov/genome/browse#!/eukaryotes/). Even

more accessible methods for non-model organisms such as phylogenomics, targeted genomic sequencing approaches, and comparative transcriptome efforts have begun to provide foundational datasets which may help resolve long standing evolutionary questions and open new paths of inquiry for insects (Yeates et al., 2016), spiders (Garrison et al., 2016; Wheeler et al., 2018), diplopods (Rodriguez et al., 2018), and other arthropod groups (Schwentner et al., 2017). Within mygalomorphs, second-generation sequencing approaches have recently been applied to the study of venoms (Undheim et al., 2013), chemosensory systems (Frías-López et al., 2015), cryptic speciation (Leavitt et al., 2015), and higher-level systematics (Hedin et al., 2018). At the family level, publicly available sequence data for mygalomorph spiders has increased exponentially in the last five years due to large-scale phylogenomic analyses however; utilization of high-throughput information to search for signatures of selection at the species level is terra incognita in mygalomorph research. The ability to carry out such studies at the species/population interface is hindered by a lack of appropriate foundational genomic datasets, as is the case for many non-model or 'obscure model organisms' (Matz, 2017); only one mygalomorph spider genome has been partially sequenced, for the tarantula *Acanthoscurria geniculata*, but remains in the scaffolding stage (Sanggaard et al., 2014) and has likely been diverging from trapdoor spiders for ~114MY (Garrison et al., 2016). The overarching goal of this study is to build genomic resources and generate preliminary functional annotations for transcriptomes of an ecologically diverse trapdoor spider sister species complex.

The *Aptostichus atomarius* complex is a closely related set of sister species pairs, a sibling species complex, distributed throughout the Coastal Ranges in the California Floristic Province. Of the seven members, two species are chaparral dwelling, two are coastal dune endemics, and three inhabit the inland hills and valleys of central California west of the Central

Valley. The two dune species represent independent colonization of dune habitats, and though they share phenotypic features of light pigmentation and reduced abdominal patterning (Bond & Stockman, 2008), they are not sister taxa (Chapter 2). *Aptostichus miwok* occupies dune habitats north of the San Francisco Bay and *A. stephencolberti* is distributed along beaches further to the south (Figure 1). We have utilized RNAseq derived sequences to generate draft transcriptome assemblies, annotations, and search for gene families under selection within the *A. atomarius* complex; we specifically test for positive selection in detected orthologs along branches of the species tree leading to dune endemic members. We also assess transcriptome level conservation across the complex and between *A. atomarius* members and two outgroup *Aptostichus* species representing varying levels of taxonomic distance from the species complex ingroup.

Materials and Methods:

Adult female spiders were collected from known localities with mitochondrial evidence for clade assignment (Bond, 2012) for five of the six currently recognized species in the *atomarius* complex (*A. atomarius, angelinajolieae*, *A. stephencolberti*, *A. miwok*, and *A. stanfordianus* North); one individual from the putative cryptic species *A. stanfordianus* South (see Chapter 2) was also obtained. Two outgroup taxa, *A. barackobamai* and *A. simus,* were also sampled for this study. After burrow excavation, all spiders were placed in individual containers with sterile tissue wipers molded into a burrow shape, transported back to the lab, and held for two weeks under the same conditions (room temp, minimal light exposure, daily hydration, no food). After a multi-week holding period, spiders were removed from their artificial burrows and flash frozen in preparation for RNA extraction. The prosomal region of each spider was cut diagonally in half and, with the distal portion of one leg, was ground in liquid nitrogen before

being transferred to a tube containing 1mL TRIzol. RNA was extracted following the TRIzol protocol with an additional RNA purification step using the RNeasy kit (Qiagen). Samples were checked for high quality via spectrometry and gel electrophoresis and sent to the Genomic Services Center at HudsonAlpha (Huntsville, Alabama) for paired end sequencing on the Illumina HiSeq platform (50bp, 25-50 million reads). Collection and processing of spiders in this study happened in three pulses – sequencing details, raw sequence statistics, and locality information for each specimen is summarized in Table 1.

Assembly and Assessment of Completeness

Raw sequence reads were processed with the program FastQC to evaluate sequence quality and content. Guided by the FastQC results, residual Illumina adapters were removed with Trimmomatic (Bolger, Lohse, & Usadel, 2014) during assembly. The program Trinity (v2.2.0; Grabherr et al., 2011; Haas et al., 2013) was used to generate de novo assemblies for each of the individuals, using default paired end parameters. To estimate assembly statistics and provide expression level data for downstream interpretation of functional annotations, raw reads were mapped back to their respective assemblies using the programs RSEM (Li & Dewey, 2011) and TransRate (Smith-Unna et al., 2016). PCR duplicates were removed from raw reads using samtools rmdup (Li et al., 2009) prior to final mapping to references to ensure more accurate coverage estimation. TransRate uses the ultrafast alignment algorithm of SNAP (Scalable Nucleotide Alignment Program; Zaharia et al., 2011) to map reads back to transcriptomes and the alignment-free mapping software salmon (Patro et al., 2017) to assign multi-mapping reads and generate coverage values. TransRate generates a filtered subset of contigs based on read coverage evidence as well as descriptive statistics about each assembly. After assembly, 12S-

tRNA Val-16s mitochondrial fragments were extracted and used to match samples to previously sequenced haplotypes and confirm species identities.

BUSCOv3 (Benchmarking Universal Single-Copy Orthologs; Waterhouse et al., 2017; Siman et al., 2015) was used to determine completeness of the assembly relative to a curated, highly conserved set of single-copy orthologs housed in the OrthoDB online database. The BUSCO pipeline first translates and detects open reading frames (ORFs) within a set transcriptome contigs (using TransDecoder; http://transdecoder.github.io), then uses hidden markov models (HMMER; Finn, Clements, & Eddy, 2011) to search the curated ortholog set for matches, accepting those sequences which are recovered as reciprocal best hits to the reference species of choice. For this study BUSCO was used to determine the proportion and quality (complete, fragmented, duplicated) of 2,675 core arthropod (fly reference species) and 1066 core spider (*Parasteatoda* reference) orthologs present in each transcriptome. BUSCO analyses were executed on the CyVerse Discovery Platform (*www.cyverse.org*) for all species.

The transcriptomes were further evaluated for taxonomic identity of sequence clusters using MCSC decontamination (Lafonde-Lapalme et al., 2017). MCSC uses hierarchical clustering approach and incorporates taxonomic information from BLAST (Altschul et al., 1990) hits to the UniRef90 cluster database to determine which sequences likely represent the focal organism and which may represent contaminating organisms. Contamination can arise from sources within and on the surface of the extracted tissues or potentially during sample/library preparation and sequencing via sample bleeding (Mitra et al., 2015). Though the expectation is minimal contamination given the tissue types chosen, MCSC was used to exclude transcripts with no homology to known spider or arthropod transcripts in the final set of contigs. MCSC was employed at the phylum level; Arthropoda best hits were preferentially retained. Taxonomic

distributions based on BLAST hits for each of the species were parsed from the MCSC results and 'good' transcripts represented in both the MCSC and TransRate filtered files were used for downstream ortholog inference.

Functional Annotation

Annotations were added to the full set of transcripts for each species using the Trinotate pipeline. First, untranslated transcriptome sequences and predicted open reading frames for each species were subjected BLAST+ (Camacho et al., 2008) searches of the UniProt peptide database (blastx and blastp respectively). Additional blastp and blastx searches were conducted using proteins predicted from the reference tarantula transcriptome (Sanggaard et al., 2014 Supplementary Data 4) as a database. Next, HMMER was used to search for protein family domains using the PfamA database (Punta et al., 2012), signalP (Petersen et al., 2011) was used to search for signal peptide cleavage sites, tmHMM (Krogh et al., 2001) was used to identify transmembrane regions, and RNAmmer (Lagesen et al., 2007) was used to detect any ribosomal RNA present in the samples. Trinotate output includes eggnog (Powell et al., 2012) and KEGG (Kanehisa et al., 2012) associated terms for all annotated contigs when able. All results were loaded into a boilerplate sqlite database before being exported into a tab-delimited report that could be parsed in downstream analyses.

OrthoFinder (Emms & Kelly, 2015) and the online ortholog visualization tool OrthoVenn (Wang et al., 2015) were used to identify and compare sets of orthologs across the *Aptostichus* samples and within the *atomarius* ingroup. OrthoFinder offers improved accuracy and recovery relative to several other ortholog detection programs by overcoming sequence length biases in ortholog detection (Emms & Kelly, 2015). The full complement of coding sequences predicted from each transcriptome and the filtered set (TransRate/MCSC overlap) was processed with

OrthoFinder to determine orthogroup overlap and identify species-specific orthogroups. OrthoVenn is an online orthology server which combines OrthoMCL, BLAST homology searches of the swissprot reference database, and inparalog detection with orthAgogue (Ekseth, Kuiper, & Mironov, 2013) to generate interactive visualizations of whole genome/transcriptome comparisons. In OrthoVenn, the filtered and translated transcripts were analyzed for the full *A. atomarius* complex ingroup.

Detection of Gene Families Under Selection

The FUSTr pipeline (Families Under Seletction in Transcriptomes; Cole & Brewer, 2017) was used to explore patterns of selection 1) within the *atomarius* complex and 2) within dune endemic species. For detection of genes under selection, the full set of transcripts was utilized for each species under the expectation that rare or lowly expressed transcripts may contribute to a pattern of gene family expression in a biologically meaningful way. This approach provides the maximum amount of transcriptome wide information while still allowing for incorporation of confidence estimates from TransRate, MCSC, and RSEM in post-analysis interpretation of findings if necessary. FUSTr first translates sequences and predicts open reading frames (TransDecoder), infers homology using blastp and the transitive clustering algorithm of SiLix (Miele, Penel, & Duret, 2011), generates multiple sequence alignments of clusters using mafft (Katoh & Standley, 2013), and builds phylogenetic trees for each family using FastTree (Price, Dehal, & Arkin, 2009) prior to detection of selection. In families containing at least 15 members, site-specific tests for positive selection (amino acid level) are performed using codeml v4.9 (Yang, 2007) and log likelihood values are compared to those of models excluding positive selection. The result of FUSTr analysis is a list of gene families detected, and a file highlighting those containing at least one site where the ratio of non-

synonymous to synonymous changes (dN/dS ratios, ω) exceeded 1, indicating strong positive selection.

Tests for positive selection along branches leading to dune endemic species *A. miwok* and *A. stephencolberti* were implemented using the COATS pipeline (unpublished, Brewer in prep), which is designed to examine selection within the context of a species tree. The species tree generated in Chapter 2 with the most corroboration across analyses (Figure 1 legend) was given to the pipeline for the multi-species analysis pathway depicted in Figure 2. Briefly, TransDecoder predicted ORFs are subjected to an all versus all blastp search, reciprocal best hit loci are used to generate fasta files with orthologous sets of loci, orthologous sets are searched using a reference taxon (in our case the dune species *A. stephencolberti*), orthologs are aligned using mafft, pal2nal.pl (Mikita, Torrence, & Bork, 2006) is used to assign codon positions to sequences using the translated ORF and corresponding nucleotide sequences, poorly aligned sites in alignments are masked using Aliscore/Alicut (Kuck, 2009), alignments with too few taxa are removed, and multi-species PAML (Yang, 2007) analyses are performed on the remaining alignments. A selection of representative sequences from alignments of orthogroups under selection (top results of FUSTr and COATS) were submitted to the I-TASSER server (http://zhanglab.ccmb.med.umich.edu/I-TASSER) for automated comparison of tertiary structure to known structural models housed in the PDB (Protein Data Bank).

Results and Discussion:

Raw read counts ranged from ~27 to 61 million paired reads, averaging ~29 million for the 25M read sequencing design (*A. atomarius*, *A. angelinajolieae*, *A. miwok*, *A. stanfordianus* North, and *A. stephencolberti*) and ~49 million for the 50M design (*A. stanfordianus* South, *A. barackobamai*, *A. simus*). Mean base quality scores as assessed by FastQC were >30 for all raw

reads, however post sequencing adapter contamination was detected and removed using Trimmomatic during assembly. Pre- and post-assembly statistics for each transcriptome can be found in Table 1; total number of assembled contiguous sequences ranged from 30,871- 61,516 with a mean length of 636 and average GC content of 40%. *A. stephencolberti* had the fewest contigs (30,871), while *A. stanfordianus* North had the most (61,516). On average, there were ~35,700 unique genes with isoform group size ranging from 2-38. Isoform distribution was less expansive for earlier sequencing events (25M PE samples), group size decreased drastically for all assemblies beyond the 3-isoform category (Figure 3). RSEM mapping rates prior to de-duplication ranged from 71.7-86.6%, with larger more isoform rich transcriptomes averaging 72% and less diverse assemblies averaging 84%. Assessment of completeness via TransRate resulted in 'good' sequence files containing ~17,260 contigs on average. Mapping rates determined by SNAP and salmon were lower than those generated via RSEM with an average mapping rate of 66% and 'good' mapping rates averaging 58%. Mitochondrial matching of samples to previously sequenced localities was successful in all but two cases: *A. atomarius* and *A. stanfordianus* South may represent a previously unrecognized clade of *Aptostichus* occurring south of the *A. angelinajolieae* range (see Figure 1, angelinajolieae-like). This clade was found to be sister to *A. angelinajolieae* in the recent revision of the genus (Bond 2012), but was not explicitly analyzed in the species tree analyses of Chapter 2. Original species names have been retained for the purposes of this study, pending further examination of speciation within the complex.

Completeness as assessed by BUSCO showed that *Aptostichus* transcriptomes were ~64% 'complete' when compared to the *Parasteatoda* reference sequences. The smallest transcriptome, *A. stephencolberti* was the least complete (52%) while *A. stanfordianus* South

was the most (72%). The proportion of single-copy, duplicated, fragmented and missing genes can be seen in Figure 4 for all species. Of the genes missing, 77 were missing from all of the *Aptostichus* transcriptomes. Missing sequences were found to represent 5 functional annotation clusters by the online functional annotation tool DAVID (Huang et al., 2009a; Huang et al., 2009b). Two KEGG pathways were identified, having multiple components missing – the Fanconi anemia and glycerophospholipid metabolism pathways. A table of the associated pathways and IDs in each cluster can be found in the supplemental materials (Supplemental Doc 1).

Decontamination with MCSC revealed high taxonomic affinity with Arthropoda for sequences that had matches to the uniref90 database (Figure 5); however, most transcripts had no similarity to sequences in the database. Despite this, MCSC recovered ~27,247 sequences on average which passed the taxonomy/clustering filter. The full complement of transcripts was processed with OrthoFinder and high confidence sequences representing overlap between MCSC and TransRate were processed with OrthoVenn, generating a rich resource of orthologous clusters for species level comparisons. For the *atomarius* complex ingroup, OrthoFinder assigned 96,946 genes (88.1% of total) to 18,273 orthogroups. Fifty percent of all genes were in orthogroups with 6 or more genes (G50 was 6) and were contained in the largest 6,577 orthogroups (O50 was 6,577). There were 5,770 orthogroups with all species present and 2,127 of these consisted entirely of single-copy genes. When the outgroup taxa were compared as well, OrthoFinder assigned 13,4045 genes (89.1% of total) to 19,773 orthogroups. Fifty percent of all genes were in orthogroups with 8 or more genes (G50 was 8) and were contained in the largest 6,230 orthogroups (O50 was 6230). There were 4,799 orthogroups with all species present and 1,338 of these consisted entirely of single-copy genes. Table 2 shows total numbers of orthologs

(diagonal), species-specific orthogroups (diagonal, parentheses), total orthogroup overlap between species (lower left triangle) and one-to-one ortholog overlap between species (upper right triangle). Uncorrected pairwise distances were calculated for alignments of single copy orthogroups recovered in the OrthoFinder analysis including outgroups (n=1,338) using the EMBOSS utility distmat (Rice, Longden, & Bleasby 2000) and visualized using R (Figure 6). Figure 7 illustrates the *A. atomarius* ingroup overlap of clusters as determined by OrthoVenn. In total, the high confidence filtering of transcripts yielded 1,296 orthogroup clusters with representative sequences from all species; more species-specific clusters were detected with this method (tips of venn diagram) and there were only 717 single copy gene clusters.

FUSTr detected 46 gene families under some degree of positive selection (Supp. Table 1) within the atomarius complex ingroup, with the number of sites under selection ranging from 1 (n=26) to 18 (n=1). Four of the five top clusters under selection were composed of venom related peptides. The cluster of orthologs with the most sites under selection shared significant homology with the ICK (inhibitor cysteine knot) protein family, a group of hyperstable small peptides which have been detected in most spider venom proteomes (King and Hardy, 2013). The specific peptides detected in Aptostichus most closely resemble the Aptotoxins (a.k.a. Cyrtautoxins; Herzig et al., 2010), isolated from the mygalomorph spider Apomastus schlingeri Bond and Opell 2002 with BLAST identities ranging from 42-59% (Figure 8). When the Aptostichus ICK peptide structure was compared to the PDB database, it was found to most resemble U4-hexatoxin-Hi1a with a very high TM-align score of 0.962 (Figure 9). Not only do these venoms act as strong paralytic insecticides, they are remarkably resistant to proteases and environmental degradation (extreme pH, organic solvents, temperature extremes) making them candidates for orally active therapeutics (Saez et al., 2010). The cluster with the second highest

number of sites under selection belonged to the Kunitz family of venom peptides (Figure 10), which are serine protease inhibitors (ArachnoServer; Herzig et al., 2010). Other venom peptides detected in the top 20 families under selection included Techylectin-like homologs (agglutinate in human erythrocytes and Gram+/- bacteria), and Prokinektin-2-like proteins (CsTx-20, neurotoxic enhancer). The cluster with the third highest number of sites under selection was an alpha-tocopherol (vitamin E) transferase family, with 8 sites under strong positive selection. Only two families were found to be under selection in the dune endemic spiders retinol dehydrogenase and Cytochrome P450. Both of these families were also detected in the complete ingroup analysis as well, so this is not likely a dune specific result.

The COATS pipeline revealed 16 orthologous clusters under strong positive selection that met the 0.05 FDR (false discovery rate) threshold cutoff. Six of these groups matched the input species tree topology. Among the six groups with the appropriate species tree topology (Table 3) were Cytochrome P450 2c15 (as in the FUSTr analysis), Niemann Pick C1-like, and Kainate 2 isoform-like (ionotropic glutamate receptor) as identified by NCBI-BLAST. Both Niemann Pick and Kainate/glutamate receptor sequences were detected in a recent distal leg-tissue specific transcriptome analysis of the mygalomorph spider *Macrothele calpeiana*, and may play a role in chemosensory function (Frias-Lopez et al., 2015). *Aptostichus* sequences display strong similarity (64-85% pairwise identity) at the nucleotide level to four of the six chemoreception candidate genes identified from leg tissue in that study (2 Niemann Pick C2 and 2 glutamate receptor genes).

Additionally, the COATS pipeline detected selection in a few proteins belonging to families with some venom associations – sulfotransferase, A disintegrin and metalloproteinase with thrombospondin motif 5 (ADAMTs5), and even cytochrome p450. Sulfotransferase,

thrombin inhibitor/metalloproteinase, and the cytochrome p450 family categories were found to be highly differentially expressed in the salivary gland secretions of the aptly named Australian paralysis tick (*Ixodes holocyclus*; Rodriguez-Valle et al., 2018). Sulfotransferases are also prominently expressed in the venom transcriptome of the Australian scorpion *Urodacus yaschenkoi* (Luna-Ramirez et al., 2015), and ADAMTs5 is phylogenetically closely related and structurally similar to snake venom metalloproteinases (Takeda 2015). Venom peptide evolution in spiders is thought to progress in short bursts, perhaps in response to colonization of novel habitats, followed by long periods of stasis under strong purifying selection. When compared to the venoms of evolutionarily 'young' lineages such as cone snails and snakes, spider venoms display remarkable conservation over large taxonomic distances (Sunagar & Moran, 2015).

For *Aptostichus*, this work provides a foundation for future studies of the connection between speciation, genome-wide divergence, and adaptation to coastal dune habitats. The changes in phenotype seen in dune lineages likely represent the shallowest level of response to dune colonization; for reasons yet to be determined, there appears to be positive selection at the amino acid level for genes related to venom production, metabolism, and sensory systems. To a colonizing organism, dune habitat would present many abiotic and biotic elements that differ from inland habitats and might, over evolutionary timescales, result in signals of selective pressure. Drought, disturbance, and the unique chemical composition of dune soils have led to the development of specific community structures in sand dune ecosystems particularly across the dune-inland gradient (McLachlan, 1991). Implications of *Aptostichus* dune colonization might include 1) higher levels of oxidative stress (from temperature extremes, increased salinity, and a decrease in soil moisture) requiring or resulting in altered metabolic responses 2) a diet that is divergent in species composition from inland habitats and a concurrent decrease in venom

efficacy 3) altered macro and micronutrient availability 4) changes in the microbiome or composition of burrow associated soil bacteria/fungi 5) engineering challenges associated with constructing and maintaining a burrow in shifting sand or 6) an altered signaling landscape due to substrate and vegetation changes resulting in behavioral modifications to male search strategies. Some, or many, of these elements may have led to the observed patterns in dune *Aptostichus* transcripts, however, the complexity of both the habitat and transcriptional patterns will require much more fine-scale analysis to make strong connections between ecology and species-specific adaptations.

Conclusions:

There is great potential in this system for further comparative studies, both between dune species and their inland sisters and between independent dune lineages. Biological and technical replicates will be needed to further facilitate understanding the quantitative differences among species within the *atomarius* complex. Additionally, tissue specific and transcriptomes sampled from males may be very revealing in this group – increasing resolution and specificity of datasets will make inferring function easier and examining males, with their reduced life span, altered phenotype, and epigean life stage, would provide a more complete picture of dune adaptation. To extract the maximal amount of insight from resources like those generated in this study, complementary natural history studies must be carried out as well. What are they eating? When do they move across the landscape and why? How are they communicating, what kinds of interactions are they having with each other? Are there species -specific parasitoid pressures that might impact population dynamics and chemical communication? More detailed knowledge of the constraints imposed upon these spiders and the associated life history strategies they employ

will help guide future work and provide better context for the results of the current study. Guided by this study, areas of interest might include specific differences in composition and nutritional content of diet, abiotic dune parameters, and secretion of volatile compounds which might be associated with inter or intra species signaling.

The transcriptome assemblies presented here represent a novel genomic resource for researchers interested in spider and chelicerate evolution or species level variation in transcription. We have developed a preliminary transcript level reference of shared orthologs for a closely related set of mygalomorph spiders, detected genes under putative positive selection in independent colonizers of dune habitats, and recovered gene families containing novel peptides across the *atomarius* species complex. While they may not represent ideal laboratory subjects and have not received much scientific attention, mygalomorphs harbor a vast amount of evolutionary insight regarding early animal evolution, physiology, and synthesis of potent chemical cocktails. This oversight is now well within our ability to correct, with additional resources being added and curated daily in online databases and software development proceeding at a rapid pace. Developing foundational datasets for even the most obscure organisms is now possible, and may lead to significant advances in our understanding of this group's fascinating and ancient evolutionary history.

References:

Altschul S.F., Gish W., Miller W., Myers E.W., Lipman D.J. (1990). Basic local alignment search tool. *Journal of Molecular Biology*, 215, 403-10.

Bolger, A.M., Lohse, M., & Usadel, B. (2014). Trimmomatic: A flexible trimmer for Illumina Sequence Data. *Bioinformatics*, btu170.

Bond, J.E. (2012). Phylogenetic treatment and taxonomic revision of the trapdoor spider genus Aptostichus Simon (Araneae, Mygalomorphae, Euctenizidae). *ZooKeys*, (252), 1.

Bond, J.E., Hedin, M.C., Ramirez, M.G., & Opell, B.D. (2001). Deep molecular divergence in the absence of morphological and ecological change in the Californian coastal dune endemic trapdoor spider Aptostichus simus. *Molecular Ecology*, 10(4), 899-910.

Bond, J.E., Hendrixson, B.E., Hamilton, C.A., & Hedin, M. (2012). A reconsideration of the classification of the spider infraorder Mygalomorphae (Arachnida: Araneae) based on three nuclear genes and morphology. *PLoS One*, 7(6), e38753.

Bond, J.E., & Stockman, A.K. (2008). An integrative method for delimiting cohesion species: finding the population-species interface in a group of Californian trapdoor spiders with extreme genetic divergence and geographic structuring. *Systematic Biology*, 57(4), 628-646.

Camacho C., Coulouris G., Avagyan V., Ma N., Papadopoulos J., Bealer K., & Madden T.L. (2008). BLAST+: architecture and applications. *BMC Bioinformatics*, 10:421.

Cole, T. J., & Brewer, M. S. (2018). FUSTr: a tool to find gene Families Under Selection in Transcriptomes. *PeerJ*, 6, e4234.

Criscuolo, F., Font-Sala, C., Bouillaud, F., Poulin, N., & Trabalon, M. (2010). Increased ROS production: a component of the longevity equation in the male mygalomorph, Brachypelma albopilosa. *PloS One*, 5(10), e13104.

Diego-García, E., Cologna, C.T., Cassoli, J.S., & Corzo, G. (2016). Spider Transcriptomes from Venom Glands: Molecular Diversity of Ion Channel Toxins and Antimicrobial Peptide Transcripts. *Spider Venoms*, 223-249.

Ekseth, O.K., Kuiper, M., & Mironov, V. (2013). orthAgogue: an agile tool for the rapid prediction of orthology relations. *Bioinformatics*, 30(5), 734-736.

Emms, D.M., & Kelly, S. (2015). OrthoFinder: solving fundamental biases in whole genome comparisons dramatically improves orthogroup inference accuracy. *Genome Biology*, 16(1), 157.

Finn, R.D., Clements, J., & Eddy, S.R. (2011). HMMER web server: interactive sequence similarity searching. *Nucleic Acids Research*,Web Server Issue 39:W29-W37.

Frías-López, C., Almeida, F.C., Guirao-Rico, S., Vizueta, J., Sánchez-Gracia, A., Arnedo, M.A., & Rozas, J. (2015). Comparative analysis of tissue-specific transcriptomes in the funnel-web spider Macrothele calpeiana (Araneae, Hexathelidae). *PeerJ*, 3, e1064.

Garrison, N.L., Rodriguez, J., Agnarsson, I., Coddington, J.A., Griswold, C.E., Hamilton, C.A., Hedin, M., Kocot, K.M., Ledford, J.M., & Bond, J.E. (2016). Spider phylogenomics: untangling the Spider Tree of Life. *PeerJ*, 4, e1719.

Grabherr M.G., Haas B.J., Yassour M., Levin J.Z., Thompson D.A., Amit I., Adiconis X., Fan L., Raychowdhury R., Zeng Q., Chen Z., Mauceli E., Hacohen N., Gnirke A., Rhind N., di Palma F., Birren B.W., Nusbaum C., Lindblad-Toh K., Friedman N., & Regev A. (2011). Full-length transcriptome assembly from RNA-Seq data without a reference genome. *Nature Biotechnology,* 29(7):644-652

Gregory, T.R., & Shorthouse, D.P. (2003). Genome sizes of spiders. Journal of Heredity, 94(4), 285-290.

Haas, B.J., Papanicolaou, A., Yassour, M., Grabherr, M., Blood, P.D., Bowden, J., Couger, B.M., Eccles, D., Li, B., Lieber, M., MacManes, M.D., Ott, M., Orvis, J., Pochet, N., Strozzi, F., Weeks, N., Westerman, R., William, T., Dewey, C.N., Henschel, R., LeDuc, R.D., Friedman, N., & Regev, A. (2013). De novo transcript sequence reconstruction from RNA-seq using the Trinity platform for reference generation and analysis. *Nature Protocols*, 8(8), 1494.

Hamilton, C.A., Lemmon, A.R., Lemmon, E.M., & Bond, J.E. (2016). Expanding anchored hybrid enrichment to resolve both deep and shallow relationships within the spider tree of life. *BMC Evolutionary Biology*, 16(1), 212.

Hedin, M., Derkarabetian, S., Ramírez, M.J., Vink, C., & Bond, J.E. (2018). Phylogenomic reclassification of the world's most venomous spiders (Mygalomorphae, Atracinae), with implications for venom evolution. *Scientific Reports*, 8(1), 1636.

Herzig, V., Wood, D.L., Newell, F., Chaumeil, P.A., Kaas, Q., Binford, G.J., Nicholson, G.M, Gorse, D., & King, G.F. (2010). ArachnoServer 2.0, an updated online resource for spider toxin sequences and structures. *Nucleic Acids Research*, 39, D653-D657.

Huang D.W., Sherman B.T., & Lempicki R.A. (2009). Systematic and integrative analysis of large gene lists using DAVID Bioinformatics Resources. *Nature Protocols*, 4(1):44-57.

Huang D.W., Sherman B.T., & Lempicki R.A. (2009). Bioinformatics enrichment tools: paths toward the comprehensive functional analysis of large gene lists. *Nucleic Acids Research*, 37(1), 1-13.

Kanehisa, M., Goto, S., Sato, Y., Furumichi, M., and Tanabe, M. (2012). KEGG for integration and interpretation of large-scale molecular datasets. *Nucleic Acids Research*, 40, D109-D114.

Katoh, K., & Standley, D.M. (2013). MAFFT multiple sequence alignment software version 7: improvements in performance and usability. *Molecular Biology and Evolution*, 30(4), 772-780.

King, G.F., & Hardy, M.C. (2013). Spider-venom peptides: structure, pharmacology, and potential for control of insect pests. *Annual Review of Entomology*, 58, 475-496.

Krogh A., Larsson B., von Heijne G., Sonnhammer E.L. (2001). Predicting transmembrane protein topology with a hidden Markov model: application to complete genomes. *Journal of Molecular Biology*, 305(3), 567-80.

Kück, P. (2009). ALICUT: a Perlscript which cuts ALISCORE identified RSS. Department of Bioinformatics, Zoologisches Forschungsmuseum A. Koenig (ZFMK), Bonn, Germany, version, 2.

Lafond-Lapalme, J., Duceppe, M.O., Wang, S., Moffett, P., & Mimee, B. (2017). A new method for decontamination of de novo transcriptomes using a hierarchical clustering algorithm. *Bioinformatics*, 33(9), 1293-1300.

Lagesen, K., Hallin, P.F., Rodland, E., Staerfeldt, H.H., Rognes, T., & Ussery, D.W. (2007). RNammer: consistent annotation of rRNA genes in genomic sequences. *Nucleic Acids Research*, 35(9), 3100-3108.

Leavitt, D.H., Starrett, J., Westphal, M.F., & Hedin, M. (2015). Multilocus sequence data reveal dozens of putative cryptic species in a radiation of endemic Californian mygalomorph spiders (Araneae, Mygalomorphae, Nemesiidae). *Molecular Phylogenetics and Evolution*, 91, 56-67.

Li, B., & Dewey, C.N. (2011). RSEM: accurate transcript quantification from RNA-Seq data with or without a reference genome. *BMC Bioinformatics*, 12(1), 323.

Li, H., Handsaker, B., Wysoker, A., Fennell, T., Ruan, J., Homer, N., Marth G., Abecasis, G.,& Durbin, R. (2009). The sequence alignment/map format and SAMtools. *Bioinformatics*, 25(16), 2078-2079.

Luna-Ramírez, K., Quintero-Hernández, V., Juárez-González, V.R., & Possani, L.D. (2015). Whole transcriptome of the venom gland from Urodacus yaschenkoi scorpion. *PloS One*, 10(5), e0127883.

Main, B.Y. (1978). Biology of the arid-adapted Australian trapdoor spider *Anidiops villosus* (rainbow). *Bulletin of the British Arachnological Society*, 4, 161-175.

Mason, L.D., Tomlinson, S., Withers, P.C., & Main, B.Y. (2013). Thermal and hygric physiology of Australian burrowing mygalomorph spiders (*Aganippe spp*.). *Journal of Comparative Physiology B*, 183(1), 71-82.

Matz, M.V. (2017). Fantastic beasts and how to sequence them: ecological genomics for obscure model organisms. *Nature*, 36(37), 38.

McLachlan, A. (1991). Ecology of coastal dune fauna. *Journal of Arid Environments*, 21, 229-243.

Miele, V., Penel, S., & Duret, L. (2011). Ultra-fast sequence clustering from similarity networks with SiLiX. *BMC Bioinformatics*, 12(1), 116.

Mitra, A., Skrzypczak, M., Ginalski, K., & Rowicka, M. (2015). Strategies for achieving high sequencing accuracy for low diversity samples and avoiding sample bleeding using illumina platform. *PloS One*, 10(4), e0120520.

Patro R., Duggal G., Love M.I., Irizarry R.A., Kingsford C. (2017). Salmon: fast and bias-aware quantification of transcript expression using dual-phase inference. *Nature Methods*, 14(4):417-419. doi:10.1038/nmeth.4197.

Pérez-Miles, F., Guadanucci, J. P.L., Jurgilas, J.P., Becco, R., & Perafán, C. (2017). Morphology and evolution of scopula, pseudoscopula and claw tufts in Mygalomorphae (Araneae). *Zoomorphology*, 136(4), 435-459.

Petersen T.N., Brunak S., von Heijne, G., & Nielsen, H. (2011). SignalP 4.0: discriminating signal peptides from transmembrane regions. *Nature Methods*, 8, 785-786.

Powell, S., Szklarczyk, D., Trachana, K., Roth, A., Kuhn. M., Muller, J., Arnold, R., Rattei, T., Letunic, I., Doerks, T., Jensen, L.J., von Mering, C., & Bork, P. (2012). eggNOG v3.0: orthologous groups covering 1133 organisms at 41 different taxonomic ranges. *Nucleic Acids Research*, 40(Database Issue), D284-9.

Price, M.N., Dehal, P.S., & Arkin, A.P. (2009). FastTree: computing large minimum evolution trees with profiles instead of a distance matrix. *Molecular biology and evolution*, 26(7), 1641-1650.

Punta, P.C. Coggill, R.Y. Eberhardt, J. Mistry, J. Tate, C. Boursnell, N. Pang, K. Forslund, Ceric, J. Clements, A. Heger, L. Holm, E.L.L. Sonnhammer, S.R. Eddy, A. Bateman, R.D. Finn. (2012). The Pfam protein families database. *Nucleic Acids Research*, 40(Database Issue), D290-D301

Rodriguez, J., Jones, T.H., Sierwald, P., Marek, P.E., Shear, W.A., Brewer, M.S., Kocot, K.M. & Bond, J.E. (2018). Step-wise evolution of complex chemical defenses in millipedes: a phylogenomic approach. *Scientific Reports*, 8(1), 3209.

Saez, N.J., Senff, S., Jensen, J.E., Er, S.Y., Herzig, V., Rash, L.D., & King, G.F. (2010). Spider-venom peptides as therapeutics. *Toxins*, 2(12), 2851-2871.

Sanggaard, K.W., Bechsgaard, J.S., Fang, X., Duan, J., Dyrlund, T.F., Gupta, V., ... & Han, L. (2014). Spider genomes provide insight into composition and evolution of venom and silk. *Nature communications*, 5, 3765.

Schlinger, E.I. (1987). The biology of Acroceridae (Diptera): True endoparasitoids of spiders. Pp. 319-326, In Ecophysiology of Spiders. (W. Nentwig, ed.). Springer-Verlag, Berlin.

Schwentner, M., Combosch, D.J., Nelson, J.P., & Giribet, G. (2017). A phylogenomic solution to the origin of insects by resolving crustacean-hexapod relationships. *Current Biology*, 27(12), 1818-1824.

Simão, F.A., Waterhouse, R.M., Ioannidis, P., Kriventseva, E.V., & Zdobnov, E.M. (2015). BUSCO: assessing genome assembly and annotation completeness with single-copy orthologs. *Bioinformatics*, 31(19), 3210-3212.

Smith-Unna R.D., Boursnell C.,Patro R., Hibberd J.M., Kelly S. (2016). TransRate: reference free quality assessment of de-novo transcriptome assemblies. *Genome Research* doi: http://dx.doi.org/10.1101/gr.196469.115

Sunagar, K., & Moran, Y. (2015). The rise and fall of an evolutionary innovation: contrasting strategies of venom evolution in ancient and young animals. *PLoS Genetics,* 11(10), e1005596.

Suyama, M., Torrents, D., & Bork, P. (2006). PAL2NAL: robust conversion of protein sequence alignments into the corresponding codon alignments. *Nucleic Acids Research*, 34, W609-W612.

Takeda, S. (2016). ADAM and ADAMTS family proteins and snake venom metalloproteinases: A structural overview. *Toxins*, 8(5), 155.

Rice, P., Longden, I., & Bleasby, A. (2000). EMBOSS: the European molecular biology open software suite.

Rodriguez-Valle, M., Moolhuijzen, P., Barrero, R.A., Ong, C.T., Busch, G., Karbanowicz, T., Booth, M., Clark, R., Koehback, J., Ijaz, H., Broady, K., Agnew, K., Knowles, A.G., Bellgard, M.I., & Tabor, A.E. (2018). Transcriptome and toxin family analysis of the paralysis tick, Ixodes holocyclus. *International Journal for Parasitology*, 48(1), 71-82.

Undheim, E.A., Sunagar, K., Herzig, V., Kely, L., Low, D.H., Jackson, T.N., Jones, A., Kurniawan, N., King, G.F., Ali, S.A., Antunes, A., Ruder, T., & Fry B.G. (2013). A proteomics and transcriptomics investigation of the venom from the barychelid spider Trittame loki (brush-foot trapdoor). *Toxins*, 5(12), 2488-2503.

Wang, Y., Coleman-Derr, D., Chen, G., & Gu, Y. Q. (2015). OrthoVenn: a web server for genome wide comparison and annotation of orthologous clusters across multiple species. *Nucleic Acids Research*, 43(W1), W78-W84.

Waterhouse, R.M., Seppey, M., Simão, F.A., Manni, M., Ioannidis, P., Klioutchnikov, G., Kriventseva, E.V., & Zdobnov, E.M. (2017). BUSCO applications from quality assessments to gene prediction and phylogenomics. *Molecular biology and evolution*, 35(3), 543-548.

Wheeler, W.C., Coddington, J.A., Crowley, L.M., Dimitrov, D., Goloboff, P.A., Griswold, C.E., et al. (2017). The spider tree of life: phylogeny of Araneae based on target gene analyses from an extensive taxon sampling. *Cladistics*, 33(6), 574-616.

World Spider Catalog (2018). World Spider Catalog. Natural History Museum Bern, online at http://wsc.nmbe.ch, version 19.0, accessed on 1 March 2018. doi: 10.24436/2

Yang, Z. (2007). PAML 4: phylogenetic analysis by maximum likelihood. *Molecular Biology and Evolution*, 24(8), 1586-1591.

Yeates, D.K., Meusemann, K., Trautwein, M., Wiegmann, B., & Zwick, A. (2016). Power, resolution and bias: recent advances in insect phylogeny driven by the genomic revolution. *Current Opinion in Insect Science*, 13, 16-23.

Zaharia M., Bolosky W.J., Curtis K., Fox A., Patterson D., Shenker S., Stoica I., Karp R.M., & Sittler, T. (2011). Faster and More Accurate Sequence Alignment with SNAP. arXiv:1111.5572v1

Table 1: Sequencing metadata and annotation results

Sample ID	MY4009	AUMS62	AUMS20	AUMS29	AUMS33	AUMS20723	AUMS01	AUMS22
Species ID	atomarius	angelinajolieae	stephencolberti	miwok	stanfordianus_N	stanfordianus_S	barackobamai	simus
Design	25M,PE	25M,PE	25M,PE	25M,PE	25M,PE	50M,PE	50M,PE	50M,PE
Sequencing ID	SL7743	SL10683	SL10681	SL10684	SL10682	SL267690	SL267688	SL267689
Sequencer	D09NRACXX	C0EFRACXX	C0EFRACXX	C0EFRACXX	C0EFRACXX	CBM18ANXX	CBM18ANXX	CBM18ANXX
Read Number	27431535	30880739	30904990	28351749	28168870	67199206	58216062	50721762
Read Length	50	50	50	50	50	50	50	50
Contigs	35444	46796	30871	47390	61516	50708	43524	36628
Genes	34781	45664	30227	30340	58265	38912	34635	30340
ORFs	14714	17997	14717	18348	21229	23075	21709	18577
UniProt (blastx)	11432	13499	11519	13397	16348	15645	15100	13296
UniProt (blastp)	8226	9880	8415	9905	11546	10996	10801	9334
Tarantula	17186	20201	16804	20307	25580	23724	22085	19607
UniRef90	14257	17186	14300	17177	21334	20207	19118	16836
lat	35.41695	36.571374	36.704522	38.307402	38.417361	36.432667	38.70425	36.704522
long	-120.55722	-121.904289	-121.803911	-123.053548	-122.662169	-121.228455	-122.93653	-121.803911

Table 2: Orthofinder result -- total numbers of orthologs (diagonal), species-specific orthogroups (diagonal, parentheses), total orthogroup overlap between species (lower left triangle) and one-to-one ortholog overlap between species (upper right triangle).

	BO	SM	AJ	AT	MI	SFN	SFS	SC
BO	18918 (13)	6291	7261	6590	7515	7223	7825	6119
SM	8470	14946 (14)	5871	5511	6103	5852	6095	5194
AJ	9498	7980	16580 (1)	7502	8402	8338	8169	6938
AT	8497	7327	8896	13872 (2)	7332	7258	7057	6563
MI	9635	8077	10047	8750	16710 (5)	8678	7996	7232
SFN	9808	8298	10394	8942	10733	19008 (5)	7769	6873
SFS	10236	8394	10553	9116	10232	10511	20503 (9)	6318
SC	8032	6926	8362	7787	8623	8548	8246	13508 (3)

Loci	Length	LRT.p.value	fdr	Sp_tree	top blast ID
AM-stephen-m.10023	77	1.15E-22	4.37E-19	-	hypothetical protein
stephen-m.7645	1954	1.14E-15	2.16E-12	-	myosin heavy chain iX7
AM-stephen-m.12020	144	2.41E-15	3.04E-12	-	sulfotransferase 1c2
AM-stephen-m.1363	153	1.76E-12	1.66E-09	-	disintegrin and metalloproteinase with thrombospondin modifs 5
AM-stephen-m.6082	322	1.74E-07	0.000131809	+	Niemann Pick C1
AM-stephen-m.774	459	2.52E-07	0.000158774	+	cytochrome p450 2c15
AM-stephen-m.10656	850	0.000002631	0.001422639	+	glutamate receptor ionotropic, kainate 2 isoform X1
AM-stephen-m.2039	259	4.91E-06	0.00232515	-	Brain-specific angiogenisis inhibitor 1 associated protein 2-like isoform X1
AM-stephen-m.5533	331	0.000016753	0.00704557	+	Platelet-activating factor acetylhydrolase isoform X2
AM-stephen-m.1654	84	2.44E-05	0.008695113	-	hp B7P43 GO7732
AM-stephen-m.649	78	2.53E-05	0.008695113	-	F36G3.2-like, acetyltransferase family
AM-stephen-m.9849	362	4.65E-05	0.014675114	+	RNA exonuclease 1-like protein
AM-stephen-m.1196	263	0.000108407	0.031563173	-	FMRFamide receptor-like, neuropeptide
stephen-m.8284	310	0.000152592	0.041254399	+	Hadh, fatty acid beta-oxidization
AM-stephen-m.5873	189	0.000191395	0.048295347	-	RPABC1 dna directed rna polymerase

Table 2: COATS top 20 families under positive selection, yellow highlights indicate agreement with species tree, green chemosensory function, red venom-related peptides.

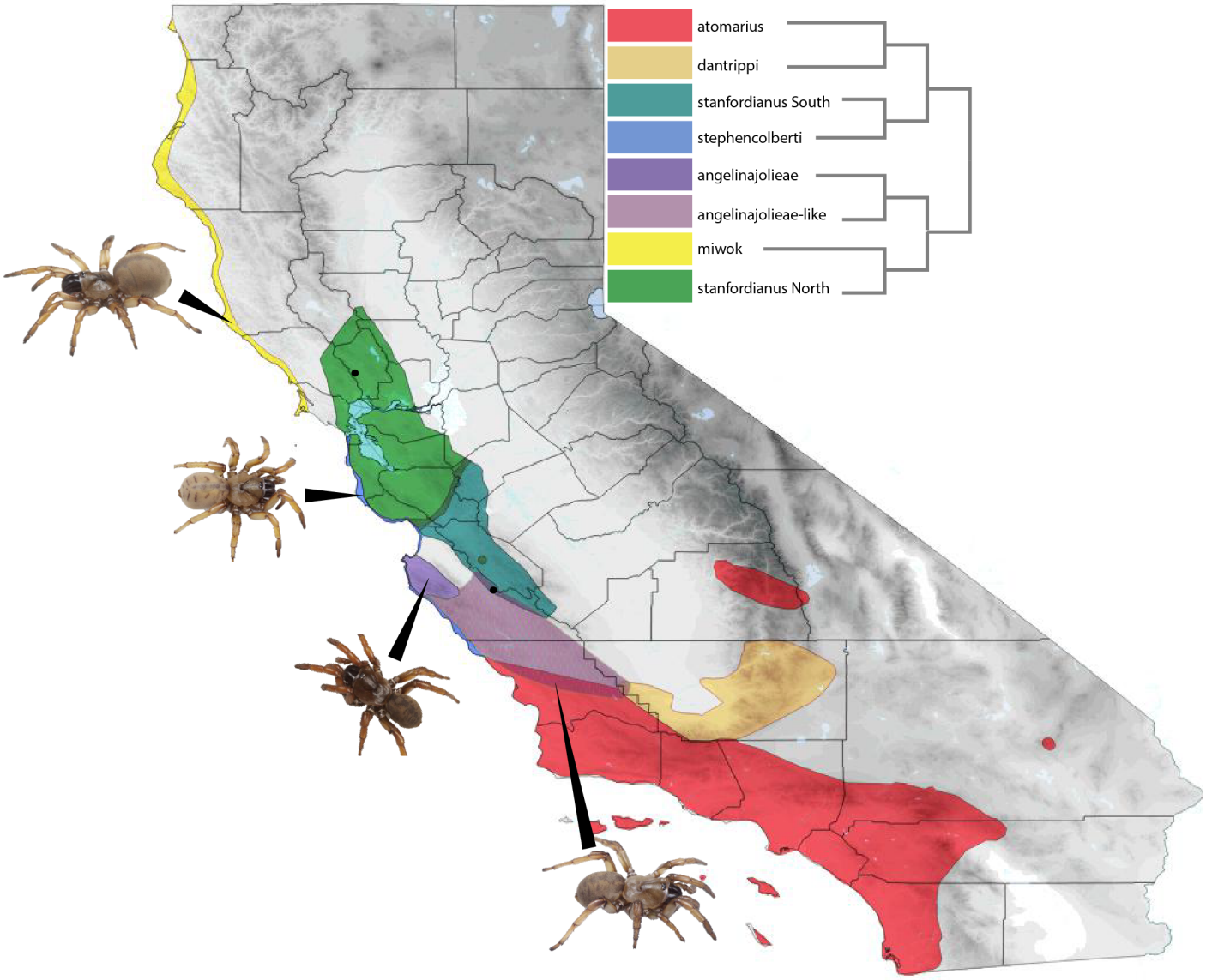

Figure 1: Generalized distribution map of atomarius complex, sampling locations of representative transcriptomes indicated with arrows and black dots. Putative species tree and delimitations in legend correspond to map colors. Pictured from top left to bottom right: A. miwok, A. stephencolberti, A. angelinajolieae, and A. atomarius.

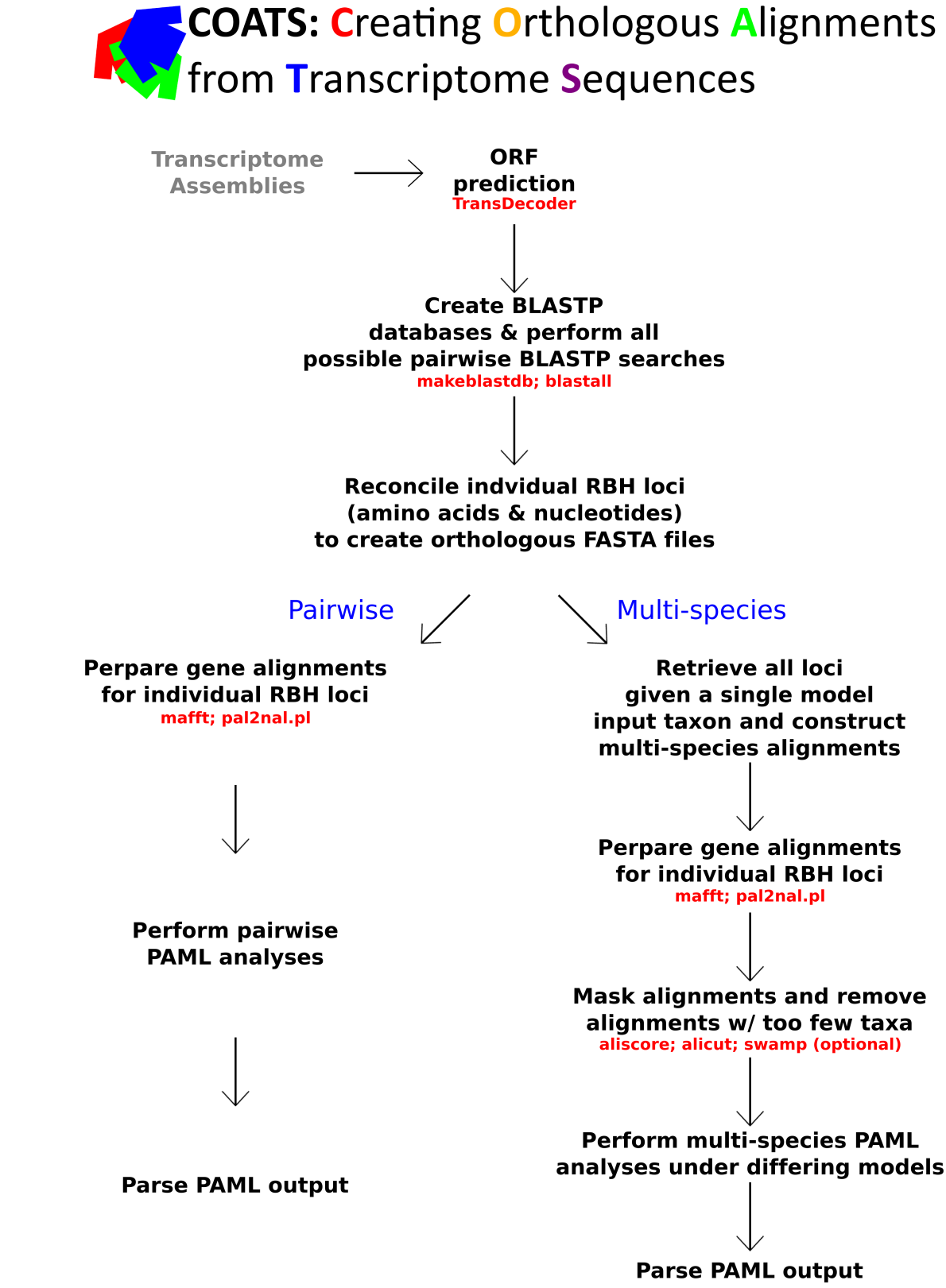

Figure 2: COATS pipeline summary

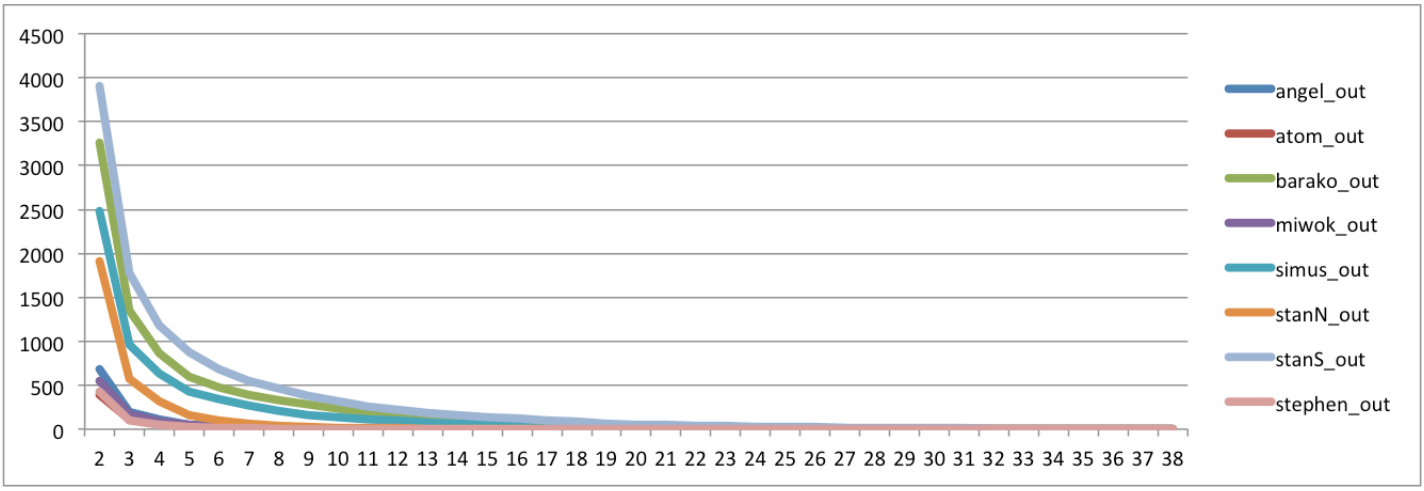

Figure 3: Isoform count distribution of assembled transcriptomes. x axis = number of genes; y axis = number of isoforms associated with genes

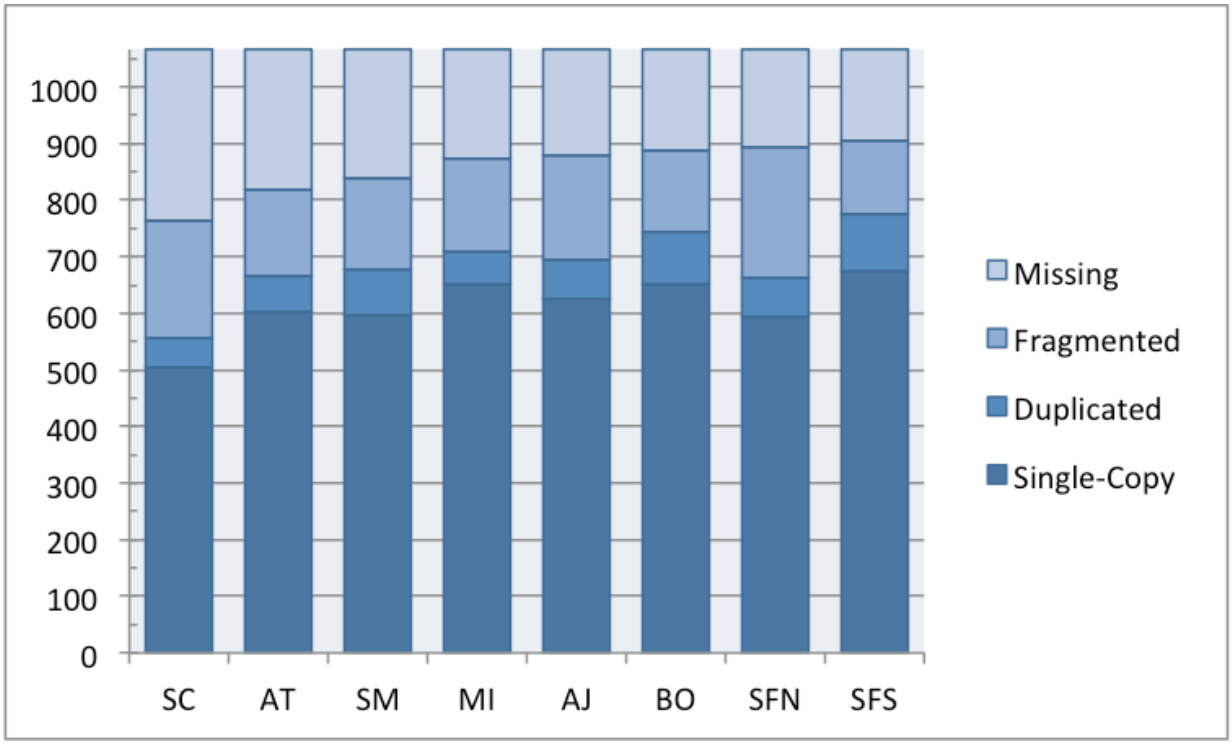

Figure 4: BUSCO completeness compared to 1066 Parasteatoda reference genes.

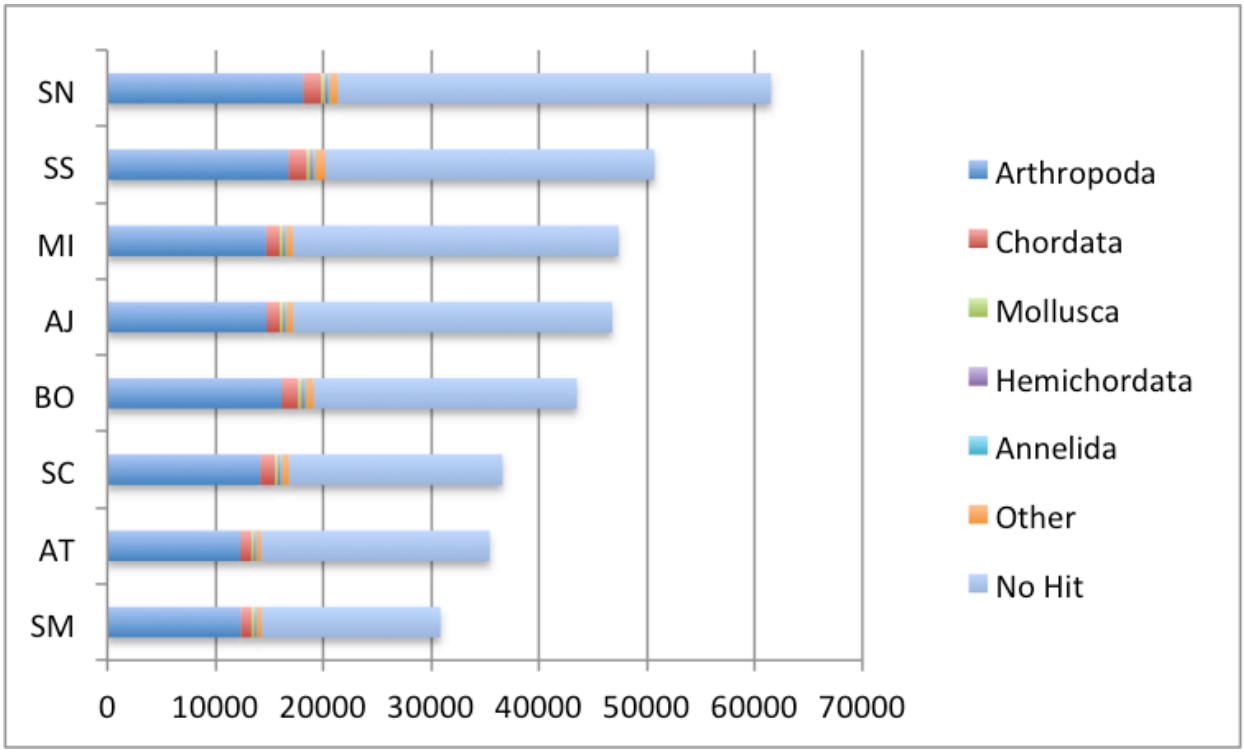

Figure 5: Taxonomic distribution as determined by MCSC decontamination

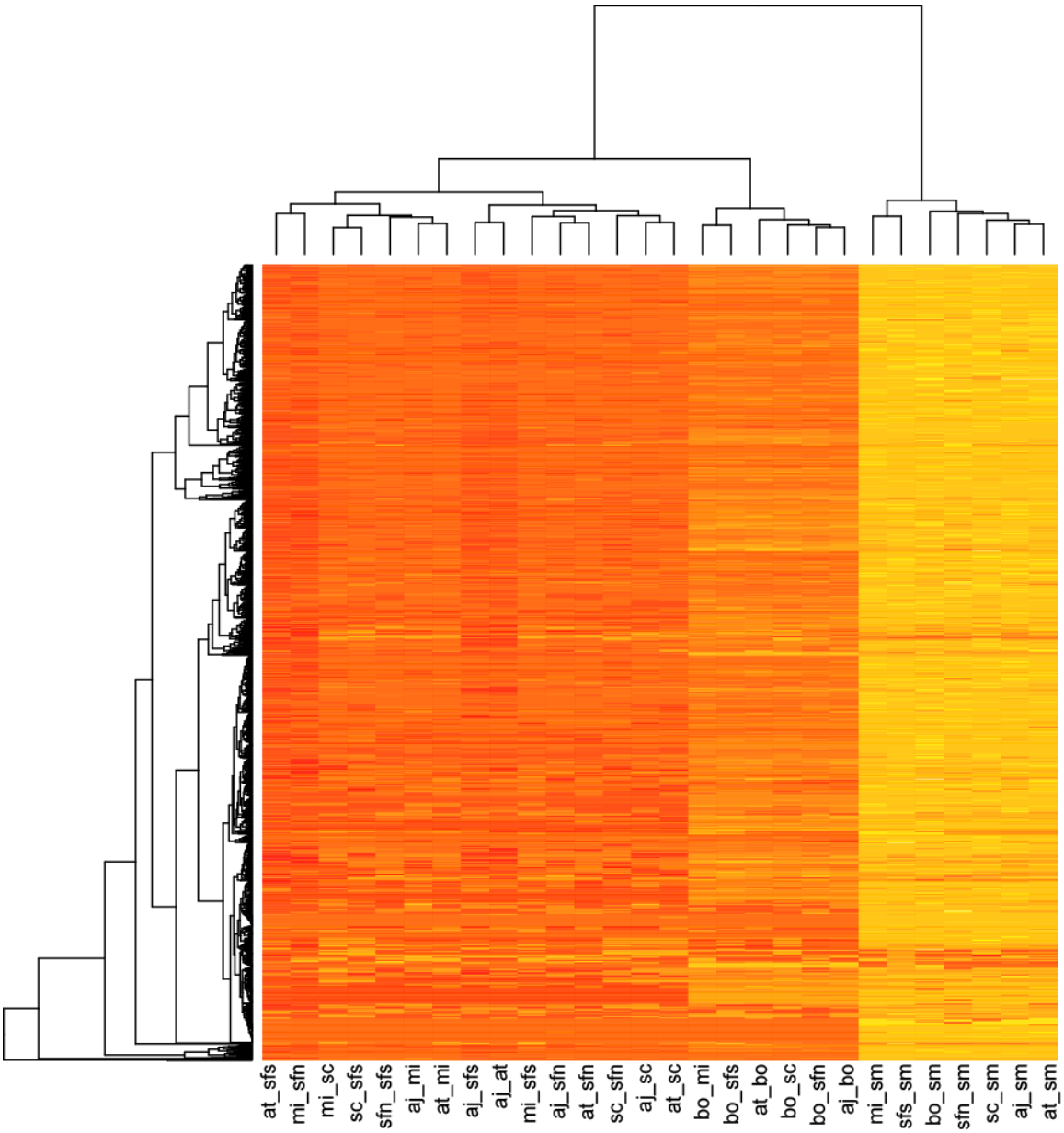

Figure 6: Heatmap of uncorrected pairwise divergence values for each single copy orthogroup detected by OrthoFinder in the analysis including outgroups. red=low, yellow=high. At=atomarius, aj=angelinajolieae, bo=barackobamai, sc=stephencolberti, sfn=stanfordianus North, sfs=stanfordianus South, mi=miwok, sm=simus.

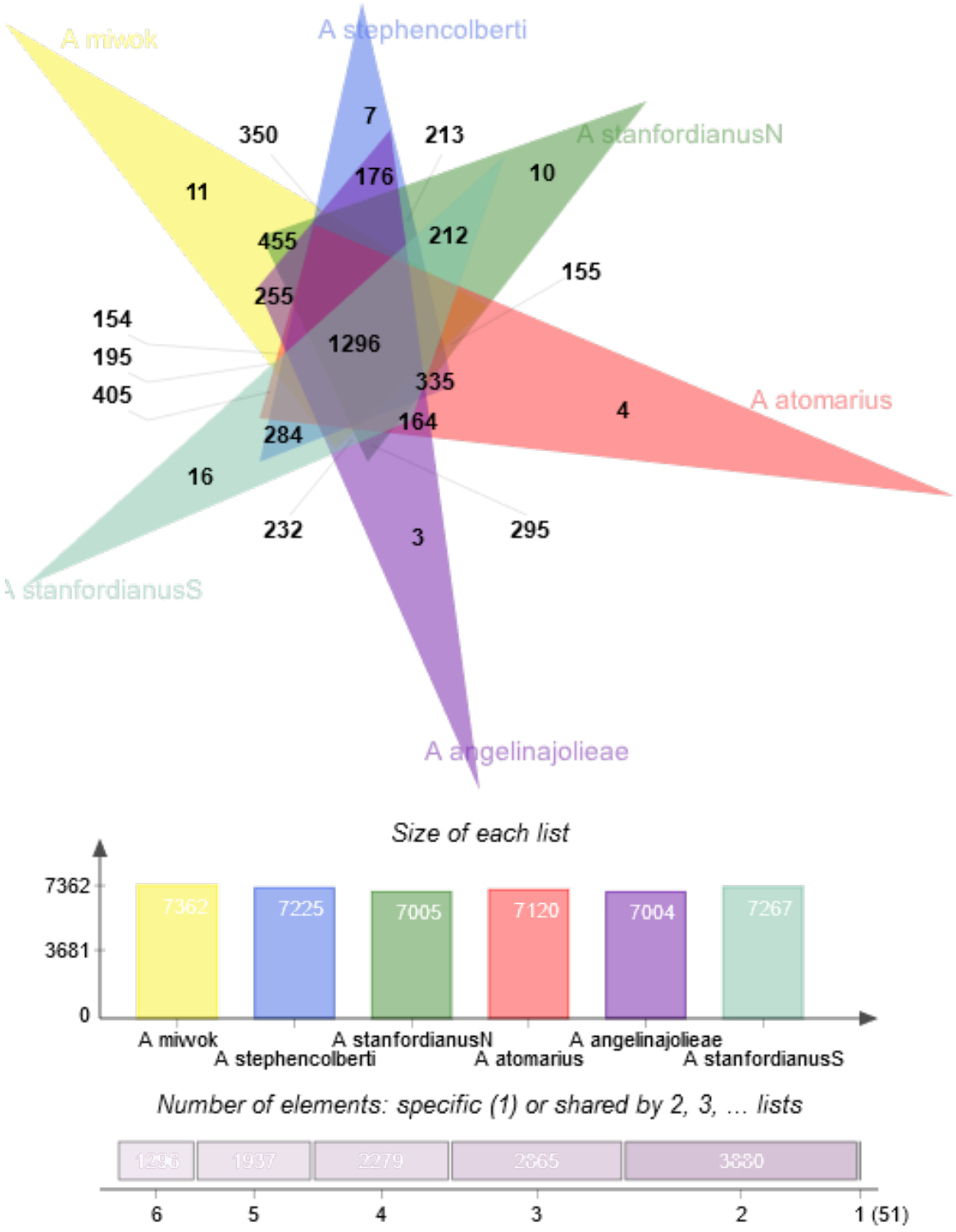

Figure 7: OrthoVenn output of total ingroup analysis

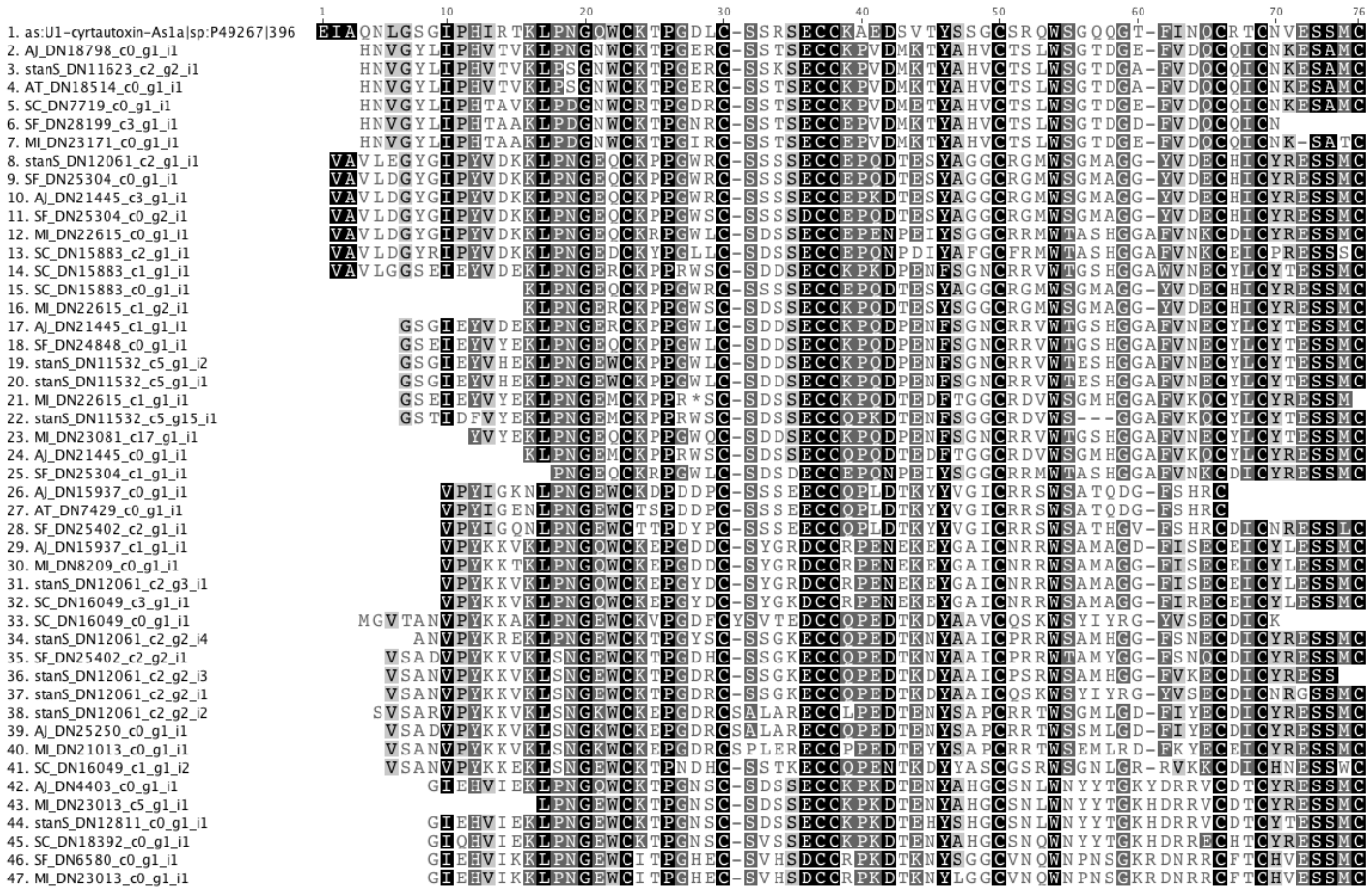

Figure 8: MSA of Aptostichus ICK family peptides to best hit from ArachnoServer database

Figure 9: TM-hmm alignment of representative Aptostichus ICK (colored cartoon structure) to best PDB structural hit (purple line)

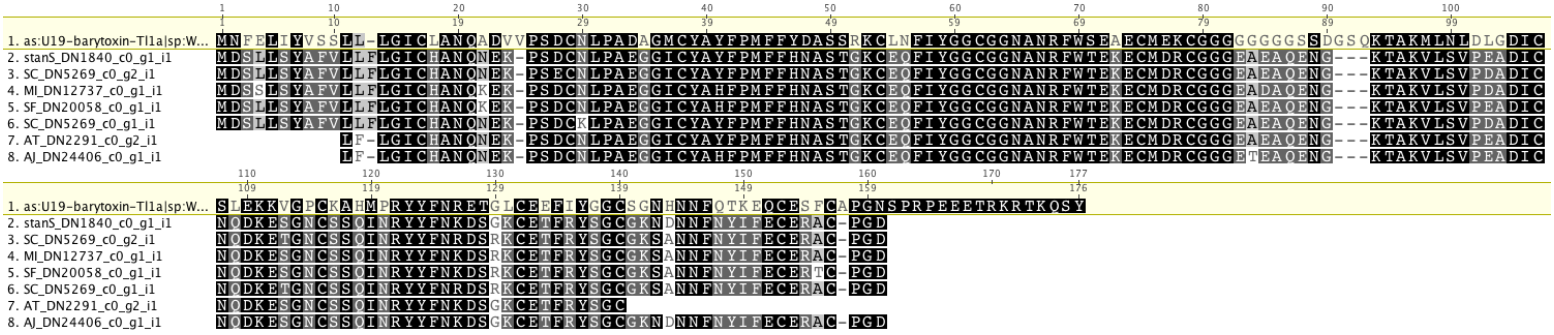

Figure 10: MSA of Aptostichus Kunitz-type venom peptide to best hit in ArachnoServer database

Appendix I

Supplemental Table 1: AHE Loci Summary; AEID = locus identification, LEN = length, OCC = occupancy, ID = percent identity, PID = pairwise identity, THIT = transcriptome hit, TG = transcriptome group ID.

AEID	LEN	OCC	% ID	% PID	THIT	TG
L1	662	97.67%	46.40%	93.90%	SC_DN11456_c0_g1_i1	156
L2	736	95.35%	70.70%	97.10%	SF_DN20421_c0_g1_i1	297
L3	784	100.00%	54.50%	95.60%	SF_DN14086_c0_g2_i1	275
L4	883	97.67%	37.40%	94.30%	SC_DN16188_c0_g1_i1	202
L5	808	100.00%	72.60%	97.30%	SF_DN14086_c0_g2_i1	275
L6	812	95.35%	56.80%	95.00%	AT_DN19885_c0_g1_i1	69
L7	787	97.67%	62.30%	96.30%	MI_DN27342_c0_g1_i1	137
L8	776	100.00%	62.40%	95.30%	SF_DN14086_c0_g2_i1	275
L9	678	90.70%	48.10%	93.10%	SF_DN14086_c0_g2_i1	275
L10	685	97.67%	61.60%	93.50%	SF_DN14086_c0_g2_i1	275
L11	710	62.79%	64.10%	95.70%	SF_DN14086_c0_g2_i1	275
L12	785	97.67%	68.00%	96.50%	AT_DN19885_c0_g1_i1	69
L13	724	76.74%	68.50%	96.00%	SF_DN14086_c0_g1_i1	274
L14	879	100.00%	66.40%	97.40%	AJ_DN11414_c0_g1_i1	2
L15	624	79.07%	59.10%	95.30%	SF_DN32220_c0_g1_i1	405
L16	722	100.00%	35.30%	89.70%	SF_DN32220_c0_g1_i1	405
L17	737	86.05%	47.50%	93.90%	SF_DN32220_c0_g1_i1	405
L18	841	100.00%	65.90%	96.20%	SF_DN32220_c0_g1_i1	405
L19	693	88.37%	55.40%	93.90%	SF_DN30341_c0_g1_i1	378

L20	789	100.00%	51.20%	95.90%	SF_DN30341_c0_g1_i1	378
L21	772	100.00%	44.90%	93.30%	SF_DN3399_c0_g1_i1	410
L22	733	83.72%	67.30%	96.30%	SF_DN25880_c2_g1_i1	330
L23	624	83.72%	13.60%	84.20%	SF_DN25880_c2_g1_i1	330
L24	705	95.35%	34.50%	93.80%	SF_DN25880_c2_g1_i1	330
L25	805	100.00%	58.40%	95.30%	SF_DN11030_c0_g1_i1	265
L26	639	65.12%	72.80%	95.20%	AT_DN2912_c0_g2_i1	81
L27	753	83.72%	62.00%	96.30%	SF_DN11030_c0_g1_i1	265
L28	353	55.81%	83.90%	96.60%	AT_DN2912_c0_g2_i1	81
L29	481	65.12%	52.40%	94.00%	SC_DN15190_c0_g1_i1	176
L30	516	69.77%	68.00%	95.60%	AT_DN2912_c0_g2_i1	81
L31	1193	100.00%	86.20%	98.80%	AT_DN14439_c0_g1_i1	46
L32	641	93.02%	43.50%	91.40%	SF_DN30967_c0_g1_i1	388
L33	747	90.70%	65.50%	96.20%	SC_DN15455_c0_g1_i1	179
L34	836	100.00%	58.90%	96.10%	MI_DN2033_c0_g2_i1	109
L35	692	79.07%	39.70%	90.00%	MI_DN22950_c4_g1_i1	123
L36	765	88.37%	23.40%	91.30%	SC_DN7031_c0_g1_i1	252
L37	812	97.67%	52.60%	96.80%	SF_DN26369_c1_g1_i1	332
L38	832	100.00%	40.30%	95.00%	SC_DN7031_c0_g1_i1	252
L39	845	97.67%	53.00%	93.20%	SF_DN11010_c0_g1_i1	264
L40	642	67.44%	47.80%	93.10%	SF_DN11010_c0_g1_i1	264
L41	787	100.00%	63.00%	95.20%	SF_DN17630_c0_g1_i1	283
L42	691	100.00%	39.10%	92.60%	AJ_DN24258_c0_g1_i1	32

L43	806	100.00%	63.30%	96.10%	SC_DN14368_c0_g2_i1	167
L44	758	93.02%	65.30%	95.60%	SF_DN20191_c0_g2_i1	294
L45	667	90.70%	63.90%	95.40%	SC_DN8602_c0_g1_i1	259
L46	773	100.00%	63.30%	96.40%	MI_DN23502_c0_g1_i1	134
L47	704	100.00%	30.00%	83.90%	AT_DN22474_c0_g1_i1	79
L48	835	95.35%	65.50%	93.70%	SF_DN30553_c0_g2_i1	385
L49	777	100.00%	47.60%	93.10%	SC_DN10974_c0_g1_i1	154
L50	830	95.35%	50.40%	95.40%	MI_DN23333_c0_g1_i1	132
L51	833	100.00%	44.90%	91.40%	SF_DN31520_c0_g1_i1	394
L52	779	93.02%	37.70%	93.30%	SF_DN3264_c0_g1_i1	409
L53	805	100.00%	40.20%	93.40%	SC_DN18342_c0_g1_i1	226
L54	665	69.77%	58.90%	94.90%	AT_DN4775_c0_g1_i1	83
L55	716	97.67%	58.40%	91.60%	SF_DN13617_c0_g1_i1	272
L56	748	90.70%	78.60%	97.30%	SF_DN24909_c0_g3_i1	321
L57	851	100.00%	60.40%	96.20%	SF_DN20215_c0_g1_i1	296
L58	745	93.02%	17.70%	91.90%	SF_DN20215_c0_g1_i1	296
L59	780	97.67%	47.70%	93.80%	SF_DN20215_c0_g1_i1	296
L60	771	97.67%	45.90%	91.70%	SC_DN15791_c0_g1_i1	188
L61	719	67.44%	45.30%	89.90%	AJ_DN22540_c7_g1_i1	27
L62	768	100.00%	73.60%	95.60%	SC_DN15791_c0_g1_i1	188
L63	652	62.79%	68.10%	94.70%	SF_DN20215_c0_g1_i1	296
L64	680	81.40%	45.10%	92.50%	SC_DN15791_c0_g1_i1	188
L65	797	100.00%	59.60%	93.90%	SF_DN20215_c0_g1_i1	296

L66	772	93.02%	53.00%	94.00%	SC_DN778_c0_g1_i1	256
L67	760	100.00%	53.40%	93.90%	SC_DN6242_c0_g1_i1	247
L68	609	97.67%	71.10%	95.80%	SF_DN24160_c0_g2_i1	314
L69	827	95.35%	79.70%	97.60%	SF_DN11586_c0_g1_i1	270
L70	762	100.00%	71.00%	97.10%	AJ_DN18148_c0_g1_i1	8
L71	920	100.00%	55.00%	93.00%	SC_DN15492_c1_g2_i1	183
L72	701	97.67%	92.40%	99.30%	SF_DN11586_c0_g1_i1	270
L73	736	100.00%	64.70%	95.70%	AJ_DN18148_c0_g1_i1	8
L74	642	86.05%	54.50%	94.80%	SF_DN16462_c0_g1_i1	279
L75	634	97.67%	54.30%	92.10%	SF_DN30315_c0_g1_i1	374
L76	771	97.67%	9.20%	90.00%	AJ_DN15302_c0_g1_i1	4
L77	837	100.00%	63.40%	95.40%	MI_DN26522_c0_g1_i1	136
L78	761	100.00%	46.10%	94.40%	AT_DN2942_c0_g1_i1	82
L79	802	95.35%	60.50%	93.60%	SC_DN15969_c0_g1_i1	193
L80	767	83.72%	45.20%	94.10%	SF_DN23239_c0_g1_i1	305
L81	787	95.35%	46.40%	93.60%	SF_DN23239_c0_g1_i1	305
L82	780	97.67%	68.20%	95.90%	SF_DN23239_c0_g1_i1	305
L83	828	95.35%	65.00%	95.90%	MI_DN26522_c0_g1_i1	136
L84	850	100.00%	36.20%	94.60%	SF_DN11263_c0_g1_i1	268
L85	772	95.35%	35.40%	94.00%	SF_DN11263_c0_g1_i1	268
L86	846	100.00%	59.00%	95.70%	SF_DN11263_c0_g1_i1	268
L87	834	100.00%	42.30%	93.10%	SC_DN2483_c0_g1_i1	234
L88	781	100.00%	54.50%	95.90%	MI_DN6566_c0_g1_i1	142

L89	680	97.67%	58.10%	95.60%	SF_DN11263_c0_g1_i1	268
L90	880	100.00%	53.90%	95.50%	SF_DN747_c0_g1_i1	423
L91	879	100.00%	47.00%	94.20%	AT_DN19864_c0_g1_i1	68
L92	863	100.00%	55.00%	92.50%	SF_DN747_c0_g1_i1	423
L93	724	97.67%	55.50%	91.50%	SF_DN747_c0_g1_i1	423
L94	309	60.47%	74.10%	96.60%	AT_DN19864_c0_g1_i1	68
L95	822	100.00%	48.50%	93.50%	SF_DN747_c0_g1_i1	423
L96	805	100.00%	59.80%	94.00%	AJ_DN16317_c0_g1_i1	5
L97	895	97.67%	36.20%	87.20%	SF_DN31524_c0_g1_i1	395
L98	1266	100.00%	36.20%	93.20%	SC_DN16342_c3_g1_i1	207
L99	761	95.35%	42.80%	91.70%	SF_DN31524_c0_g1_i1	395
L100	719	95.35%	41.00%	92.30%	SC_DN16275_c2_g2_i5	204
L101	604	83.72%	61.10%	95.10%	SF_DN31006_c0_g1_i1	389
L102	816	97.67%	70.30%	97.30%	AT_DN13706_c0_g1_i1	45
L104	625	76.74%	40.60%	93.30%	SF_DN30451_c0_g1_i1	384
L105	693	100.00%	66.40%	96.40%	SC_DN17752_c0_g2_i1	222
L106	609	97.67%	75.20%	96.90%	AJ_DN20984_c0_g1_i1	13
L107	829	100.00%	68.30%	97.30%	AJ_DN20984_c0_g1_i1	13
L108	710	95.35%	43.10%	94.30%	SF_DN29218_c0_g1_i1	364
L109	692	58.14%	32.10%	83.20%	SF_DN18365_c0_g1_i1	288
L110	895	100.00%	58.80%	95.30%	SF_DN18365_c0_g1_i1	288
L111	764	100.00%	54.20%	93.90%	SC_DN16510_c0_g1_i1	212
L112	753	97.67%	27.10%	90.50%	SC_DN16510_c0_g1_i1	212

L113	775	93.02%	52.40%	93.80%	AT_DN17657_c0_g1_i1	51
L114	849	100.00%	43.60%	93.60%	SF_DN28874_c5_g4_i1	347
L115	947	100.00%	64.70%	95.90%	SF_DN28874_c5_g4_i1	347
L116	837	100.00%	58.40%	96.00%	SF_DN27829_c10_g1_i1	340
L117	561	95.35%	35.30%	91.10%	AT_DN20645_c0_g1_i1	72
L118	726	93.02%	54.00%	93.20%	SF_DN27829_c10_g1_i1	340
L119	1015	100.00%	47.80%	90.00%	SC_DN16091_c1_g1_i1	195
L120	774	100.00%	49.50%	94.30%	SF_DN27829_c10_g1_i1	340
L121	775	100.00%	40.80%	95.10%	AT_DN20645_c0_g1_i1	72
L122	605	97.67%	47.90%	90.70%	SF_DN27829_c10_g1_i1	340
L123	651	95.35%	43.00%	94.40%	SC_DN6210_c0_g1_i2	246
L124	865	100.00%	59.30%	94.80%	SC_DN6210_c0_g1_i2	246
L125	711	97.67%	48.50%	93.70%	SF_DN19927_c1_g1_i1	291
L126	763	97.67%	37.40%	87.00%	SF_DN19927_c1_g1_i1	291
L127	807	97.67%	59.20%	93.00%	SF_DN19927_c1_g1_i1	291
L128	780	100.00%	65.80%	94.60%	SC_DN6210_c0_g1_i2	246
L129	852	97.67%	70.00%	95.40%	SF_DN19927_c1_g1_i1	291
L130	807	100.00%	51.80%	95.10%	SC_DN12610_c0_g2_i1	160
L131	546	81.40%	44.70%	93.30%	SF_DN31580_c0_g1_i1	399
L132	725	97.67%	43.00%	92.50%	SF_DN29182_c0_g1_i1	363
L133	740	100.00%	33.90%	91.70%	AJ_DN8804_c0_g1_i1	37
L134	713	81.40%	58.60%	94.40%	SF_DN32174_c0_g1_i1	404
L135	499	86.05%	72.10%	97.00%	MI_DN7114_c0_g2_i1	143

L136	688	100.00%	50.30%	91.00%	AJ_DN9111_c0_g1_i1	38
L137	807	100.00%	9.50%	86.40%	SF_DN23354_c0_g1_i1	306
L138	784	97.67%	66.10%	96.80%	MI_DN14274_c0_g1_i1	97
L139	725	100.00%	53.20%	94.70%	SF_DN10136_c0_g1_i1	262
L140	742	97.67%	57.10%	95.10%	SF_DN10136_c0_g1_i1	262
L141	738	100.00%	61.90%	96.70%	SF_DN10136_c0_g1_i1	262
L142	857	97.67%	52.50%	94.30%	MI_DN14274_c0_g1_i1	97
L143	889	100.00%	51.50%	94.60%	SF_DN10136_c0_g1_i1	262
L144	784	83.72%	55.10%	95.20%	SF_DN10136_c0_g1_i1	262
L145	746	95.35%	21.00%	86.70%	SC_DN15028_c0_g1_i1	173
L146	723	97.67%	6.10%	88.10%	SF_DN30941_c0_g1_i1	386
L147	894	97.67%	6.40%	88.10%	SC_DN15028_c0_g1_i1	173
L148	746	95.35%	30.30%	87.50%	AJ_DN20731_c0_g1_i1	11
L149	956	100.00%	38.90%	92.80%	MI_DN19830_c0_g1_i1	106
L151	822	97.67%	4.30%	85.30%	SF_DN30941_c0_g1_i1	386
L152	840	97.67%	10.40%	90.70%	SC_DN15028_c0_g1_i1	173
L153	903	100.00%	38.00%	93.20%	MI_DN19830_c0_g1_i1	106
L154	730	100.00%	23.60%	85.50%	AT_DN13205_c0_g1_i1	43
L155	837	95.35%	5.90%	83.80%	SF_DN30941_c0_g1_i1	386
L156	922	97.67%	23.10%	85.80%	SC_DN15028_c0_g1_i1	173
L157	961	100.00%	14.50%	91.80%	AJ_DN20731_c0_g1_i1	11
L158	701	83.72%	51.40%	96.30%	SC_DN7261_c0_g1_i1	253
L159	784	100.00%	61.50%	96.80%	SF_DN29787_c0_g2_i1	371

L160	700	97.67%	60.10%	95.10%	SC_DN18297_c0_g1_i1	224
L161	815	100.00%	49.90%	95.10%	SF_DN29078_c0_g1_i1	360
L162	763	97.67%	8.40%	87.80%	SF_DN29078_c0_g1_i1	360
L163	748	97.67%	39.70%	95.10%	SC_DN17047_c0_g1_i1	214
L164	573	97.67%	73.10%	96.30%	SF_DN29078_c0_g1_i1	360
L165	732	86.05%	79.10%	97.20%	SC_DN17047_c0_g1_i1	214
L166	967	100.00%	75.20%	96.90%	SC_DN15754_c1_g2_i1	187
L167	784	97.67%	84.90%	98.40%	SF_DN26871_c2_g1_i1	334
L168	570	93.02%	32.60%	90.10%	SF_DN28435_c11_g1_i1	344
L169	845	100.00%	63.30%	95.70%	SC_DN16099_c0_g1_i2	196
L170	757	97.67%	51.70%	90.70%	AJ_DN22075_c0_g1_i3	21
L171	772	97.67%	47.70%	94.40%	SF_DN25447_c3_g1_i1	328
L172	653	90.70%	48.40%	94.30%	SC_DN16099_c0_g1_i3	197
L173	803	95.35%	53.30%	94.50%	AJ_DN22075_c0_g1_i3	21
L174	773	88.37%	70.40%	95.70%	MI_DN22909_c0_g1_i1	122
L175	638	76.74%	57.80%	93.10%	AT_DN18017_c2_g1_i1	54
L176	625	60.47%	69.90%	95.70%	SC_DN16099_c0_g3_i1	198
L177	745	97.67%	57.20%	95.40%	SF_DN26427_c2_g1_i1	333
L178	896	97.67%	43.30%	92.20%	MI_DN12938_c0_g1_i1	94
L179	687	67.44%	35.70%	93.30%	SF_DN1596_c0_g1_i1	278
L180	2251	100.00%	78.60%	97.50%	SF_DN21017_c0_g1_i1	298
L181	814	100.00%	44.00%	92.40%	SC_DN2735_c0_g1_i1	239
L182	913	97.67%	31.70%	92.40%	SC_DN2735_c0_g1_i1	239

L183	862	95.35%	37.00%	88.10%	AJ_DN26694_c0_g1_i1	35
L184	995	97.67%	55.70%	95.50%	AJ_DN22547_c7_g2_i1	28
L185	366	53.49%	88.50%	98.00%	MI_DN22763_c4_g1_i2	117
L186	795	83.72%	63.10%	95.90%	SF_DN22807_c0_g1_i1	303
L187	475	58.14%	86.90%	97.60%	AJ_DN22407_c12_g1_i1	24
L188	648	93.02%	49.80%	89.60%	SC_DN16135_c4_g1_i1	201
L189	753	95.35%	38.10%	91.30%	SF_DN22807_c0_g2_i1	304
L190	578	76.74%	82.70%	97.70%	MI_DN20787_c0_g1_i1	111
L191	598	62.79%	87.00%	97.80%	SC_DN15465_c0_g1_i1	180
L192	592	65.12%	80.70%	96.70%	SC_DN16135_c4_g1_i1	201
L193	800	100.00%	61.00%	96.10%	SC_DN18333_c0_g1_i1	225
L194	812	53.49%	11.70%	68.60%	SF_DN28937_c13_g2_i2	349
L195	792	97.67%	49.60%	92.30%	SC_DN18333_c0_g1_i1	225
L196	690	65.12%	70.10%	94.80%	AT_DN19152_c0_g1_i1	65
L197	762	100.00%	59.80%	92.70%	SF_DN25070_c0_g1_i1	325
L198	1007	100.00%	59.00%	89.50%	AT_DN19152_c0_g1_i1	65
L199	856	97.67%	58.90%	95.00%	SC_DN18333_c0_g1_i1	225
L200	916	100.00%	73.80%	97.30%	SC_DN18333_c0_g1_i1	225
L201	678	95.35%	47.10%	94.60%	SF_DN27332_c2_g2_i1	335
L202	658	81.40%	57.40%	95.40%	MI_DN9443_c0_g5_i1	148
L203	620	67.44%	73.50%	96.70%	SF_DN27332_c2_g2_i1	335
L204	696	81.40%	55.50%	95.20%	SF_DN27332_c2_g2_i1	335
L205	739	97.67%	59.30%	96.10%	MI_DN20370_c0_g1_i1	110

L206	781	97.67%	64.50%	95.30%	SF_DN29136_c0_g1_i1	362
L207	703	100.00%	52.20%	92.40%	SC_DN17631_c0_g2_i1	218
L208	232	79.07%	13.40%	80.30%	SC_DN16217_c16_g1_i1	203
L209	790	90.70%	57.10%	95.80%	AJ_DN24581_c0_g1_i1	33
L210	832	100.00%	60.70%	93.00%	SC_DN19856_c0_g1_i1	233
L211	818	93.02%	54.30%	95.20%	SF_DN2495_c0_g1_i1	322
L212	803	100.00%	43.80%	93.60%	SC_DN3311_c0_g1_i1	240
L213	618	97.67%	51.30%	94.40%	AT_DN20831_c0_g1_i1	74
L214	685	83.72%	34.30%	91.60%	SC_DN3311_c0_g1_i1	240
L215	726	97.67%	59.50%	95.90%	SF_DN2495_c0_g1_i1	322
L216	763	93.02%	42.50%	94.60%	SF_DN2495_c0_g1_i1	322
L217	886	100.00%	75.40%	97.80%	AJ_DN25774_c0_g1_i1	34
L218	715	97.67%	57.20%	94.90%	SF_DN28932_c3_g1_i1	348
L219	818	95.35%	40.70%	88.80%	SF_DN28932_c3_g1_i1	348
L220	739	100.00%	54.10%	94.30%	SF_DN28932_c3_g1_i1	348
L221	796	93.02%	55.30%	90.90%	SF_DN28932_c3_g1_i1	348
L222	560	95.35%	60.50%	95.00%	SF_DN28932_c3_g1_i1	348
L223	738	97.67%	37.70%	92.10%	SF_DN28932_c3_g1_i1	348
L224	1071	100.00%	71.00%	96.50%	AT_DN15684_c0_g1_i2	47
L225	672	97.67%	59.50%	94.90%	SF_DN28932_c3_g1_i1	348
L226	755	83.72%	64.50%	96.10%	SC_DN15629_c0_g2_i1	184
L227	839	100.00%	58.90%	95.60%	SF_DN28932_c3_g1_i1	348

L228	835	100.00%	72.60%	98.00%	MI_DN22983_c8_g1_i1	125
L229	644	100.00%	35.10%	93.80%	SF_DN29123_c0_g1_i1	361
L230	803	100.00%	55.40%	93.80%	SF_DN29123_c0_g1_i1	361
L231	795	100.00%	48.80%	91.30%	SF_DN29807_c0_g1_i1	372
L232	725	97.67%	67.40%	95.10%	SF_DN29807_c0_g1_i1	372
L233	507	67.44%	50.90%	88.90%	SF_DN17993_c1_g1_i1	286
L234	568	90.70%	49.80%	94.00%	SC_DN17676_c0_g2_i1	220
L235	631	100.00%	66.60%	96.60%	MI_DN14560_c0_g1_i1	98
L236	1148	100.00%	58.20%	97.40%	SC_DN3843_c0_g1_i1	241
L237	774	90.70%	81.80%	98.40%	AJ_DN19321_c0_g1_i1	9
L238	736	97.67%	52.60%	94.60%	MI_DN23653_c0_g1_i1	135
L239	746	97.67%	52.40%	95.60%	SF_DN23539_c0_g1_i1	310
L240	731	95.35%	40.50%	94.30%	SC_DN2486_c0_g1_i1	236
L241	656	97.67%	60.70%	96.30%	SC_DN2486_c0_g1_i1	236
L242	738	90.70%	11.10%	87.00%	AT_DN21401_c0_g1_i1	76
L243	740	100.00%	69.70%	95.70%	SF_DN1117_c0_g2_i1	267
L244	675	86.05%	60.40%	93.40%	SF_DN1117_c0_g2_i1	267
L245	630	62.79%	74.00%	95.90%	SC_DN17685_c0_g1_i1	221
L246	922	95.35%	74.10%	97.00%	SF_DN19957_c0_g1_i1	292
L247	672	100.00%	71.90%	95.90%	SC_DN13581_c1_g1_i1	163
L248	552	95.35%	69.70%	94.10%	SF_DN19957_c0_g1_i1	292
L249	947	100.00%	54.60%	91.90%	MI_DN8477_c0_g1_i1	144
L250	670	88.37%	45.40%	93.30%	SF_DN29654_c0_g1_i1	368

L251	873	100.00%	57.20%	95.60%	AT_DN20034_c0_g1_i1	70
L252	806	100.00%	30.30%	93.20%	SC_DN11679_c0_g1_i1	159
L253	767	100.00%	59.80%	96.10%	SF_DN4089_c0_g1_i1	414
L254	489	74.42%	68.30%	95.00%	SF_DN29745_c0_g1_i1	370
L255	760	100.00%	43.80%	91.00%	AJ_DN9681_c0_g1_i1	40
L256	666	74.42%	53.90%	93.90%	SC_DN17079_c0_g1_i1	215
L257	870	100.00%	51.10%	94.30%	AJ_DN16796_c0_g2_i1	6
L258	945	100.00%	64.00%	96.30%	SF_DN31605_c0_g1_i1	400
L259	814	90.70%	72.60%	97.30%	SF_DN31605_c0_g1_i1	400
L260	781	97.67%	56.60%	94.20%	SF_DN10192_c1_g2_i1	263
L261	845	97.67%	17.20%	90.20%	SC_DN14594_c0_g1_i1	170
L262	846	97.67%	75.20%	97.10%	SF_DN10192_c1_g2_i1	263
L263	794	88.37%	51.80%	95.50%	SF_DN29050_c0_g1_i1	358
L264	696	88.37%	79.60%	98.30%	SF_DN29050_c0_g1_i1	358
L265	664	86.05%	72.60%	97.40%	SF_DN29050_c0_g1_i1	358
L266	807	90.70%	59.40%	96.50%	SC_DN13209_c0_g1_i1	162
L267	873	100.00%	80.90%	98.00%	SF_DN29050_c0_g1_i1	358
L268	637	79.07%	74.30%	96.30%	SF_DN29050_c0_g1_i1	358
L269	539	79.07%	80.30%	97.60%	SC_DN13209_c0_g1_i1	162
L270	780	95.35%	55.40%	91.50%	SF_DN29050_c0_g1_i1	358
L272	967	100.00%	92.00%	99.30%	SF_DN14054_c0_g2_i1	273
L273	587	100.00%	86.70%	98.40%	SC_DN100_c1_g1_i1	150
L274	803	86.05%	39.00%	93.60%	SF_DN14054_c0_g2_i1	273

L275	500	67.44%	33.20%	93.70%	SF_DN6046_c0_g1_i1	419
L276	689	100.00%	48.90%	93.20%	SC_DN5570_c0_g1_i1	245
L277	723	97.67%	66.10%	94.50%	SF_DN234_c0_g2_i1	307
L278	583	90.70%	53.20%	93.60%	SC_DN5570_c0_g1_i1	245
L279	754	97.67%	68.00%	97.40%	SC_DN5570_c0_g1_i1	245
L280	769	88.37%	55.80%	95.60%	SF_DN29046_c0_g1_i1	356
L281	764	100.00%	33.00%	93.00%	MI_DN23201_c5_g1_i1	129
L282	776	97.67%	81.30%	98.10%	AT_DN19169_c0_g1_i1	66
L283	525	97.67%	33.90%	91.10%	AT_DN19169_c0_g1_i1	66
L284	541	90.70%	44.50%	93.00%	SF_DN22710_c0_g1_i1	302
L285	792	100.00%	26.80%	86.80%	AT_DN19169_c0_g1_i1	66
L286	621	60.47%	66.20%	94.40%	AT_DN19169_c0_g1_i1	66
L287	831	100.00%	73.30%	97.10%	MI_DN16928_c0_g1_i1	100
L288	738	100.00%	62.10%	94.50%	AT_DN12785_c0_g1_i1	41
L289	824	100.00%	61.90%	95.20%	AJ_DN9407_c0_g1_i1	39
L290	783	100.00%	58.50%	93.30%	SF_DN31250_c0_g1_i1	393
L291	749	97.67%	54.20%	95.40%	SC_DN14118_c0_g1_i1	166
L292	822	100.00%	50.20%	91.70%	SF_DN31250_c0_g1_i1	393
L293	1588	86.05%	22.40%	90.30%	SF_DN29030_c1_g2_i2	354
L294	815	100.00%	70.60%	96.70%	SF_DN31250_c0_g1_i1	393
L295	629	100.00%	75.80%	96.60%	AT_DN16362_c0_g3_i1	49
L297	211	53.49%	87.70%	96.80%	SC_DN16343_c2_g2_i1	208
L298	770	95.35%	51.00%	93.90%	SF_DN31526_c0_g1_i1	396

L299	833	100.00%	45.30%	92.80%	SF_DN3830_c0_g1_i1	412
L300	802	100.00%	51.60%	95.50%	AT_DN5955_c0_g1_i1	84
L301	795	97.67%	76.60%	97.40%	SF_DN17838_c0_g1_i1	285
L302	776	93.02%	60.40%	96.20%	SF_DN17838_c0_g1_i1	285
L303	779	100.00%	67.90%	95.80%	SC_DN15111_c0_g1_i1	175
L304	775	97.67%	16.10%	92.90%	SC_DN15111_c0_g1_i1	175
L305	764	100.00%	70.70%	97.20%	SF_DN32146_c0_g1_i1	402
L306	772	95.35%	63.20%	95.90%	SF_DN32146_c0_g1_i1	402
L307	779	100.00%	72.00%	96.70%	SF_DN32146_c0_g1_i1	402
L308	844	100.00%	76.80%	97.60%	SF_DN32146_c0_g1_i1	402
L309	411	83.72%	54.50%	89.00%	SF_DN31038_c0_g1_i1	390
L310	518	90.70%	73.90%	95.20%	AT_DN18445_c0_g1_i1	63
L311	739	79.07%	78.80%	97.40%	SF_DN6327_c0_g1_i1	422
L312	836	97.67%	44.10%	95.00%	SF_DN6327_c0_g1_i1	422
L313	951	100.00%	63.50%	96.80%	SF_DN6327_c0_g1_i1	422
L314	856	100.00%	69.60%	97.60%	AT_DN22174_c0_g1_i1	78
L315	701	88.37%	58.50%	95.20%	SF_DN17268_c0_g1_i1	281
L316	859	97.67%	55.20%	93.90%	SF_DN17268_c0_g1_i1	281
L317	632	95.35%	70.30%	95.10%	AT_DN9162_c0_g1_i1	93
L318	782	90.70%	55.60%	95.20%	MI_DN8712_c0_g1_i1	145
L319	733	95.35%	66.70%	95.30%	SF_DN17268_c0_g1_i1	281
L320	787	100.00%	44.50%	92.60%	SF_DN750_c0_g1_i1	424
L321	832	100.00%	63.50%	95.30%	SC_DN2485_c0_g1_i1	235

L322	655	88.37%	37.10%	90.70%	SF_DN31527_c0_g1_i1	397
L323	663	83.72%	72.20%	96.30%	SF_DN28422_c3_g1_i1	343
L324	823	100.00%	61.40%	96.10%	SF_DN28422_c3_g1_i1	343
L325	558	69.77%	52.50%	95.40%	AT_DN8557_c0_g1_i1	89
L326	551	60.47%	78.40%	96.80%	AT_DN17878_c0_g1_i1	52
L327	854	100.00%	58.10%	95.70%	SC_DN18409_c0_g1_i1	228
L328	100	41.86%	81.00%	92.80%	AT_DN18092_c2_g1_i1	55
L329	1378	97.67%	59.10%	93.80%	AT_DN18312_c3_g1_i3	60
L331	769	97.67%	41.20%	95.10%	SF_DN30364_c0_g1_i1	382
L332	667	95.35%	35.20%	94.00%	SC_DN6566_c0_g2_i1	251
L333	548	88.37%	52.40%	93.40%	SF_DN8309_c0_g1_i1	425
L334	550	97.67%	56.70%	94.30%	SF_DN8309_c0_g1_i1	425
L335	504	83.72%	47.00%	90.80%	SF_DN8309_c0_g1_i1	425
L336	735	100.00%	50.70%	93.40%	SF_DN8309_c0_g1_i1	425
L337	770	100.00%	72.50%	96.40%	SC_DN18823_c0_g1_i1	230
L338	611	90.70%	55.50%	94.90%	SF_DN31064_c0_g1_i1	391
L339	754	100.00%	56.80%	92.80%	SF_DN31064_c0_g1_i1	391
L340	811	100.00%	42.30%	92.30%	SC_DN170_c0_g1_i1	216
L341	773	100.00%	68.40%	96.60%	SF_DN31064_c0_g1_i1	391
L342	572	90.70%	6.30%	88.90%	AT_DN21433_c0_g1_i1	77
L343	684	100.00%	31.10%	89.40%	SC_DN10882_c0_g2_i1	153
L344	846	95.35%	38.40%	91.00%	MI_DN28664_c0_g1_i1	141
L345	788	100.00%	43.40%	94.10%	SF_DN8607_c0_g1_i1	428

L346	883	100.00%	59.30%	95.10%	MI_DN28664_c0_g1_i1	141
L347	740	90.70%	83.00%	98.40%	SF_DN3511_c0_g1_i1	411
L348	743	97.67%	49.70%	94.20%	SC_DN8115_c0_g1_i1	258
L349	695	100.00%	58.10%	94.60%	MI_DN27549_c0_g1_i1	138
L350	711	100.00%	60.60%	94.80%	SF_DN3915_c0_g1_i1	413
L351	439	72.09%	68.30%	94.70%	MI_DN23132_c2_g1_i1	128
L352	812	97.67%	64.30%	95.40%	SF_DN28987_c7_g1_i4	351
L353	757	100.00%	39.90%	93.10%	SC_DN15706_c0_g1_i1	186
L354	958	100.00%	56.70%	94.30%	SC_DN11539_c0_g1_i1	157
L355	685	93.02%	41.20%	90.60%	SF_DN25326_c0_g1_i1	327
L356	750	100.00%	60.40%	91.40%	MI_DN22040_c0_g1_i1	114
L357	676	93.02%	45.70%	94.10%	SF_DN25326_c0_g1_i1	327
L358	645	65.12%	60.60%	94.00%	SC_DN2545_c0_g1_i1	238
L359	634	69.77%	59.10%	96.00%	SF_DN25326_c0_g1_i1	327
L360	849	95.35%	43.50%	94.10%	AJ_DN22264_c10_g1_i2	22
L361	720	100.00%	49.60%	93.30%	SF_DN21118_c0_g1_i1	299
L362	731	100.00%	69.10%	96.70%	AJ_DN23410_c0_g1_i1	30
L363	911	100.00%	61.90%	94.30%	SF_DN21118_c0_g1_i1	299
L364	786	97.67%	44.90%	94.60%	SF_DN21118_c0_g1_i1	299
L365	902	100.00%	58.00%	93.00%	SF_DN21118_c0_g1_i1	299
L366	678	100.00%	44.70%	90.40%	AJ_DN23410_c0_g1_i1	30
L367	673	86.05%	25.30%	88.80%	SF_DN27692_c0_g1_i1	338
L368	736	100.00%	32.90%	91.90%	SF_DN27692_c0_g1_i1	338

L369	771	93.02%	49.70%	92.50%	AJ_DN21072_c0_g2_i1	14
L370	873	97.67%	52.90%	92.90%	AT_DN7491_c0_g1_i1	87
L371	665	62.79%	74.90%	96.80%	SF_DN21666_c0_g1_i1	301
L372	852	100.00%	39.30%	93.10%	SC_DN15238_c0_g1_i1	178
L373	721	100.00%	54.10%	94.50%	SF_DN8335_c0_g1_i1	426
L374	706	100.00%	50.10%	93.10%	AJ_DN21305_c0_g1_i1	16
L375	523	62.79%	74.40%	96.40%	SC_DN19684_c0_g1_i1	232
L376	763	100.00%	81.40%	97.70%	MI_DN22186_c0_g1_i1	116
L377	646	88.37%	55.00%	96.00%	AJ_DN21373_c0_g2_i1	17
L378	717	100.00%	59.60%	95.00%	SC_DN4086_c0_g1_i1	242
L379	785	93.02%	51.30%	91.90%	SC_DN4086_c0_g1_i1	242
L380	809	100.00%	61.90%	96.30%	SF_DN12631_c0_g1_i1	271
L381	786	95.35%	62.60%	92.20%	SF_DN12631_c0_g1_i1	271
L382	492	62.79%	67.10%	94.70%	SF_DN6082_c0_g2_i1	421
L383	622	58.14%	94.20%	99.10%	SF_DN29048_c0_g1_i1	357
L384	765	100.00%	57.90%	92.90%	AJ_DN18118_c0_g1_i1	7
L385	716	86.05%	54.10%	94.80%	SC_DN7754_c0_g1_i1	254
L386	802	100.00%	74.60%	97.60%	SC_DN7754_c0_g1_i1	254
L387	626	69.77%	62.00%	95.40%	SF_DN23681_c1_g1_i1	311
L388	728	100.00%	70.70%	97.20%	SF_DN19819_c0_g1_i1	290
L390	705	62.79%	68.10%	95.90%	MI_DN23440_c0_g1_i1	133
L391	721	60.47%	65.70%	96.30%	SF_DN32386_c0_g1_i1	408
L392	781	97.67%	49.40%	95.20%	SC_DN18539_c0_g1_i1	229

L393	817	97.67%	76.90%	97.40%	SF_DN17801_c0_g1_i1	284
L394	794	97.67%	77.00%	97.20%	SC_DN11658_c0_g1_i1	158
L395	701	90.70%	50.50%	94.70%	SF_DN23513_c0_g1_i1	308
L396	745	83.72%	36.50%	93.60%	SF_DN23513_c0_g2_i1	309
L397	752	97.67%	67.00%	96.90%	SF_DN23513_c0_g2_i1	309
L398	831	83.72%	76.20%	96.80%	SC_DN15228_c0_g1_i1	177
L399	922	100.00%	55.10%	95.00%	AT_DN18098_c2_g1_i1	56
L400	926	100.00%	79.30%	98.10%	AJ_DN20823_c1_g2_i1	12
L401	702	86.05%	67.40%	96.50%	SF_DN27615_c25_g1_i1	337
L402	567	69.77%	60.70%	95.60%	SC_DN16295_c4_g1_i1	205
L403	673	97.67%	71.90%	96.10%	SF_DN25270_c0_g1_i1	326
L404	862	100.00%	58.60%	95.40%	MI_DN13056_c0_g1_i1	95
L405	696	97.67%	47.80%	94.20%	SC_DN16295_c4_g1_i1	205
L406	525	65.12%	54.90%	93.60%	SF_DN27615_c11_g1_i1	336
L407	867	97.67%	67.20%	95.10%	SF_DN27615_c11_g1_i1	336
L408	760	97.67%	45.50%	87.50%	SF_DN27615_c11_g1_i1	336
L409	941	100.00%	61.10%	94.90%	AJ_DN22375_c6_g1_i1	23
L410	526	62.79%	82.50%	97.20%	SF_DN24319_c0_g1_i1	316
L411	825	100.00%	58.20%	95.20%	MI_DN23205_c0_g2_i1	130
L412	810	95.35%	55.70%	92.10%	SF_DN27615_c11_g1_i1	336
L413	856	93.02%	62.60%	94.70%	SC_DN16115_c3_g1_i1	199
L414	664	97.67%	69.00%	97.10%	AJ_DN20008_c3_g1_i1	10
L415	919	100.00%	61.80%	96.80%	SF_DN27615_c11_g1_i1	336

L416	996	100.00%	49.40%	94.90%	SF_DN27615_c11_g1_i1	336
L417	528	81.40%	55.90%	92.90%	SF_DN30354_c0_g1_i1	381
L418	727	97.67%	45.80%	94.30%	SF_DN30354_c0_g1_i1	381
L419	470	55.81%	23.20%	91.90%	MI_DN22902_c8_g1_i1	121
L420	560	69.77%	75.20%	96.70%	SF_DN30354_c0_g1_i1	381
L421	649	97.67%	71.00%	96.80%	SF_DN30344_c0_g1_i1	379
L422	1177	100.00%	1.90%	79.40%	MI_DN23256_c5_g1_i2	131
L423	713	76.74%	63.30%	95.60%	SC_DN4107_c0_g1_i1	243
L424	704	90.70%	39.10%	92.90%	SF_DN30344_c0_g1_i1	379
L425	813	100.00%	51.40%	94.90%	SF_DN31101_c0_g1_i1	392
L426	850	100.00%	52.10%	93.00%	SF_DN31101_c0_g1_i1	392
L427	666	97.67%	54.70%	91.30%	SC_DN14436_c1_g1_i1	168
L428	744	74.42%	59.10%	95.50%	SC_DN14436_c1_g1_i1	168
L429	722	76.74%	65.90%	96.80%	AT_DN6246_c0_g1_i1	85
L430	579	100.00%	48.00%	92.10%	SF_DN11336_c0_g1_i1	269
L431	854	97.67%	53.90%	94.30%	AT_DN13303_c0_g1_i1	44
L432	660	76.74%	68.60%	96.60%	SF_DN11336_c0_g1_i1	269
L433	447	100.00%	54.40%	94.70%	SF_DN11336_c0_g1_i1	269
L434	743	100.00%	43.60%	92.90%	SC_DN7760_c0_g1_i1	255
L435	1306	100.00%	59.00%	92.70%	AJ_DN23652_c0_g1_i1	31
L436	898	100.00%	43.50%	94.00%	SF_DN11039_c0_g1_i1	266
L437	789	95.35%	62.00%	95.00%	SF_DN6034_c0_g1_i1	418
L438	1547	67.44%	0.30%	73.80%	AJ_DN22513_c4_g1_i1	26

L439	667	97.67%	49.60%	93.40%	AT_DN1931_c0_g1_i1	67
L440	857	88.37%	36.30%	92.90%	SC_DN15877_c2_g2_i1	191
L441	766	90.70%	53.30%	95.70%	MI_DN22780_c0_g1_i2	118
L442	717	100.00%	75.20%	97.10%	AT_DN18100_c2_g1_i2	57
L443	738	97.67%	56.60%	94.80%	AT_DN8790_c0_g1_i1	90
L444	753	97.67%	45.70%	94.00%	SC_DN16458_c0_g1_i1	210
L445	817	79.07%	31.00%	89.60%	SF_DN24018_c0_g1_i1	312
L446	523	93.02%	59.70%	94.00%	SC_DN18837_c0_g1_i1	231
L447	818	100.00%	13.10%	91.30%	SF_DN27943_c17_g2_i1	341
L448	859	100.00%	62.20%	94.80%	MI_DN14069_c0_g1_i1	96
L449	710	90.70%	65.80%	95.20%	MI_DN18802_c1_g1_i1	104
L450	644	97.67%	53.40%	92.70%	MI_DN23046_c10_g1_i 1	126
L451	758	100.00%	64.40%	95.20%	MI_DN18802_c1_g1_i1	104
L452	830	100.00%	55.20%	95.00%	AT_DN18204_c1_g1_i1	58
L453	816	97.67%	61.30%	95.00%	SF_DN17323_c0_g1_i1	282
L454	692	100.00%	65.90%	95.30%	MI_DN18802_c1_g1_i1	104
L455	777	97.67%	46.60%	92.90%	SF_DN27943_c17_g2_i1	341
L456	882	95.35%	62.90%	95.00%	SF_DN17323_c0_g1_i1	282
L457	636	100.00%	70.90%	95.90%	MI_DN18802_c4_g1_i1	105
L458	808	95.35%	68.90%	97.00%	SC_DN15701_c0_g1_i1	185
L459	773	100.00%	57.60%	96.10%	AT_DN18204_c1_g1_i1	58
L460	813	100.00%	56.80%	94.20%	SF_DN17323_c0_g1_i1	282

L461	700	100.00%	36.90%	91.50%	MI_DN23081_c4_g2_i1	127
L462	711	95.35%	55.60%	95.60%	SC_DN15701_c0_g1_i1	185
L463	774	53.49%	58.50%	94.40%	SF_DN27943_c17_g2_i1	341
L464	312	100.00%	85.60%	97.30%	SC_DN13672_c4_g1_i1	164
L465	808	93.02%	64.90%	95.70%	SF_DN17323_c0_g1_i1	282
L466	695	95.35%	47.80%	93.20%	SC_DN10003_c0_g1_i1	149
L467	677	100.00%	84.50%	98.50%	MI_DN18802_c4_g1_i1	105
L468	780	86.05%	70.40%	96.90%	SF_DN17323_c0_g1_i1	282
L469	522	86.05%	65.50%	96.00%	AT_DN18204_c1_g1_i1	58
L470	702	69.77%	16.20%	82.20%	SF_DN17323_c0_g1_i1	282
L471	496	58.14%	47.80%	94.70%	SF_DN27943_c17_g2_i1	341
L472	515	90.70%	80.80%	97.10%	AT_DN18315_c2_g2_i4	61
L473	744	88.37%	33.60%	95.40%	SC_DN13823_c0_g1_i1	165
L474	778	90.70%	81.20%	97.90%	SF_DN28798_c20_g1_i1	346
L475	605	100.00%	50.60%	95.40%	SC_DN13823_c0_g1_i1	165
L476	717	97.67%	64.40%	96.70%	SF_DN16716_c0_g2_i1	280
L477	770	97.67%	41.30%	89.70%	MI_DN28302_c0_g2_i1	140
L478	805	100.00%	50.20%	94.10%	SF_DN30316_c0_g1_i1	375
L479	757	97.67%	39.40%	93.10%	SF_DN30316_c0_g1_i1	375
L480	906	97.67%	50.30%	92.40%	SF_DN27615_c25_g1_i1	337
L481	661	81.40%	48.60%	90.60%	MI_DN21794_c1_g1_i1	112
L482	686	100.00%	55.40%	95.70%	SF_DN26302_c1_g1_i1	331
L483	826	100.00%	60.40%	96.30%	SF_DN29641_c0_g1_i1	367

L484	820	100.00%	52.00%	96.50%	SF_DN29641_c0_g1_i1	367
L485	789	100.00%	59.40%	94.80%	SF_DN31615_c0_g1_i1	401
L486	734	100.00%	80.90%	97.80%	AT_DN20141_c0_g2_i1	71
L487	701	100.00%	63.90%	95.50%	SC_DN16533_c0_g1_i1	213
L488	1005	76.74%	57.30%	95.50%	SF_DN32316_c0_g1_i1	407
L489	711	100.00%	22.50%	89.80%	MI_DN17176_c0_g1_i1	101
L490	682	95.35%	45.20%	94.70%	SC_DN17634_c0_g1_i1	219
L491	627	100.00%	66.00%	95.20%	SC_DN17634_c0_g1_i1	219
L492	791	100.00%	39.10%	94.60%	SF_DN32167_c0_g1_i1	403
L493	774	100.00%	53.90%	93.00%	SF_DN32167_c0_g1_i1	403
L494	627	100.00%	57.40%	94.80%	SF_DN32167_c0_g1_i1	403
L495	811	97.67%	63.40%	96.30%	SF_DN32167_c0_g1_i1	403
L496	769	100.00%	57.20%	93.20%	AJ_DN21666_c0_g2_i1	19
L497	1018	100.00%	69.90%	95.00%	SC_DN16117_c0_g1_i1	200
L498	899	100.00%	65.30%	95.20%	AT_DN17201_c0_g1_i1	50
L499	942	95.35%	72.70%	97.10%	AT_DN16069_c0_g1_i1	48
L500	1787	100.00%	44.50%	94.00%	MI_DN20281_c0_g1_i1	108
L501	1775	97.67%	79.30%	97.10%	MI_DN17378_c0_g1_i1	102
L502	1642	100.00%	71.50%	95.30%	SC_DN14868_c0_g1_i1	171
L503	824	100.00%	75.70%	97.50%	AT_DN7294_c0_g2_i1	86
L504	773	95.35%	70.60%	97.30%	SF_DN28301_c2_g1_i2	342
L505	701	100.00%	72.00%	98.00%	SC_DN14868_c0_g3_i1	172
L506	724	100.00%	35.50%	93.70%	SC_DN16507_c0_g1_i1	211

L507	767	86.05%	55.30%	94.20%	SC_DN16507_c0_g1_i1	211
L508	724	100.00%	71.50%	96.90%	SC_DN16360_c0_g1_i1	209
L509	1064	97.67%	18.10%	89.10%	AJ_DN22487_c13_g1_i1	25
L510	763	72.09%	49.90%	95.60%	SF_DN2419_c0_g1_i1	315
L511	522	95.35%	30.70%	93.00%	MI_DN22960_c10_g1_i 1	124
L512	827	69.77%	67.00%	97.00%	SF_DN28726_c2_g2_i1	345
L513	461	88.37%	49.70%	91.30%	SC_DN474_c0_g1_i1	244
L514	700	67.44%	8.70%	90.50%	MI_DN22960_c10_g1_i 1	124
L515	502	88.37%	60.80%	93.80%	AJ_DN15221_c0_g1_i1	3
L516	729	86.05%	55.60%	95.60%	SF_DN28726_c2_g2_i1	345
L517	682	97.67%	30.80%	90.80%	MI_DN22833_c3_g1_i1	120
L518	692	97.67%	16.00%	92.00%	SF_DN14937_c1_g1_i1	277
L519	930	100.00%	13.10%	92.80%	MI_DN22833_c2_g1_i1	119
L520	966	97.67%	6.00%	89.30%	SF_DN14937_c1_g1_i1	277
L521	866	97.67%	7.40%	86.20%	AT_DN18331_c0_g1_i1	62
L522	792	95.35%	44.90%	93.10%	AT_DN9076_c1_g1_i1	92
L523	747	62.79%	80.90%	97.90%	MI_DN21988_c3_g1_i1	113
L524	665	100.00%	61.50%	94.60%	SF_DN2020_c0_g1_i1	295
L525	757	100.00%	16.50%	92.00%	AJ_DN3475_c0_g1_i1	36
L526	728	65.12%	48.60%	89.60%	SF_DN5677_c0_g1_i1	416
L527	630	100.00%	47.90%	94.30%	SF_DN5677_c0_g1_i1	416

L528	732	95.35%	64.20%	95.70%	SF_DN5677_c0_g1_i1	416
L529	790	100.00%	43.80%	87.30%	MI_DN9167_c0_g1_i1	147
L530	854	97.67%	51.90%	91.20%	SF_DN29639_c0_g1_i1	366
L531	768	90.70%	46.40%	91.90%	SC_DN10416_c0_g1_i1	151
L532	628	60.47%	19.40%	88.50%	MI_DN22062_c0_g2_i1	115
L533	714	100.00%	67.20%	95.90%	AT_DN21068_c0_g1_i1	75
L535	796	100.00%	91.00%	99.00%	SC_DN6295_c0_g1_i1	249
L536	883	97.67%	58.20%	93.30%	SF_DN29637_c0_g1_i1	365
L537	608	97.67%	55.90%	89.70%	SF_DN21294_c0_g1_i2	300
L538	762	100.00%	36.70%	92.10%	SF_DN21294_c0_g1_i2	300
L539	748	60.47%	72.60%	97.40%	SF_DN29637_c0_g1_i1	365
L540	408	100.00%	94.60%	99.10%	SF_DN29637_c0_g1_i1	365
L541	768	55.81%	64.70%	95.10%	SF_DN29637_c0_g1_i1	365
L542	373	88.37%	94.40%	98.80%	SF_DN29637_c0_g1_i1	365
L543	742	74.42%	47.40%	95.70%	SF_DN29637_c0_g1_i1	365
L544	678	62.79%	40.00%	91.80%	SC_DN15811_c0_g2_i1	189
L545	456	97.67%	72.40%	97.00%	SF_DN29637_c0_g1_i1	365
L546	646	100.00%	77.40%	97.80%	SF_DN29637_c0_g1_i1	365
L547	738	72.09%	60.20%	95.70%	SC_DN6462_c0_g1_i1	250
L548	725	100.00%	48.10%	92.90%	SF_DN30397_c0_g1_i1	383
L549	783	100.00%	58.20%	95.50%	AT_DN18451_c0_g1_i1	64
L550	809	86.05%	51.50%	92.60%	SC_DN15066_c0_g1_i1	174
L551	770	100.00%	78.40%	97.00%	AT_DN20818_c0_g1_i1	73

L553	1040	55.81%	58.80%	96.30%	SC_DN15066_c0_g1_i1	174
L554	531	93.02%	90.00%	98.30%	SF_DN24714_c2_g1_i1	318
L555	889	65.12%	61.60%	95.70%	SC_DN15066_c0_g1_i1	174
L556	640	100.00%	78.30%	96.10%	SF_DN24714_c1_g2_i1	317
L557	867	100.00%	55.60%	95.10%	SF_DN18089_c0_g1_i1	287
L558	908	97.67%	45.40%	91.60%	MI_DN27759_c0_g1_i1	139
L559	829	83.72%	41.70%	93.50%	SF_DN29976_c0_g1_i1	373
L560	733	100.00%	70.50%	95.90%	SF_DN30326_c0_g1_i1	377
L561	847	81.40%	82.50%	97.80%	SC_DN15470_c0_g1_i1	181
L562	692	65.12%	71.40%	96.60%	MI_DN17505_c0_g1_i1	103
L563	522	100.00%	48.70%	92.60%	SC_DN7888_c1_g1_i1	257
L564	969	95.35%	66.60%	97.10%	AJ_DN21267_c0_g1_i1	15
L565	835	97.67%	60.70%	92.40%	SC_DN7888_c1_g1_i1	257
L566	740	100.00%	83.20%	98.50%	SF_DN30326_c0_g1_i1	377
L567	743	100.00%	48.60%	96.30%	AT_DN8195_c0_g1_i1	88
L568	999	97.67%	74.10%	97.80%	SC_DN2497_c0_g1_i1	237
L569	755	67.44%	74.70%	97.40%	SC_DN10852_c0_g1_i1	152
L570	738	100.00%	58.00%	95.10%	SF_DN4826_c0_g2_i1	415
L571	863	100.00%	45.70%	96.90%	SF_DN4826_c0_g2_i1	415
L572	839	83.72%	62.10%	91.80%	MI_DN9048_c0_g1_i1	146
L573	727	65.12%	68.40%	96.10%	SC_DN9769_c0_g1_i1	261
L574	681	100.00%	57.30%	92.90%	SF_DN30323_c0_g1_i1	376
L575	728	100.00%	51.20%	95.30%	SF_DN6049_c0_g1_i1	420

L576	920	60.47%	50.30%	94.50%	SF_DN6049_c0_g1_i1	420
L577	428	88.37%	39.50%	91.70%	SF_DN6049_c0_g1_i1	420
L578	778	100.00%	64.90%	95.60%	AJ_DN21449_c0_g1_i1	18
L579	921	97.67%	47.10%	93.00%	SC_DN15841_c0_g1_i1	190
L580	825	100.00%	61.70%	96.70%	SC_DN15841_c0_g1_i1	190
L581	827	90.70%	62.80%	95.60%	AT_DN13179_c0_g1_i1	42
L582	726	97.67%	40.60%	91.60%	SF_DN28954_c16_g1_i1	350
L583	805	97.67%	14.00%	92.50%	SC_DN16298_c8_g1_i3	206
L584	682	100.00%	73.20%	97.60%	SF_DN27760_c0_g1_i1	339
L585	733	100.00%	48.40%	94.00%	AJ_DN10025_c0_g1_i1	1
L586	751	88.37%	56.50%	95.40%	SC_DN18346_c0_g1_i1	227
L587	718	100.00%	68.70%	95.50%	SF_DN24787_c0_g2_i1	320
L588	766	97.67%	18.00%	90.70%	SF_DN24787_c0_g2_i1	320
L589	838	88.37%	49.80%	93.30%	SF_DN24787_c0_g2_i1	320
L590	638	95.35%	46.40%	94.50%	SF_DN24787_c0_g1_i1	319
L591	539	100.00%	55.10%	92.80%	SF_DN24787_c0_g1_i1	319
L592	784	97.67%	34.60%	92.00%	AJ_DN21930_c3_g1_i1	20
L593	642	76.74%	24.10%	93.70%	SF_DN25013_c0_g1_i1	323
L594	704	62.79%	59.70%	94.20%	SF_DN25013_c0_g1_i1	323
L595	643	97.67%	70.30%	95.70%	AT_DN17950_c0_g1_i1	53
L596	696	97.67%	50.00%	95.30%	SF_DN25013_c0_g2_i1	324
L597	919	100.00%	60.80%	95.20%	SF_DN25013_c0_g2_i1	324
L598	788	97.67%	47.80%	95.10%	SF_DN25013_c0_g2_i1	324

L599	848	100.00%	56.50%	94.90%	SF_DN25013_c0_g2_i1	324
L600	780	100.00%	50.10%	96.10%	AT_DN17950_c0_g1_i1	53
L601	792	76.74%	2.00%	83.70%	SF_DN31577_c0_g1_i1	398
L602	614	95.35%	67.40%	96.40%	SF_DN31577_c0_g1_i1	398
L603	721	90.70%	33.40%	88.60%	SF_DN32252_c0_g1_i1	406
L604	693	100.00%	33.60%	91.70%	SC_DN17230_c0_g1_i1	217
L605	852	97.67%	38.80%	92.20%	SC_DN17230_c0_g1_i1	217
L606	799	100.00%	47.40%	94.80%	SF_DN30950_c0_g1_i1	387
L607	841	100.00%	39.60%	90.20%	SF_DN30950_c0_g1_i1	387
L608	683	88.37%	73.90%	95.10%	SF_DN8419_c0_g1_i1	427
L609	673	93.02%	8.30%	86.10%	SF_DN8419_c0_g1_i1	427
L610	706	100.00%	59.10%	93.60%	SC_DN18276_c0_g1_i1	223
L611	818	69.77%	37.30%	92.70%	SF_DN30349_c0_g1_i1	380
L612	628	100.00%	16.40%	92.90%	SF_DN30349_c0_g1_i1	380
L613	772	100.00%	55.60%	96.00%	SF_DN30349_c0_g1_i1	380
L614	792	95.35%	72.60%	96.00%	SF_DN30349_c0_g1_i1	380
L615	697	100.00%	31.40%	88.00%	SC_DN15479_c0_g1_i1	182
L616	806	100.00%	4.80%	88.40%	SF_DN19300_c0_g1_i1	289
L617	767	100.00%	39.10%	83.90%	SF_DN19300_c0_g1_i1	289
L618	1814	67.44%	70.50%	96.90%	AJ_DN23377_c0_g1_i1	29
L619	631	100.00%	51.30%	93.00%	AT_DN9060_c0_g1_i1	91
L620	843	76.74%	54.40%	95.30%	SF_DN29038_c0_g1_i1	355
L621	642	67.44%	41.60%	90.90%	SF_DN29038_c0_g1_i1	355

L622	739	100.00%	62.70%	94.80%	SC_DN6284_c0_g1_i1	248
L623	776	90.70%	75.90%	98.00%	SC_DN14457_c0_g1_i1	169
L624	838	62.79%	40.10%	92.00%	MI_DN20197_c0_g1_i1	107
L625	565	100.00%	70.40%	95.90%	SF_DN25504_c2_g2_i1	329
L626	800	72.09%	55.80%	95.80%	SF_DN14301_c0_g1_i1	276
L627	498	100.00%	47.80%	94.10%	SF_DN29070_c0_g1_i1	359
L628	753	60.47%	75.40%	97.70%	AT_DN18219_c0_g1_i1	59
L630	521	90.70%	8.80%	76.60%	SF_DN29070_c0_g1_i1	359
L631	671	93.02%	31.00%	89.00%	SF_DN14301_c0_g1_i1	276
L632	798	100.00%	50.00%	94.10%	SC_DN11388_c0_g2_i1	155
L633	789	62.79%	64.40%	97.00%	SF_DN14301_c0_g1_i1	276
L634	526	100.00%	80.80%	97.00%	SF_DN29070_c0_g1_i1	359
L635	830	100.00%	72.80%	97.60%	SF_DN29738_c0_g1_i1	369
L636	831	100.00%	66.70%	96.40%	MI_DN16677_c0_g1_i1	99
L637	990	100.00%	52.40%	96.40%	SC_DN13148_c0_g1_i1	161
L638	1358	100.00%	22.00%	93.60%	SF_DN29009_c6_g1_i1	353
L639	865	81.40%	50.90%	93.50%	SC_DN13148_c0_g1_i1	161
L640	746	97.67%	70.20%	96.70%	SC_DN13148_c0_g1_i1	161
L641	835	97.67%	56.80%	94.40%	SF_DN5944_c0_g1_i1	417
L642	701	95.35%	38.40%	93.90%	SC_DN15879_c0_g1_i1	192
L643	744	93.02%	44.20%	94.70%	SC_DN16030_c0_g1_i1	194
L644	752	95.35%	45.90%	93.30%	SF_DN20068_c0_g1_i1	293
L645	773	97.67%	51.20%	95.50%	SF_DN20068_c0_g1_i1	293

L646	732	95.35%	38.00%	90.30%	SC_DN16030_c0_g1_i1	194
L647	604	69.77%	43.90%	91.70%	SF_DN20068_c0_g1_i1	293
L648	637	83.72%	49.30%	94.00%	SF_DN24093_c0_g2_i1	313
L649	763	95.35%	64.20%	95.90%	SC_DN903_c0_g1_i1	260
L650	787	62.79%	54.90%	94.00%	SF_DN24093_c0_g2_i1	313
L651	735	95.35%	56.20%	94.90%	SF_DN24093_c0_g2_i1	313
L652	770	76.74%	63.00%	96.60%	SF_DN29006_c11_g2_i3	352
L653	690	75.00%	60.00%	94.80%	AT_DN2699_c0_g1_i1	80